Search for electroweak diboson production in association with a high-mass dijet system in semileptonic final states in pp collisions at $\sqrt{s} = 13$ TeV with the ATLAS detector

G. Aad *et al.*[*]
(ATLAS Collaboration)

(Received 21 May 2019; published 22 August 2019)

This paper reports on a search for electroweak diboson ($WW/WZ/ZZ$) production in association with a high-mass dijet system, using data from proton-proton collisions at a center-of-mass energy of $\sqrt{s} = 13$ TeV. The data, corresponding to an integrated luminosity of 35.5 fb^{-1}, were recorded with the ATLAS detector in 2015 and 2016 at the Large Hadron Collider. The search is performed in final states in which one boson decays leptonically, and the other boson decays hadronically. The hadronically decaying W/Z boson is reconstructed as either two small-radius jets or one large-radius jet using jet substructure techniques. The electroweak production of $WW/WZ/ZZ$ in association with two jets is measured with an observed (expected) significance of 2.7 (2.5) standard deviations, and the fiducial cross section is measured to be $45.1 \pm 8.6(\text{stat.})^{+15.9}_{-14.6}(\text{syst.})$ fb.

DOI: 10.1103/PhysRevD.100.032007

I. INTRODUCTION

Vector-boson scattering (VBS) is a key process for probing the non-Abelian gauge structure of the electroweak (EW) sector of the Standard Model (SM), since it involves both the self-couplings of the vector bosons and their coupling with the Higgs boson. In the absence of the SM Higgs boson, the amplitudes for VBS would increase as a function of partonic center-of-mass energy and ultimately violate unitarity [1,2]. The discovery of a Higgs boson in 2012 at the LHC [3,4], with measured properties [5–8] consistent with those of the SM Higgs boson, represents a major milestone in the understanding of electroweak symmetry breaking. The study of the VBS process provides an important check of the SM by testing whether the Higgs mechanism is the sole source of electroweak symmetry breaking. Theories of new phenomena beyond the SM that alter the quartic gauge couplings [9,10], or include the presence of additional resonances [11,12], predict enhancements of VBS at high transverse momentum of the vector bosons and at high invariant mass of the diboson system.

The experimental signature of VBS is characterized by the presence of a pair of vector bosons and two forward jets, $VVjj$ ($V = W, Z, \gamma$), with a large separation in rapidity of jets and a large dijet invariant mass. Multiple processes can produce the same final state of two bosons and two jets. The production of $VVjj$ at tree level has an EW contribution involving only electroweak-interaction vertices, and a strong contribution (QCD induced) involving two strong-interaction vertices. The EW production is further divided into two components. The first component is EW VBS production with actual scattering of the two electroweak bosons. The scattering occurs via quartic gauge vertices, or triple gauge vertices involving the s- or t-channel exchange of a Higgs boson or a W/Z boson. The second component is EW non-VBS production that has electroweak vertices only, but where the two bosons do not scatter. The EW non-VBS component cannot be separated from the EW VBS component in a gauge invariant way [13] and contributes significantly to the total cross section. It is therefore included in the signal generation. Representative Feynman diagrams at tree level are shown in Fig. 1. Both the ATLAS and CMS Collaborations have searched for experimental evidence of VBS. So far, electroweak $VVjj$ production is only observed in the same-sign $W^{\pm}W^{\pm}jj$ channel [14] and $WZjj$ channel [15] in the fully leptonic final states using data collected at a center-of-mass energy of $\sqrt{s} = 13$ TeV. Evidence of electroweak $VVjj$ production is also obtained in the $W^{\pm}W^{\pm}jj$ [16–18] and $Z\gamma jj$ [19] channels using pp collisions at $\sqrt{s} = 8$ TeV. Limits on fiducial cross sections of electroweak $VVjj$ production are reported for the $WZjj$ [20,21], $ZZjj$ [22], $Z\gamma jj$ [23] and $W\gamma jj$ [24] channels. Constraints on anomalous quartic gauge couplings are reported in Refs. [16–19,21,23–27].

[*]Full author list given at the end of the article.

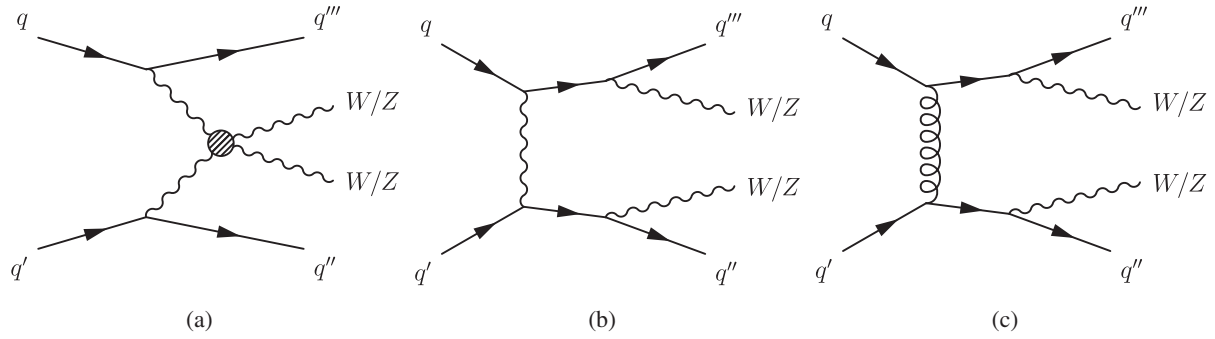

FIG. 1. Representative Feynman diagrams for (a) EW $VVjj$ production via VBS, (b) EW $VVjj$ production via non-VBS contribution, and (c) QCD $VVjj$ production.

Reference [26] reports a study similar to the one in this paper, albeit focused on EW production of $VVjj$ in the $WV \to \ell\nu qq$ channel only and performed at $\sqrt{s} = 8$ TeV. This paper presents a study of the EW production of $VVjj$ ($V = W$, Z) with the vector-boson pair decaying semileptonically. A larger data sample is used and additional diboson signal processes with similar final states are included.

Three VV semileptonic decay channels are explored: a Z boson decaying into a pair of neutrinos, $Z \to \nu\nu$[1]; a W boson decaying into a charged lepton (an electron or muon, denoted by ℓ) and a neutrino, $W \to \ell\nu$; and a Z boson decaying into a pair of light charged leptons, $Z \to \ell\ell$. In all cases, the other vector boson V is required to decay into a pair of quarks, $V \to qq$, leading to $ZV \to \nu\nu qq$, $WV \to \ell\nu qq$ and $ZV \to \ell\ell qq$ final states. These processes overlap in the fiducial region of the measurement because of the geometrical acceptance of the detector for leptons and jets. The decay channels are selected as 0-, 1- and 2-lepton final states, where the 1-lepton (2-lepton) final state receives only contribution from $WV \to \ell\nu qq$ ($ZV \to \ell\ell qq$) processes, and the 0-lepton final state receives about equal contributions from $WV \to \ell\nu qq$ and $ZV \to \nu\nu qq$ processes.

Two different reconstruction techniques for the $V \to qq$ decay are considered: resolved and merged. The resolved reconstruction attempts to identify two separate small-radius jets (small-R jet denoted by j) of hadrons from the $V \to qq$ decay, while the merged reconstruction uses jet substructure techniques to identify the $V \to qq$ decay reconstructed as a large-radius jet (large-R jet denoted by J). The latter applies when the momentum transfer in $VVjj$ production is high, and as a consequence the qq pair from the V boson decay is collimated. In this case, hadrons from the two quarks overlap in the detector and are more efficiently reconstructed as a single large-R jet. In total, six final states are included in this study: 0-, 1- and 2-lepton final states, each using resolved or merged $V \to qq$ reconstruction techniques.

In order to extract the signal and to measure the cross section for the EW production of $VVjj$ in a fiducial volume, multivariate discriminants, which combine observables sensitive to the kinematics of the VBS process, are used to separate EW-induced $VVjj$ production from QCD-induced $VVjj$ production.

This analysis measures the cross section of EW $VVjj$ production in a region of kinematic phase space close to the acceptance of the detector. Fiducial cross sections are measured in the 0-, 1- and 2-lepton channels, where lepton refers to e and μ. Final states with V decaying into one or more τ-leptons (both leptonically and hadronically decaying τ-leptons) are included as signal, but the contribution of V from top quark decay is not considered as signal.

II. ATLAS DETECTOR

The ATLAS experiment is described in Ref. [28]. ATLAS is a multipurpose detector with a forward-backward symmetric cylindrical geometry and a solid-angle[2] coverage of nearly 4π. The inner tracking detector (ID), covering the region $|\eta| < 2.5$, consists of a silicon pixel detector, a silicon microstrip detector and a straw-tube transition-radiation tracker. The inner detector is surrounded by a thin superconducting solenoid providing a 2 T magnetic field, and by a finely segmented lead/liquid-argon (LAr) electromagnetic calorimeter covering the region $|\eta| < 3.2$. A steel/scintillator-tile hadronic calorimeter provides coverage in the central region $|\eta| < 1.7$.

[1]To simplify the notation, antiparticles are not explicitly labeled in this paper.

[2]The ATLAS experiment uses a right-handed coordinate system with its origin at the nominal interaction point (IP) in the center of the detector and the z axis along the axis of the beam pipe. The x axis points from the IP to the center of the LHC ring, and the y axis points upwards. Cylindrical coordinates (r, ϕ) are used in the transverse plane, ϕ being the azimuthal angle around the z axis. The pseudorapidity is defined in terms of the polar angle θ as $\eta = -\ln\tan(\theta/2)$. Angular distance is measured in units of $\Delta R \equiv \sqrt{(\Delta\eta)^2 + (\Delta\phi)^2}$.

The end cap and forward regions are instrumented with LAr calorimeters for both EM and hadronic energy measurements up to $|\eta| = 4.9$. A muon spectrometer (MS) system incorporating large superconducting toroidal air-core magnets surrounds the calorimeters. Three layers of precision wire chambers provide muon tracking in the range $|\eta| < 2.7$, while dedicated fast chambers are used for triggering in the region $|\eta| < 2.4$. The trigger system is composed of two stages [29]. The first stage, implemented with custom hardware, uses information from calorimeters and muon chambers to reduce the event rate to a maximum of 100 kHz. The second stage, called the high-level trigger, reduces the data acquisition rate to about 1 kHz on average. The high-level trigger is software-based and runs reconstruction algorithms similar to those used in the offline reconstruction.

III. DATA AND MONTE CARLO SIMULATION

A. Data

The data were collected with the ATLAS detector in 2015 and 2016 from pp collisions at a center-of-mass energy of $\sqrt{s} = 13$ TeV, corresponding to a total integrated luminosity of 35.5 fb^{-1}.

The recorded 2-lepton channel and 1-lepton channel events were selected with a mixture of either multiple single-electron or single-muon triggers with varying transverse energy E_{T} (electron) and transverse momentum p_{T} (muon) thresholds, and quality and isolation requirements, that depended on the LHC running conditions. The lowest E_{T} or p_{T} requirement without trigger prescaling was 26 GeV for both the electrons and muons. Events for the 0-lepton channel were recorded with nonprescaled missing transverse momentum ($E_{\mathrm{T}}^{\mathrm{miss}}$) triggers where the $E_{\mathrm{T}}^{\mathrm{miss}}$ threshold depended on the LHC running conditions. The lowest threshold used is 110 GeV. The $E_{\mathrm{T}}^{\mathrm{miss}}$ triggers used are fully efficient for events passing the selection described below. The $E_{\mathrm{T}}^{\mathrm{miss}}$ triggers are also used in the 1-lepton channel to compensate for single-muon trigger inefficiency due to the difference in acceptance between the muon tracking and triggering.

Events in this analysis have all detector systems operating normally. Collision vertices are formed from tracks with $p_{\mathrm{T}} > 400$ MeV, and the one with the highest $\sum p_{\mathrm{T}}^2$ of its associated tracks is selected as the primary vertex.

B. Signal and background simulation

Monte Carlo (MC) simulation is used to model signal and background processes. The simulated samples are used to optimize the event selection, to develop the multivariate discriminant, and to estimate the irreducible background yields.

The EW $VVjj$ signal samples were generated using MadGraph5_aMC@NLO 2.4.3 [30] with amplitudes of $\mathcal{O}(\alpha_{\mathrm{EW}}^6\alpha_{\mathrm{S}}^0)$, where α_{EW} (α_{S}) is the EW (strong) coupling constant. Both the VBS amplitudes and non-VBS amplitudes of the $VVjj$ process with one boson decaying hadronically and the other leptonically were included, using factorized on-shell decays for the gauge bosons. The NNPDF30LO [31] PDF set was used. The parton showers and hadronization were modeled with Pythia 8.186 [32] using the A14 set of tuned parameters (tune) for the underlying event [33].

The main background sources are Z and W bosons produced in association with jets (Z + jets and W + jets), as well as significant contributions from top quark production (both $t\bar{t}$ pair and single-top) and QCD-induced vector-boson pair production. The Z + jets and W + jets events were simulated using the Sherpa 2.2.1 [34] event generator. Matrix elements were calculated for up to two partons at NLO and up to four partons at LO using the Comix [35] and OpenLoops [36] programs. QCD-induced diboson processes with one of the bosons decaying hadronically and the other leptonically were simulated using Sherpa 2.2.1. They were simulated for up to one additional parton at NLO and up to three additional partons at LO using the Comix and OpenLoops programs. There is no overlap between the QCD-induced diboson samples and the EW $VVjj$ signal samples, as the former include diagrams of $\mathcal{O}(\alpha_{\mathrm{EW}}^4\alpha_{\mathrm{S}}^2)$. For Z + jets, W + jets and diboson simulation, the matrix-element calculations were merged with the Sherpa parton shower using the ME + PS@NLO prescription [37]. The NNPDF30NNLO [38] PDF set was used in conjunction with a dedicated parton-shower tuning developed by the Sherpa authors. For the Z + jets and W + jets samples, boson decays into all lepton flavors (e, μ, τ) are included. For the generation of top quark pairs, the Powheg-Box v2 [39–41] event generator with the CT10 [42] PDF set in the matrix-element calculations was used. Electroweak t-channel, s-channel and Wt-channel single-top-quark events were generated using the Powheg-Box v1 event generator [43–45]. This event generator uses the four-flavor scheme for the NLO matrix-element calculations together with the fixed four-flavor PDF set CT10f4 [42]. For all top quark processes, top quark spin correlations are preserved (for the t-channel, top quark decay is simulated using MadSpin [46]). The parton showers, fragmentation, and underlying event were simulated using Pythia 6.428 [47] with the CTEQ6L1 [48] PDF set and the corresponding Perugia 2012 tune (P2012) [49]. The top quark mass was set to 172.5 GeV. The EvtGen v1.2.0 program [50] was used to simulate the decay of bottom and charm hadrons for the Powheg-Box samples.

All simulated processes are normalized using the currently available state-of-the-art theoretical predictions for their cross sections. Cross sections are calculated with up to next-to-next-to-leading-order (NNLO) QCD corrections for Z + jets and W + jets production [51]. Cross sections for diboson production are calculated at NLO including LO contributions with two additional partons [34,52]. The $t\bar{t}$

production cross section is calculated at NNLO in QCD, including resummation of next-to-next-to-leading logarithmic (NNLL) soft-gluon terms [53,54]. The single-top production cross sections are calculated to NLO in QCD [55], including the soft-gluon resummation at NNLL [56] for the Wt process.

MC events were processed with a detailed detector simulation [57] based on GEANT4 [58]. Additional inelastic simulated pp collisions generated with PYTHIA 8.186 using the A2 set of tuned parameters [59] and the MSTW2008LO [60] PDF set were overlaid in order to model both the in- and out-of-time effects from additional pp collisions in the same and neighboring bunch crossings (pileup). MC samples are reweighted to match the pileup conditions in the data. All simulated events are processed using the same reconstruction algorithms as the data.

IV. OBJECT RECONSTRUCTION

Electrons are identified as isolated energy clusters in the electromagnetic calorimeter matched to ID tracks, and are required to have transverse energy $E_{\mathrm{T}} > 7$ GeV and pseudorapidity $|\eta| < 2.47$. A likelihood-based requirement [61] is imposed to reduce the background from nonprompt electrons or hadrons misidentified as electrons. Electrons are classified as either "loose," "medium" or "tight" according to the likelihood-based identification criteria described in Ref. [61].

Muons are reconstructed by a combined fit to the ID and MS tracks, and are required to have $p_{\mathrm{T}} > 7$ GeV and $|\eta| < 2.5$. Muons must pass identification requirements, based on the number of hits in the ID and MS subsystems, and the significance of the difference $|q/p_{\mathrm{MS}} - q/p_{\mathrm{ID}}|$ [62], where q is the charge and $p_{\mathrm{MS}}(p_{\mathrm{ID}})$ is the momentum of the muon measured in the MS (ID). Similarly to electrons, muons are classified as either loose, medium or tight, following the criteria in Ref. [62].

All electrons and muons are required to be isolated by using selections based on the sum of the p_{T} of tracks (excluding the track associated with the lepton) in a cone of p_{T}-dependent size around their directions. The isolation selection criteria are designed to maintain a constant efficiency of 99% in the p_{T}-η plane for reconstructed leptons from $Z \to \ell\ell$ decays. Furthermore, leptons are required to have associated tracks satisfying $|d_0/\sigma_{d_0}| < 5(3)$ and $|z_0 \times \sin\theta| < 0.5$ mm for electrons (muons), where d_0 is the transverse impact parameter relative to the beam line, σ_{d_0} is its uncertainty, and z_0 is the distance between the longitudinal position of the track along the beam line at the point where d_0 is measured and the longitudinal position of the primary vertex.

Three types of jets are employed in the analysis. Two of them are reconstructed from three-dimensional topological clusters of energy deposits in the calorimeter [63] (small-R jets and large-R jets), and the third type from inner-detector tracks (track jets). All three use the anti-k_t algorithm [64,65] but with different values of the radius parameter R. Small-R jets and large-R jets are reconstructed independently from the same energy depositions for a given event. The treatment of the resulting overlap is discussed further below.

Small-R jets are reconstructed with a radius parameter of $R = 0.4$. Energy- and η-dependent correction factors derived from MC simulations are applied to correct jets back to the particle level [66]. Pileup effects are corrected using a jet area method [67,68]. Jets are required to have $p_{\mathrm{T}} > 20$ GeV for $|\eta| < 2.5$ and $p_{\mathrm{T}} > 30$ GeV for $2.5 < |\eta| < 4.5$. A jet vertex tagger [67] is applied to jets with $p_{\mathrm{T}} < 60$ GeV and $|\eta| < 2.4$ in order to select only jets from the hard interaction which are associated with the primary vertex, and to suppress jets from pileup interactions. This tagger uses information about tracks associated with the primary vertex and pileup vertices.

Small-R jets containing b-hadrons are identified using a multivariate algorithm (b-tagging) [69] which uses information such as track impact-parameter significance and the position of explicitly reconstructed secondary decay vertices. The chosen b-tagging algorithm has an efficiency of 70% for b-quark jets in simulated $t\bar{t}$ events, with a light-flavor jet rejection factor of about 380 and a c-jet rejection factor of about 12 [70].

Large-R jets are reconstructed with the radius parameter increased to $R = 1.0$. In order to mitigate the effects of pileup and soft radiation, the large-R jets are trimmed [71]. Trimming takes the original constituents of the jet and reclusters them using the k_t algorithm [72] with a smaller radius parameter, R_{subjet}, to produce a collection of subjets. These subjets are discarded if they carry less than a specific fraction (f_{cut}) of the original jet p_{T}. The trimming parameters were optimized for W/Z boson tagging and are $R_{\mathrm{subjet}} = 0.2$ and $f_{\mathrm{cut}} = 5\%$. The large-R jet four-momenta are recomputed from the remaining subjets, and the jet energies are calibrated to particle level using correction factors derived from MC simulations [73]. The mass of a large-R jet (m_J) is computed using a combination of calorimeter and tracking information [74]. Large-R jets are required to have $p_{\mathrm{T}} > 200$ GeV and $|\eta| < 2.0$.

Track jets have a radius parameter of $R = 0.2$ [75]. Inner-detector tracks originating from the primary vertex, with $p_{\mathrm{T}} > 0.5$ GeV and selected by impact parameter requirements, are used in the track jet reconstruction. Track jets are required to satisfy $p_{\mathrm{T}} > 20$ GeV and $|\eta| < 2.5$. The number of track jets is an input to the multivariate discriminant described later.

An overlap-removal procedure is applied to the selected leptons and jets in order to prevent double-counting. The jet is removed if an electron and a small-R jet are separated by $\Delta R < 0.2$; the electron is removed if the separation satisfies $0.2 < \Delta R < 0.4$. The jet is removed if a muon and a small-R jet are separated by $\Delta R < 0.2$ and if the jet has less than three tracks or the energy and momentum differences

between the muon and the jet are small; otherwise the muon is removed if the separation satisfies $\Delta R < 0.4$. In order to prevent double-counting of energy from an electron inside a large-R jet, the large-R jet is removed if an electron and a large-R jet are separated by $\Delta R < 1.0$. No overlap removal is applied between large-R jets or track jets and small-R jets.

Boson tagging is applied to large-R jets in order to select those consistent with $V \to qq$ decays. A p_{T}-dependent requirement is applied to the jet substructure variable $D_2^{(\beta=1)}$, which is defined as a ratio of two-point to three-point energy correlation functions [76,77] that are based on the energies and pairwise angular separations of the particles within a jet. This variable is optimized to distinguish between jets originating from a single parton and those coming from the two-body decay of a heavy particle. A detailed description of the method and its optimization can be found in Ref. [78]. Large-R jets from $V \to qq$ decays are required to have a jet mass m_J in a p_{T}-dependent window centered around the expected value of the boson mass. The configuration of the boson tagging algorithm is called a working point, which is designed to provide constant efficiency independent of the large-R jet p_{T} for the signals studied. Two working points are used, one with 50% efficiency and the other one with 80% efficiency, with corresponding misidentification rates for jets from multijet production of ∼2% and ∼10%, respectively.

The missing transverse momentum vector, $\vec{E}_{\mathrm{T}}^{\mathrm{miss}}$, is calculated as the negative vectorial sum of the transverse momenta of calibrated electrons, muons, and small-R jets where the calibration already includes corrections for pileup. Large-R jets and track jets are not included in the $\vec{E}_{\mathrm{T}}^{\mathrm{miss}}$ calculation in order to avoid double-counting of energy between the small-R jets and large-R jets. Energy depositions due to the underlying event and other types of soft radiation are taken into account by constructing a "soft term" from ID tracks that are associated with the primary vertex but not used in any reconstructed object [79]. The track-based missing transverse momentum vector, $\vec{p}_{\mathrm{T}}^{\mathrm{miss}}$, is the negative vectorial sum of the transverse momenta of all good-quality inner-detector tracks that are associated with the primary vertex.

V. EVENT SELECTION AND BACKGROIUND ESTIMATION

Events are categorized into the 0-, 1- and 2-lepton channels depending on the number of selected electrons and muons. In addition to a leptonically decaying candidate V_{lep}, events in all three channels are required to contain a hadronically decaying candidate V_{had}, and two additional small-R jets (referred to as tagging-jets). The V_{had} candidate is reconstructed as either two small-R jets ($V \to jj$) in a resolved selection, or one large-R jet ($V \to J$) in a merged selection, and those jets are referred to as V_{had} jets. Event selection criteria are chosen to guarantee the statistical independence of the channels and to maximize the sensitivity of the analysis. This selection results in nine nonoverlapping distinct signal regions (SR): one for each of the three lepton channels and three types of V_{had} selections (resolved, and low- and high-purity merged).

The event selection for all channels and background estimations is summarized in Table I. Further details are given below.

A. Event selection

Signal events in the 0-lepton channel are typical of a hadronically decaying V boson recoiling against a large amount of missing transverse momentum stemming from either a $Z \to \nu\nu$ decay or a $W \to \ell\nu$ decay, where the lepton is outside the acceptance of the detector. An initial selection is made by requiring $E_{\mathrm{T}}^{\mathrm{miss}} > 200$ GeV, and rejecting events with electrons or muons passing the loose quality requirements. The multijet background originates primarily from the presence of mismeasured jets and noncollision phenomena. It is suppressed using a requirement on the value of the track-based missing transverse momentum, $p_{\mathrm{T}}^{\mathrm{miss}} > 50$ GeV. Three further angular selection criteria are: the azimuthal separation between the $\vec{E}_{\mathrm{T}}^{\mathrm{miss}}$ and $\vec{p}_{\mathrm{T}}^{\mathrm{miss}}$ directions satisfies $\Delta\phi(\vec{E}_{\mathrm{T}}^{\mathrm{miss}}, \vec{p}_{\mathrm{T}}^{\mathrm{miss}}) < \pi/2$; the azimuthal separation between the directions of $\vec{E}_{\mathrm{T}}^{\mathrm{miss}}$ and the nearest small-R jet satisfies $\min[\Delta\phi(\vec{E}_{\mathrm{T}}^{\mathrm{miss}}, \text{small-}R\,\text{jet})] > \pi/6$; and the azimuthal separation between the directions of $\vec{E}_{\mathrm{T}}^{\mathrm{miss}}$ and the reconstructed hadronically decaying candidate V_{had} satisfies $\Delta\phi(\vec{E}_{\mathrm{T}}^{\mathrm{miss}}, V_{\mathrm{had}}) > \pi/9$. The multijet background is found to be negligible after these selections.

The 1-lepton channel is typical of a leptonically decaying W boson. The $W \to \ell\nu$ candidates are selected by requiring one isolated lepton (electron or muon) satisfying the tight criteria with $p_{\mathrm{T}} > 27$ GeV. Events are required to have $E_{\mathrm{T}}^{\mathrm{miss}} > 80$ GeV, and must not have any additional loose leptons. In order to reconstruct the invariant mass of the WV system, needed later to construct the multivariate discriminant, the neutrino momentum four-vector is reconstructed by imposing a W boson mass constraint on the lepton–neutrino system. The neutrino transverse momentum components are set equal to the missing transverse momentum of the event and the unknown z-component of the momentum (p_z) is obtained from the resulting quadratic equation. The p_z is chosen as either the smaller, in absolute value, of the two real solutions or, if the solution is complex, its real part.

In the 2-lepton channel, the $Z \to \ell\ell$ candidates are identified by requiring two isolated same-flavor leptons satisfying the loose criteria. The leading (subleading)

TABLE I. Summary of the event selection in the 0-, 1- and 2-lepton channels.

Selection	0-lepton	1-lepton	2-lepton
Trigger	$E_{\mathrm{T}}^{\mathrm{miss}}$ triggers	Single-electron triggers single-muon or $E_{\mathrm{T}}^{\mathrm{miss}}$ triggers	Single-lepton triggers
Leptons	0 loose leptons with $p_{\mathrm{T}} > 7$ GeV	1 tight lepton with $p_{\mathrm{T}} > 27$ GeV 0 loose leptons with $p_{\mathrm{T}} > 7$ GeV	2 loose leptons with $p_{\mathrm{T}} > 20$ GeV ≥ 1 lepton with $p_{\mathrm{T}} > 28$ GeV
$E_{\mathrm{T}}^{\mathrm{miss}}$	>200 GeV	>80 GeV	...
$m_{\ell\ell}$	...	...	$83 < m_{ee} < 99$ GeV $(-0.0117 \times p_{\mathrm{T}}^{\mu\mu} + 85.63\ \mathrm{GeV})$ $< m_{\mu\mu} < (0.0185 \times p_{\mathrm{T}}^{\mu\mu} + 94\ \mathrm{GeV})$
Small-R jets	$p_{\mathrm{T}} > 20$ GeV if $\lvert\eta\rvert < 2.5$, and $p_{\mathrm{T}} > 30$ GeV if $2.5 < \lvert\eta\rvert < 4.5$		
Large-R jets	$p_{\mathrm{T}} > 200$ GeV, $\lvert\eta\rvert < 2$		
$V_{\mathrm{had}} \to J$	V boson tagging, $\min(\lvert m_J - m_W\rvert, \lvert m_J - m_Z\rvert)$		
$V_{\mathrm{had}} \to jj$	$64 < m_{jj} < 106$ GeV, jj pair with $\min(\lvert m_{jj} - m_W\rvert, \lvert m_{jj} - m_Z\rvert)$, leading jet with $p_{\mathrm{T}} > 40$ GeV		
Tagging-jets	$j \notin V_{\mathrm{had}}$, not b-tagged, $\Delta R(J, j) > 1.4$ $\eta_{\mathrm{tag},j_1} \cdot \eta_{\mathrm{tag},j_2} < 0$, $m_{jj}^{\mathrm{tag}} > 400$ GeV, $p_{\mathrm{T}} > 30$ GeV		
Num. of b-jets	...	0	...
Multijet removal	$p_{\mathrm{T}}^{\mathrm{miss}} > 50$ GeV $\Delta\phi(\vec{E}_{\mathrm{T}}^{\mathrm{miss}}, \vec{p}_{\mathrm{T}}^{\mathrm{miss}}) < \pi/2$ $\min[\Delta\phi(\vec{E}_{\mathrm{T}}^{\mathrm{miss}}, \text{small-}R\text{ jet})] > \pi/6$ $\Delta\phi(\vec{E}_{\mathrm{T}}^{\mathrm{miss}}, V_{\mathrm{had}}) > \pi/9$	...	...

lepton must satisfy $p_{\mathrm{T}} > 28(20)$ GeV. Opposite charges are required for the muon pairs but not for the electron pairs, since electrons are more susceptible to charge misidentification due to the conversion of photons from bremsstrahlung, especially at high p_{T}. The dilepton invariant mass is required to be consistent with that of the Z boson: $83 < m_{ee} < 99$ GeV in the case of electrons and $(-0.0117 \times p_{\mathrm{T}}^{\mu\mu} + 85.63\ \mathrm{GeV}) < m_{\mu\mu} < (0.0185 \times p_{\mathrm{T}}^{\mu\mu} + 94\ \mathrm{GeV})$ in the case of muons. The p_{T}-dependent requirement on $m_{\mu\mu}$ recovers the selection efficiency at high $p_{\mathrm{T}}^{\mu\mu}$, which would otherwise fall due to the degraded dimuon invariant mass resolution [80].

The merged selection is applied as the first step in identifying a V_{had} candidate. If an event is not selected, then the resolved selection is used. The order is motivated by a smaller background expectation in the merged analysis. Selecting the jets that form a V_{had} candidate first and then selecting the tagging-jets from the pool of remaining jets results in an analysis with a higher sensitivity compared with doing the selection in the reverse order. The V_{had} candidates are selected in three different nonoverlapping channels.

Merged selection events are required to have at least one large-R jet. Next the boson tagging discussed in Sec. IV is applied to select the $V \to qq$ decays. Two SRs are defined, one for events passing the 50% working point of the boson tagging requirement and the other for events failing the 50%, but passing the 80% working point requirement. The former is called the high-purity (HP) signal region, and the latter the low-purity (LP) signal region. Given the different but overlappping W and Z boson tagging requirements, large-R jets are required to satisfy either W or Z boson tagging. If multiple V_{had} candidates are selected, the one minimizing $\min(\lvert m_J - m_W\rvert, \lvert m_J - m_Z\rvert)$ is selected.

The resolved selection events are required to have two small-R signal jets with a dijet invariant mass lying in the $m_{W/Z}$ window: $64 < m_{jj} < 106$ GeV. If multiple V_{had} candidates are selected, the one minimizing $\min(\lvert m_{jj} - m_W\rvert, \lvert m_{jj} - m_Z\rvert)$ is used. At least one of the jets forming the selected V_{had} candidate must have $p_{\mathrm{T}} > 40$ GeV, in order to improve the separation between the signal and the background; otherwise the event is not selected.

After selecting the V_{had} candidate, tagging-jets are selected from the remaining small-R jets that fail the b-tagging described in Sec. IV. For the merged selection, all small-R jets with $\Delta R(J, j) < 1.4$ are excluded before the tagging-jets selection. Tagging-jets are required to be in opposite hemispheres, $\eta_{\mathrm{tag},j_1} \cdot \eta_{\mathrm{tag},j_2} < 0$, and the invariant mass of the two tagging-jets must satisfy $m_{jj}^{\mathrm{tag}} > 400$ GeV. If there is more than one pair of jets satisfying these requirements, the one with the highest m_{jj}^{tag} value is chosen. In order to suppress the contribution from pileup interactions, both tagging-jets from the selected pair must have $p_{\mathrm{T}} > 30$ GeV; otherwise the event is rejected.

Finally, 1-lepton channel events are rejected if any of the small-R jets in the event is identified as a b-jet prior to the V_{had} candidate and tagging-jets selection. This reduces the contributions from top quark production.

B. Data control regions and background estimation

The dominant backgrounds for the 1-lepton channel are $W+$ jets and $t\bar{t}$ production; for the 2-lepton channel it is $Z+$ jets production; while in the 0-lepton channel, they all contribute significantly. Smaller background contributions for the 1-lepton channel arise from multijet background. Single-top and QCD-induced diboson production is a small background for all three lepton channels. The background contributions are estimated using a combination of MC and data-driven techniques. The shapes of kinematic variable distributions are taken from MC simulations in all cases except for the multijet background in the 1-lepton channel.

A $Z+$ jets control region (ZCR) is defined for each of the three SRs in the 2-lepton channel by reversing the m_J or m_{jj} requirement. Events in each of the CRs are selected in exactly the same way as those in their corresponding SRs except for the requirement on m_J or m_{jj}. For the merged selection, the leading large-R jet mass is required to be outside the large-R jet mass window of the 80% working point of the W/Z boson tagging. For the resolved selection, a requirement of $50 < m_{jj} < 64$ GeV or $m_{jj} > 106$ GeV is applied. These CRs are dominated by the $Z+$ jets contribution, with a purity higher than 95% in all regions. They are therefore used to constrain its contribution in signal regions through simultaneous fits as discussed in Sec. X.

Three $W+$ jets control regions (WCRs) are formed from events satisfying the 1-lepton signal region selection except for the invariant mass requirement of the V_{had} candidate, similar to the ZCRs. Approximately 86% and 77% of the selected events are from $W+$ jets production in the merged and resolved categories of the 1-lepton channel, respectively. The remaining events are primarily from $t\bar{t}$ production.

The three $t\bar{t}$ control regions (TopCRs) consist of events satisfying the signal region selection of the 1-lepton channel except for the b-jet requirement, which is inverted. These CRs are dominated by $t\bar{t}$ production, with a purity of 79% and 59% for merged and resolved categories respectively, and the remainder are from single-top, $V+$ jets or diboson production, for both the merged and the resolved event topologies.

In the 0-lepton channel, it is not possible to define pure control regions for $W+$ jets, $Z+$ jets and $t\bar{t}$ processes, thus events falling into the mass sideband regions of the V_{had}, similar to WCRs and ZCRs, form three different CRs (referred to as VjjCR), one for each of the corresponding SRs.

The contribution from multijet production primarily consists of events with jets or photon conversions misidentified as leptons or real but nonprompt leptons from decays of heavy-flavor hadrons. This contribution is negligible in all regions, except for the resolved 1-lepton SR. The fake-factor background method of Ref. [81] is used to estimate the multijet background contribution in the resolved topology of the 1-lepton channel. The estimated multijet contribution is about 10% of the total background in the resolved 1-lepton SR.

The m_{jj}^{tag} spectra of simulated $W+$ jets ($Z+$ jets) events are not well modeled by the MC simulation in the WCRs (ZCRs) for the three V_{had} selections in the 1-lepton (2-lepton) channel. A data-driven procedure is applied to the simulated $W+$ jets and $Z+$ jets events to correct for this shape mismodeling. Reweighting factors are derived from WCRs and ZCRs as a function of m_{jj}^{tag}, and applied to all SRs and CRs (for 0-, 1-, and 2-lepton regions) in the MC simulation of $W+$ jets and $Z+$ jets events, respectively. The non-$W+$ jets($Z+$ jets) contributions are subtracted from the spectra in data. Then the reweighting factors as a function of m_{jj}^{tag} are determined by performing a linear fit to the ratios of data to simulation in the control regions. The reweighting is done separately for the merged and resolved analyses. For $W+$ jets, the reweighting factor ranges from 1.016 (1.024) at $m_{jj}^{\mathrm{tag}} = 400$ GeV to 0.47 (0.53) at $m_{jj}^{\mathrm{tag}} = 3000$ GeV in the resolved (merged) analysis. For $Z+$ jets, the reweighting factor ranges from 1.071 (1.062) at $m_{jj}^{\mathrm{tag}} = 400$ GeV to 0.42 (0.36) at $m_{jj}^{\mathrm{tag}} = 3000$ GeV in the resolved (merged) analysis.

Additional reweighting factors are needed for the MC simulation of $W+$ jets and $Z+$ jets events in the 0-lepton channel because the phase space is so different between the 0-lepton selection and the 1- and 2-lepton selections that the reweightings described above are not applicable. These additional reweightings are derived from MC simulation as the ratio of the numbers of $W+$ jets ($Z+$ jets) events in the 1-lepton (2-lepton) and 0-lepton channels, and are applied to the MC simulation of $W+$ jets ($Z+$ jets) events in the 0-lepton channel. Good agreement between the prediction from MC simulation and the data in the VjjCR is achieved only after the two reweightings have been applied. Unless stated otherwise, the final reweighted $W+$ jets and $Z+$ jets simulated events are used everywhere in the analysis.

VI. MULTIVARIATE ANALYSIS

A multivariate method is used to enhance the separation between the signal and background. The analysis uses the Toolkit for Multivariate Data Analysis, TMVA [82], and its implementation of the boosted decision trees (BDTs) method. BDTs are constructed, trained and evaluated in each lepton channel and analysis region separately. The BDT training is carried out using simulated signal and all background MC samples. However, the events in

TABLE II. Variables used for the BDT discriminant in the merged analysis category of each lepton channel.

Variable	0-lepton	1-lepton	2-lepton
m_{jj}^{tag}	✓	...	✓
$\Delta\eta_{jj}^{\text{tag}}$	...	...	✓
$p_{\text{T}}^{\text{tag},j_2}$	✓	✓	✓
m_J	✓	...	...
$D_2^{(\beta=1)}$	✓	...	✓
$E_{\text{T}}^{\text{miss}}$	✓	...	...
$\Delta\phi(\vec{E}_{\text{T}}^{\text{miss}}, J)$	✓	...	...
η_ℓ	...	✓	...
$n_{j,\text{track}}$	✓	...	...
ζ_V	...	✓	✓
m_{VV}	...	...	✓
p_{T}^{VV}	...	...	✓
m_{VVjj}	...	✓	...
p_{T}^{VVjj}	...	...	✓
w^{tag,j_1}	✓	...	...
w^{tag,j_2}	✓	...	...

TABLE III. Variables used for the BDT discriminant in the resolved analysis category of each lepton channel analysis.

Variable	0-lepton	1-lepton	2-lepton
m_{jj}^{tag}	✓	...	✓
$\Delta\eta_{jj}^{\text{tag}}$	...	...	✓
$p_{\text{T}}^{\text{tag},j_1}$	✓	✓	...
$p_{\text{T}}^{\text{tag},j_2}$	✓	✓	✓
$\Delta\eta_{jj}$	✓	✓	✓
$p_{\text{T}}^{j_1}$	✓	...	...
$p_{\text{T}}^{j_2}$	✓	✓	✓
w^{j_1}	✓	✓	✓
w^{j_2}	✓	✓	✓
$n_{\text{tracks}}^{j_1}$	...	✓	✓
$n_{\text{tracks}}^{j_2}$	...	✓	✓
w^{tag,j_1}	✓	✓	✓
w^{tag,j_2}	✓	✓	✓
$n_{\text{tracks}}^{\text{tag},j_1}$	...	✓	✓
$n_{\text{tracks}}^{\text{tag},j_2}$	...	✓	✓
$n_{j,\text{track}}$	✓	...	✓
$n_{j,\text{extr}}$	✓	...	...
$E_{\text{T}}^{\text{miss}}$	✓	...	...
η_ℓ	...	✓	...
$\Delta R(\ell,\nu)$	...	✓	...
ζ_V	...	✓	✓
m_{VV}	...	...	✓
m_{VVjj}	...	✓	...

high-purity SR and low-purity SR are merged together for the BDT training due to an insufficient number of MC events. In order to make use of the complete set of simulated MC events for the BDT training and evaluation in an unbiased way, the MC events are split for training and validation into two subsamples of equal size following the procedure in Ref. [83]. The output distributions of the BDTs trained on the two subsamples are averaged for both the simulated and data events.

The input variables used for the BDTs are chosen in order to maximize the separation between signal and background, and are summarized in Tables II and III, for the merged and resolved category, respectively. The distributions of input variables of the BDTs are compared between data and simulation, and in general are found to be in good agreement. The small-R jets are labeled in decreasing p_{T} as j_1 and j_2 for the jets used to reconstruct the hadronically decaying boson, and as "tag, j_1" and "tag, j_2" for the tagging-jets. The invariant mass and transverse momentum of the reconstructed VV ($VVjj$) system are denoted by m_{VV} (m_{VVjj}) and p_{T}^{VV} (p_{T}^{VVjj}), respectively. Angular variables are also considered, such as the pseudorapidity gap between the tagging-jets ($\Delta\eta_{jj}^{\text{tag}}$) and between the small-$R$ V_{had} jets ($\Delta\eta_{jj}$), the angular separation of the lepton and neutrino from the W boson decay ($\Delta R(\ell,\nu)$) in the 1-lepton channel, and the azimuthal angle between the directions of $\vec{E}_{\text{T}}^{\text{miss}}$ and the large-R jet ($\Delta\phi(\vec{E}_{\text{T}}^{\text{miss}}, J)$) in the merged category of the 0-lepton channel. A topological variable named boson centrality is also used, and it is defined as $\zeta_V = \min(\Delta\eta_-, \Delta\eta_+)$, where $\Delta\eta_- = \min[\eta(V_{\text{had}}), \eta(V_{\text{lep}})] - \min[\eta_{\text{tag},j_1}, \eta_{\text{tag},j_2}]$ and $\Delta\eta_+ = \max[\eta_{\text{tag},j_1}, \eta_{\text{tag},j_2}] - \max[\eta(V_{\text{had}}), \eta(V_{\text{lep}})]$. The variable ζ_V has large values when the tagging-jets have a large separation in η, and when the two boson candidates lie between the tagging-jets in η. Variables sensitive to the quark–gluon jet separation are also included, such as the width of the small-R jets (w) [84], and the number of tracks associated with the jets (n_{tracks}). The number of track jets, $n_{j,\text{track}}$, and the number of additional small-R jets other than the V_{had} jets and tagging-jets, $n_{j,\text{extr}}$, are also found to be useful for the BDTs. In the 1-lepton channel, the pseudorapidity of the lepton (η_ℓ) is also considered.

VII. FIDUCIAL CROSS-SECTION DEFINITION

The fiducial phase space of the measurement is defined using stable final-state particles [85]. Leptons produced in the decay of a hadron or its descendants are not considered in the charged lepton requirement of the fiducial phase space. The fiducial selection is summarized in Table IV and details are given below.

TABLE IV. Fiducial phase-space definitions used for the measurement of electroweak $VVjj$ production.

Object selection		
Leptons		$p_{\mathrm{T}} > 7$ GeV, $\lvert\eta\rvert < 2.5$
Small-R jets		$p_{\mathrm{T}} > 20$ GeV if $\lvert\eta\rvert < 2.5$, and $p_{\mathrm{T}} > 30$ GeV if $2.5 < \lvert\eta\rvert < 4.5$
Large-R jets		$p_{\mathrm{T}} > 200$ GeV, $\lvert\eta\rvert < 2.0$
Event selection		
Leptonic V selection	0-lepton	Zero leptons, $p_{\mathrm{T}}^{\nu\nu} > 200$ GeV
	1-lepton	One lepton with $p_{\mathrm{T}} > 27$ GeV, $p_{\mathrm{T}}^{\nu} > 80$ GeV
	2-lepton	Two leptons, with leading (subleading) lepton $p_{\mathrm{T}} > 28(20)$ GeV $83 < m_{\ell\ell} < 99$ GeV
Hadronic V selection	Merged	One large-R jet, $\min(\lvert m_J - m_W\rvert, \lvert m_J - m_Z\rvert)$ $64 < m_J < 106$ GeV
	Resolved	Two small-R jets, $\min(\lvert m_{jj} - m_W\rvert, \lvert m_{jj} - m_Z\rvert)$ $p_{\mathrm{T}}^{j_1} > 40$ GeV, $p_{\mathrm{T}}^{j_2} > 20$ GeV $64 < m_{jj} < 106$ GeV
Tagging-jets		Two small-R non-b jets, $\eta_{\mathrm{tag},j_1} \cdot \eta_{\mathrm{tag},j_2} < 0$, highest m_{jj}^{tag} $m_{jj}^{\mathrm{tag}} > 400$ GeV, $p_{\mathrm{T}}^{\mathrm{tag},j_{1,2}} > 30$ GeV
Number of b-jets	0-lepton	…
	1-lepton	0
	2-lepton	…

Charged leptons are required to satisfy $p_{\mathrm{T}} > 7$ GeV and $|\eta| < 2.5$. Jets are clustered from all final-state particles except prompt leptons, prompt neutrinos, and prompt photons using the anti-k_t algorithm. Small-R jets are required to have $p_{\mathrm{T}} > 20$ GeV for $|\eta| < 2.5$ and $p_{\mathrm{T}} > 30$ GeV for $2.5 < |\eta| < 4.5$. Jets within $\Delta R = 0.2$ of any charged lepton (as defined above) are rejected. Jets containing a b-hadron, identified using "truth" information from the MC event record, are labeled as b-jets. Large-R jets are required to have $p_{\mathrm{T}} > 200$ GeV and $|\eta| < 2.0$, and the same trimming algorithm as for the reconstruction-level large-R jets is applied. No $D_2^{(\beta=1)}$ requirement is applied to large-R jets.

The selection of hadronically decaying bosons and tagging-jets follows the same steps and apply the same criteria as for reconstruction level, as shown in Table IV.

For the 0-, 1- and 2-lepton channels, the number of selected fiducial leptons is required to be 0, 1 and 2, respectively. Events with additional leptons for the 1- and 2-lepton channels are vetoed. The lepton p_{T} is required to be larger than 27 GeV for the 1-lepton channel; for the 2-lepton channel, the leading (subleading) lepton p_{T} must be larger than 28 (20) GeV, and the invariant mass of the lepton pair must lie within $83 < m_{\ell\ell} < 99$ GeV. For the 0-lepton channel, the transverse momentum of the neutrino system must satisfy $p_{\mathrm{T}}^{\nu\nu} > 200$ GeV; and for the 1-lepton channel, the events are required to have $p_{\mathrm{T}}^{\nu} > 80$ GeV and contain no b-jets.

VIII. SYSTEMATICAL UNCERTAINTIES

The sources of systematic uncertainty can be divided into three categories: experimental uncertainties related to the detector or to the reconstruction algorithms, uncertainties in the estimations of background contributions, and uncertainties in modeling the signal. Unless stated otherwise, the uncertainties quoted below are the uncertainties in the quantities themselves, not the impact on the analysis sensitivity.

The uncertainty in the integrated luminosity of the dataset is 2.1%. It is derived from the calibration of the luminosity scale using x-y beam-separation scans, following a methodology similar to that detailed in Ref. [86], and using the LUCID-2 detector for the baseline luminosity measurements [87]. This uncertainty is applied to the normalization of the signal and also to background contributions whose normalizations are derived from MC simulations. In addition to the luminosity uncertainty, a variation in the pileup reweighting of MC events is also included to cover the uncertainty in the ratio of the predicted to measured inelastic cross sections in Ref. [88].

The efficiencies of the lepton triggers for events with selected leptons are high, nearly 100% in the electron channel and approximately 96% in the muon channel. The corresponding uncertainties are negligible. For the selection used in the 0-lepton and 1-lepton channels, the efficiency of the $E_{\mathrm{T}}^{\mathrm{miss}}$ trigger is also close to 100% with negligible associated uncertainty. The modeling of the electron and muon reconstruction, identification and

isolation efficiencies is studied with a tag-and-probe method using $Z \to \ell\ell$ events in data and simulation at $\sqrt{s} = 13$ TeV [61,62]. Small corrections are applied to the simulation to better model the performance seen in data. These corrections have associated uncertainties of the order of 1%. Uncertainties in the lepton energy (or momentum) scale and resolution [62,89] are also taken into account.

Uncertainties in the jet energy scale and resolution for small-radius jets are estimated using MC simulation and *in situ* techniques [66]. For central jets ($|\eta| < 2.0$), the total uncertainty in the jet energy scale ranges from about 6% for jets with $p_{\mathrm{T}} = 25$ GeV to about 2% for $p_{\mathrm{T}} = 1$ TeV. There is also an uncertainty in the jet energy resolution [66], which ranges from 10% to 20% for jets with a p_{T} of 20 GeV to less than 5% for jets with $p_{\mathrm{T}} > 200$ GeV. Uncertainties in the lepton and jet energy scales and resolutions are propagated into the uncertainty in $E_{\mathrm{T}}^{\mathrm{miss}}$. Uncertainties in the energy scale and resolution of the track soft term are also propagated into the uncertainty in $E_{\mathrm{T}}^{\mathrm{miss}}$ [79]. For the b-tagging efficiency of small-R jets, correction factors are applied to the simulated event samples in order to compensate for differences between data and simulation. The corrections and uncertainties in the efficiency for tagging b-jets and in the rejection factor for light jets are determined from $t\bar{t}$ samples [90,91].

The uncertainties in the scale of the large-R jet p_{T}, mass and $D_2^{(\beta=1)}$ are of the order of 2%–5%. They are estimated using comparisons of data and simulation in Ref. [78]. An absolute uncertainty of 2% is assigned to the large-R jet energy resolution, and relative uncertainties of 20% and 15% are assigned to the resolution of the large-R jet mass and $D_2^{(\beta=1)}$, respectively.

The overall normalization of the main backgrounds ($W+$jets, $Z+$jets and $t\bar{t}$) is determined from the corresponding data control regions and is left unconstrained and floating in the global likelihood fit. For $W+$jets ($Z+$jets) events in the 0-lepton channel, additional normalization uncertainties are considered to account for the acceptance difference between the 0-lepton channel analysis and the 1-lepton (2-lepton) channel analysis, given that there are no corresponding pure control regions of 0-lepton events and the normalization is determined mainly from control regions with 1-lepton (2-lepton) events. This additional normalization uncertainty for $W+$jets ($Z+$jets) events is estimated using the ratio of the event yield in each signal region of the 0-lepton channel to that in the 1-lepton (2-lepton) channel, and by comparing this ratio obtained from the nominal MC samples generated by Sherpa with the ratio from alternative samples generated by MadGraph5_aMC@NLO. The normalization uncertainty is 8% (14%) for $W+$jets events in the merged (resolved) signal region, and 22% (42%) for $Z+$jets events in the merged (resolved) signal region. These uncertainties are applied to the $W+$jets and $Z+$jets events in the 0-lepton channel only. The normalization uncertainties in the diboson background cross sections are studied with Sherpa. The uncertainty due to missing higher-order QCD contributions (QCD scale uncertainty) is estimated by varying the renormalization (μ_{R}) and factorization (μ_{F}) scales independently by a factor ranging from one-half to two with the constraint $0.5 \leq \mu_{\mathrm{F}}/\mu_{\mathrm{R}} \leq 2$. The PDF uncertainty corresponds to the 68% confidence-level variations of the nominal PDF set NNPDF30NNLO, as well as its difference from the alternative PDF sets CT10NNLO [92] and MMHT2014NNLO [93]. The overall normalization uncertainty for the diboson background is estimated to be about 30%. For single-top-quark events, a 20% normalization uncertainty is assigned [94].

The uncertainty in the modeling of the final discriminants, the BDT output and m_{jj}^{tag}, for background processes estimated using MC simulation is assessed by comparing the nominal MC samples with alternative samples. The uncertainties are of the order of 5%–30%. The m_{jj}^{tag} reweighting as described in Sec. V B is also included as a shape systematic uncertainty for $Z+$jets and $W+$jets events by taking the difference of their respective final discriminants before and after applying the reweighting. An uncertainty in the shape of the BDT or m_{jj}^{tag} distribution for the $t\bar{t}$ background is derived by comparing the Powheg-Box sample with the distribution obtained using MadGraph5_aMC@NLO 2.2.2. Additional systematic uncertainties are estimated by comparing the nominal sample showered with Pythia 6.428 using the P2012 tune to one showered with Herwig++ 2.7.1 [95] and using the UEEE5 underlying-event tune [96]. Samples of $t\bar{t}$ events with the factorization and renormalization scales doubled or halved are compared with the nominal samples, and the observed differences are taken as an additional uncertainty. These modeling uncertainties for the $t\bar{t}$ background are 5%–30%. The shape uncertainty for diboson processes is obtained by comparing MC samples generated by Sherpa and Powheg-Box, and it is found to be of the order of 2%–30%. The shape uncertainty for single-top-quark events is ignored due to their relatively small contribution to the total background.

The following discussion describes the uncertainties in the predictions of EW $VVjj$ signal processes. The uncertainties in the signal-strength measurement, discussed in Sec. X A, include contributions from both the normalization and shape; for the fiducial cross section measurement, discussed in Sec. X B, only the shape uncertainties are taken into account for the measured fiducial cross sections, and the normalization uncertainties are included for the SM predicted fiducial cross sections.

Theoretical uncertainties for EW $VVjj$ signal processes include the PDF choice, the missing higher-order corrections, and the parton-shower modeling. The signal modeling uncertainty due to PDF uncertainties is estimated by taking the uncertainty from the PDF error sets of

NNPDF23LO and adding it in quadrature to the acceptance difference obtained using alternative PDF sets: CT10 and MMHT2014LO. The PDF uncertainties are estimated to be 3%–5%. The parton-shower uncertainty, estimated by varying relevant parameters in the A14-NNPDF tune [33], ranges from 1% to 5%. The effect of the QCD scale uncertainty, of the order of 1%–3%, is estimated by varying the factorization and renormalization scales independently by a factor of 2 with the constraint $0.5 \leq \mu_F/\mu_R \leq 2$.

The interference between EW- and QCD-induced $VVjj$ processes is not included in the MC simulation, since the EW- and QCD-induced $VVjj$ samples were generated separately. The interference effect is considered as an uncertainty affecting both the normalization and the shape of the EW $VVjj$ kinematic distributions. The effect is determined using the MadGraph5_aMC@NLO 2.4.3 MC generator at the truth level as a function of m_{jj}^{tag}. A reweighting is then applied to the simulated EW $VVjj$ samples, resulting in shape uncertainties of 5% to 10% at low and high values of the BDT score, respectively, and a similar size for the normalization uncertainties.

IX. STATISTICAL ANALYSIS

The statistical analysis relies on the profile likelihood test statistic [97] implemented with the RooFit [98] and RooStats [99] packages. A binned likelihood function $\mathcal{L}(\mu, \theta)$ is constructed as a product of Poisson probabilities over all of the bins of the fit templates considered in the analysis. This function depends on the signal-strength parameter μ, a multiplicative factor applied to the theoretical signal production cross section, and θ, a set of nuisance parameters that encodes the effects of systematic uncertainties in the signal and expected backgrounds. The binning is chosen so that the expected numbers of events ensure that the statistical uncertainty is less than 5% in most bins, while finer binning is also allowed in signal-enriched regions. The nuisance parameters are either free to float, or constrained using Gaussian or log-normal terms defined by external studies. The likelihood function for the combination of the three channels is the product of the Poisson likelihoods of the individual channels. However, only one constraint term per common nuisance parameter is included in the product.

A simultaneous maximum-likelihood fit is performed to the observed distributions of the final discriminants, BDT outputs, in the nine SRs to extract the signal rate information. The three ZCRs, WCRs and TopCRs as well as the three VjjCRs are included in the fit's likelihood calculation; the m_{jj}^{tag} distributions are used for ZCRs, WCRs and VjjCRs, while for the TopCRs only one bin for each of the three V_{had} decay channels is used. The purpose of using m_{jj}^{tag} distributions for CRs is to constrain the m_{jj}^{tag} reweighting systematic uncertainties. The different regions and the corresponding discriminants entering the likelihood fit are summarized in Table V. Signal and background contributions, including their shapes in the signal and control regions, are taken from MC simulations. For each source of systematic uncertainty, the correlations across bins of BDT distributions are taken into account and are fully correlated. The correlations between different regions, as well as those between signal and background, are also included. Moreover, normalization scale factors (SFs) are applied to the MC estimates of the $Z+$ jets, $W+$ jets and top quark contributions. These SFs are free parameters in the fit and are therefore constrained by the data in both the signal and control regions. The diboson contribution is constrained to the theoretical estimate within the corresponding uncertainties.

TABLE V. The distributions used in the global likelihood fit for the signal regions and control regions for all the categories in each channel. "One bin" implies that a single bin without any shape information is used in the corresponding fit region.

		Discriminants		
Regions		Merged high-purity	Merged low-purity	Resolved
0-lepton	SR	BDT	BDT	BDT
	VjjCR	m_{jj}^{tag}	m_{jj}^{tag}	m_{jj}^{tag}
1-lepton	SR	BDT	BDT	BDT
	WCR	m_{jj}^{tag}	m_{jj}^{tag}	m_{jj}^{tag}
	TopCR	One bin	One bin	One bin
2-lepton	SR	BDT	BDT	BDT
	ZCR	m_{jj}^{tag}	m_{jj}^{tag}	m_{jj}^{tag}

In general, one SF is introduced for each background component, common to both the SRs and CRs. One common $Z+$ jets SF is used for both the 0-lepton and 2-lepton channels, and one common $W+$ jets SF is used for both the 0-lepton and 1-lepton channels. Similarly, one common $t\bar{t}$ SF is used for both the 0-lepton and 1-lepton channels. However, independent SFs are used for the resolved and merged categories, to take into account different MC modelings in the different phase spaces of the same background component.

The test statistic q_μ is defined as the profile likelihood ratio [100], $q_\mu = -2\ln\Lambda_\mu$ with $\Lambda_\mu = \mathcal{L}(\mu, \hat{\hat{\theta}}_\mu)/\mathcal{L}(\hat{\mu}, \hat{\theta})$, where $\hat{\mu}$ and $\hat{\theta}$ are the values of the parameters that maximize the likelihood function (with the constraint $0 \leq \hat{\mu} \leq \mu$), and $\hat{\hat{\theta}}_\mu$ are the values of the nuisance parameters that maximize the likelihood function for a given value of μ. The best-fit signal strength $\hat{\mu}$ value ($\mu_{\text{EW}\,VVjj}^{\text{obs}}$) is obtained by maximizing the likelihood function with respect to all parameters. To determine whether the observed data is compatible with the background-only hypothesis, a test statistic $q_0 = -2\ln\Lambda_0$ is used.

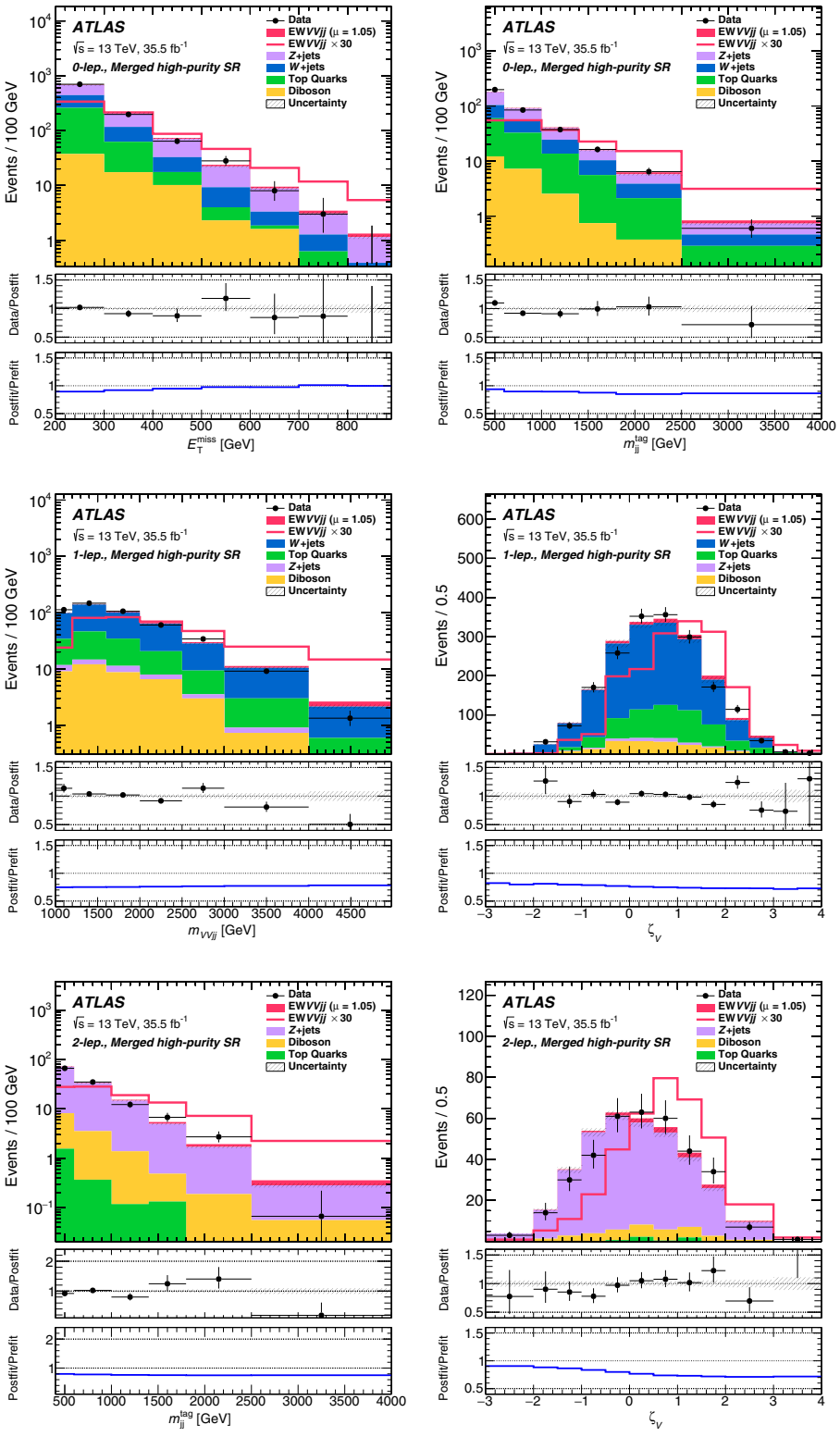

FIG. 2. The distributions for $E_{\mathrm{T}}^{\mathrm{miss}}$ (top left), m_{jj}^{tag} (top right), m_{VVjj} (middle left), ζ_V (middle right), m_{jj}^{tag} (bottom left), and ζ_V (bottom right) in the 0-lepton (top), 1-lepton (middle) and 2-lepton (bottom) channels for the high-purity merged signal region. The background contributions after the global likelihood fit are shown as filled histograms. The signal is shown as a filled histogram on top of the fitted backgrounds normalized to the signal yield extracted from data ($\mu = 1.05$), and unstacked as an unfilled histogram, scaled by the factor indicated in the legend. The size of the combined statistical and systematic uncertainty for the sum of the fitted signal and background is indicated by the hatched band. The middle pane shows the ratios of the observed data to the postfit signal and background predictions. The bottom pane shows the ratios of the postfit and pre-fit background predictions.

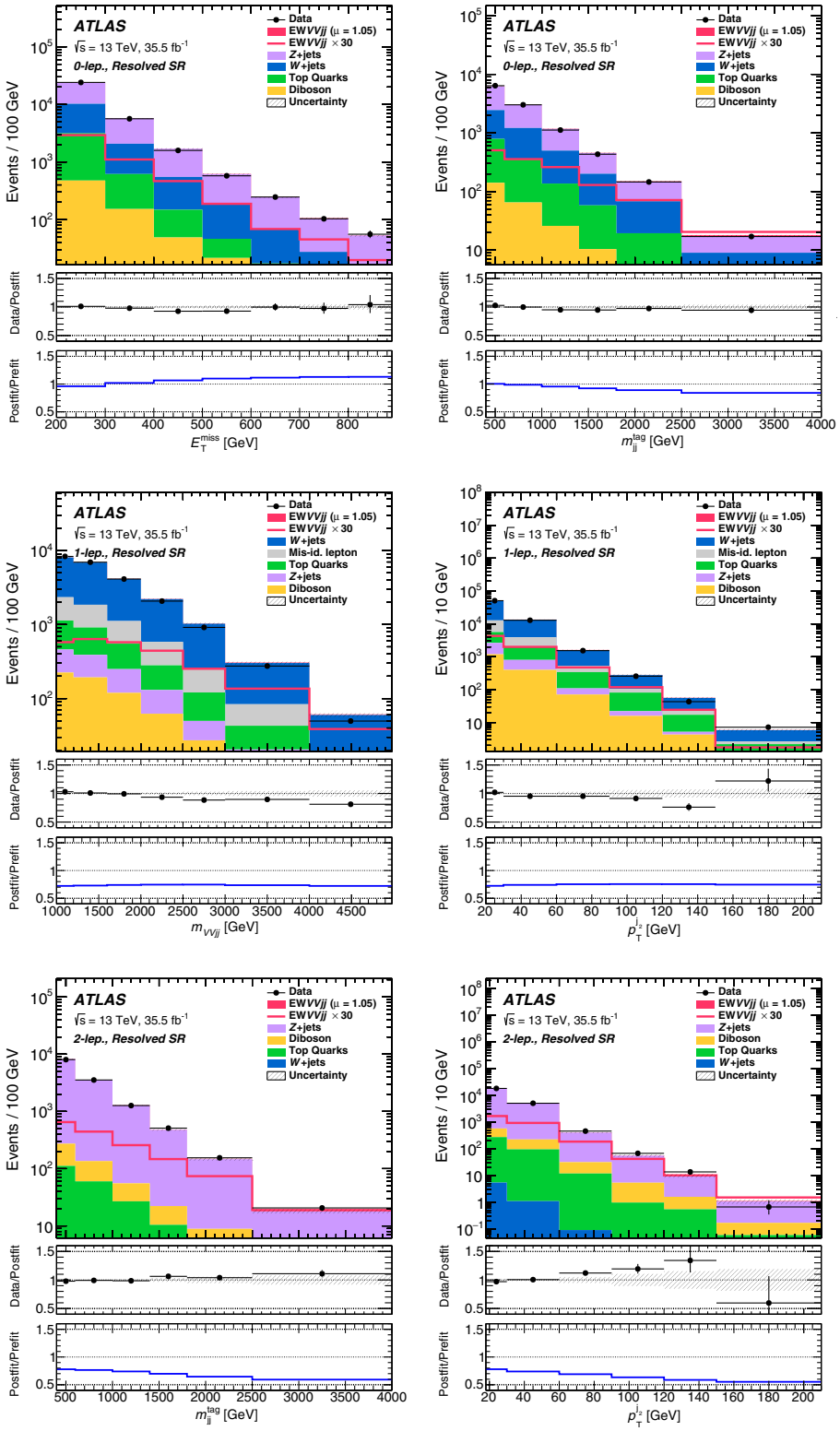

FIG. 3. The distributions for $E_{\mathrm{T}}^{\mathrm{miss}}$ (top left), m_{jj}^{tag} (top right), m_{VVjj} (middle left), $p_{\mathrm{T}}^{j_2}$ (middle right), m_{jj}^{tag} (bottom left), and $p_{\mathrm{T}}^{j_2}$ (bottom right) in the 0-lepton (top), 1-lepton (middle) and 2-lepton (bottom) channels for the resolved signal region. The background contributions after the global likelihood fit are shown as filled histograms. The signal is shown as a filled histogram on top of the fitted backgrounds normalized to the signal yield extracted from data ($\mu = 1.05$), and unstacked as an unfilled histogram, scaled by the factor indicated in the legend. The size of the combined statistical and systematic uncertainty for the sum of the fitted signal and background is indicated by the hatched band. The middle pane shows the ratios of the observed data to the postfit signal and background predictions. The bottom pane shows the ratios of the postfit and prefit background predictions.

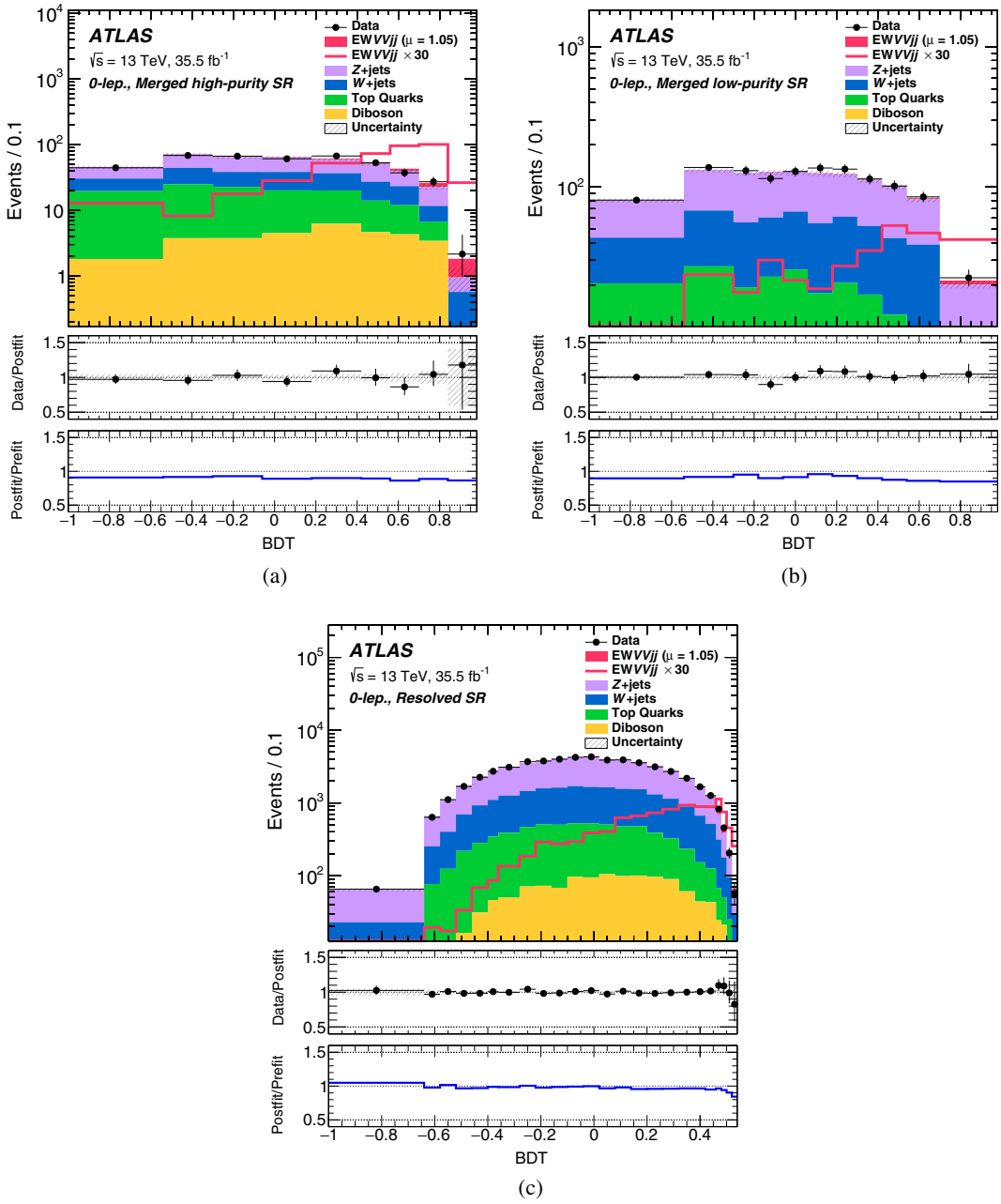

FIG. 4. Comparisons of the observed data and expected distributions of the BDT outputs of the 0-lepton channel signal regions: (a) high-purity and (b) low-purity merged signal regions; (c) the resolved signal region. The background contributions after the global likelihood fit are shown as filled histograms. The signal is shown as a filled histogram on top of the fitted backgrounds normalized to the signal yield extracted from data ($\mu = 1.05$), and unstacked as an unfilled histogram, scaled by the factor indicated in the legend. The entries in overflow are included in the last bin. The middle pane shows the ratios of the observed data to the postfit signal and background predictions. The uncertainty in the total prediction, shown as bands, combines statistical and systematic contributions. The bottom pane shows the ratios of the postfit and prefit background predictions.

X. RESULTS

A. Results for the EW *VVjj* production processes

Figures 2 and 3 show a selection of representative postfit distributions of input variables that are most discriminating for each of the lepton channels, for the merged and resolved categories, respectively. Background and EW $VVjj$ signal contributions shown are obtained from the signal-plus-background fits described previously.

The observed distributions of the BDT outputs in SRs used in the global likelihood fit are compared with the predictions, shown in Fig. 4 for the 0-lepton channel, Fig. 5 for the 1-lepton channel, and Fig. 6 for the 2-lepton channel. The data distributions are reasonably well

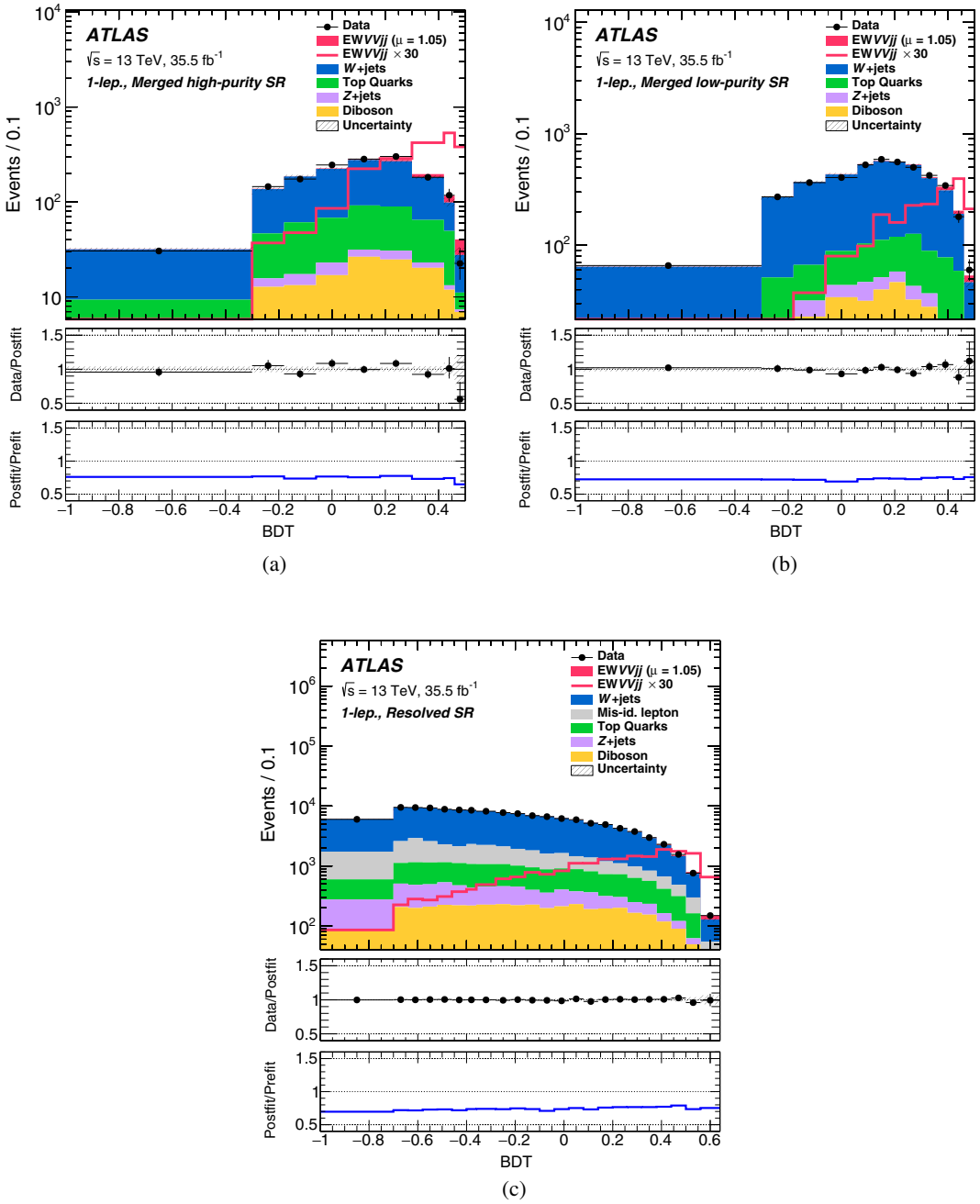

FIG. 5. Comparisons of the observed data and expected distributions of the BDT outputs of the 1-lepton channel signal regions: (a) high-purity and (b) low-purity merged signal regions; (c) the resolved signal region. The background contributions after the global likelihood fit are shown as filled histograms. The signal is shown as a filled histogram on top of the fitted backgrounds normalized to the signal yield extracted from data ($\mu = 1.05$), and unstacked as an unfilled histogram, scaled by the factor indicated in the legend. The entries in overflow are included in the last bin. The middle pane shows the ratios of the observed data to the postfit signal and background predictions. The uncertainty in the total prediction, shown as bands, combines statistical and systematic contributions. The bottom pane shows the ratios of the postfit and prefit background predictions.

reproduced by the predicted contributions in all cases, with the smallest p-value of 0.16 from the χ^2 test [101] being for the m_{jj}^{tag} distribution in the merged high-purity ZCR. The numbers of events observed and estimated in the SRs are summarized in Table VI for the 0-lepton channel, Table VII for the 1-lepton channel, and Table VIII for the 2-lepton channel. The fitted value of the signal strength is

$$\mu_{\text{EW}\,VVjj}^{\text{obs}} = 1.05^{+0.42}_{-0.40} = 1.05 \pm 0.20(\text{stat.})^{+0.37}_{-0.34}(\text{syst.}).$$

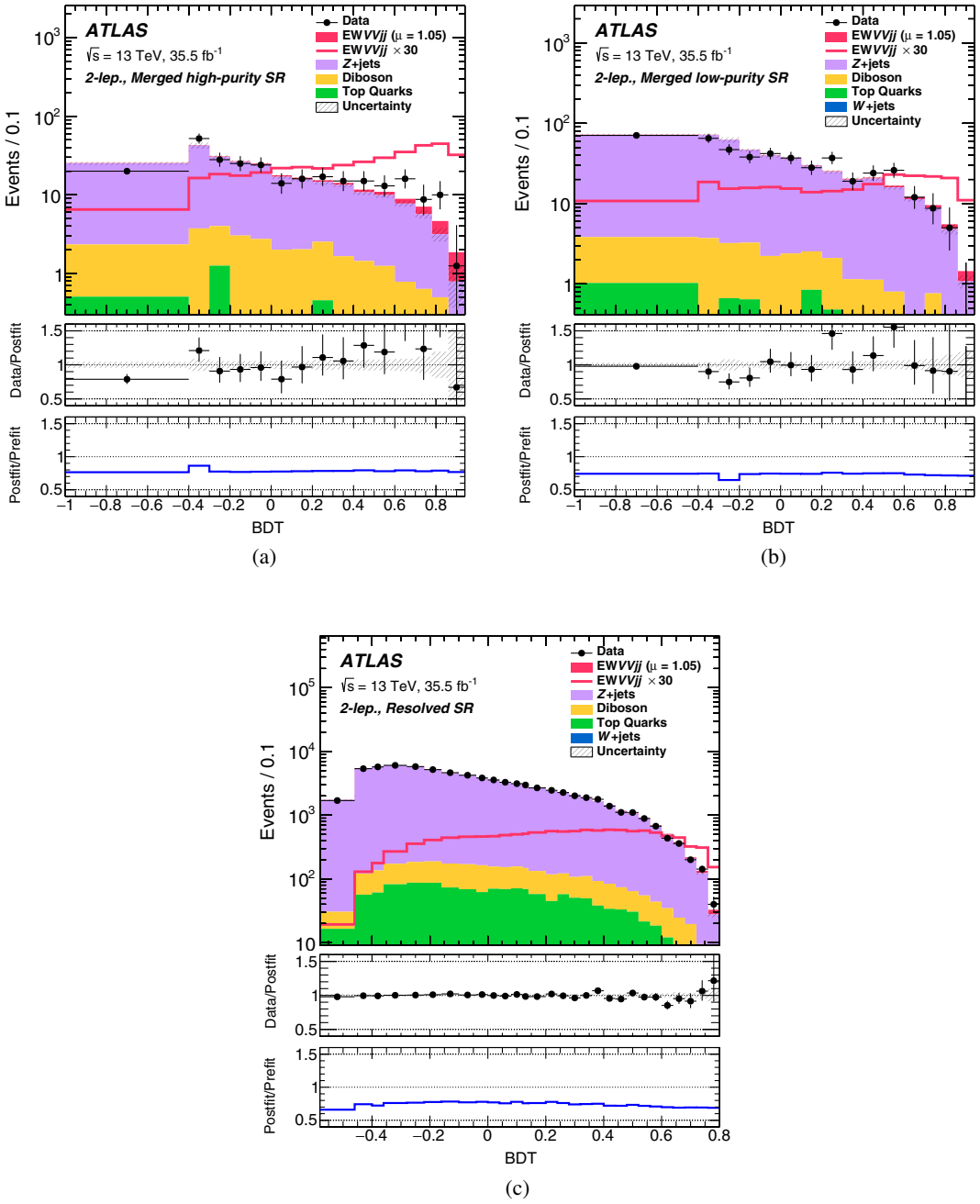

FIG. 6. Comparisons of the observed data and expected distributions of the BDT outputs of the 2-lepton channel signal regions: (a) high-purity and (b) low-purity merged signal regions; (c) the resolved signal region. The background contributions after the global likelihood fit are shown as filled histograms. The signal is shown as a filled histogram on top of the fitted backgrounds normalized to the signal yield extracted from data ($\mu = 1.05$), and unstacked as an unfilled histogram, scaled by the factor indicated in the legend. The entries in overflow are included in the last bin. The middle pane shows the ratios of the observed data to the postfit signal and background predictions. The uncertainty in the total prediction, shown as bands, combines statistical and systematic contributions. The bottom pane shows the ratios of the postfit and prefit background predictions.

The background-only hypothesis is excluded in data with a significance of 2.7 standard deviations, compared with 2.5 standard deviations expected.

Figure 7 shows the measured signal strength from the combined fit with a single signal-strength fit parameter, and from a fit where each lepton channel has its own signal-strength parameter. The probability that the signal strengths measured in the three lepton channels are compatible is 36%.

After the global maximum-likelihood fit, the uncertainties described in Sec. VIII are much reduced. The effects of systematic uncertainties on the measurement after the fit are

TABLE VI. Numbers of events observed and predicted for signal and background processes in the 0-lepton channel signal regions, obtained from signal-plus-background fits to the signal and control regions (Sec. X). The signal yields are calculated after the fit with the observed signal strength of 1.05 applied. The uncertainties combine statistical and systematic contributions. The fit constrains the background estimate towards the observed data, which reduces the total background uncertainty by correlating those uncertainties from the individual backgrounds.

Sample		Resolved	Merged HP	Merged LP
Background	$W+$jets	9200 ± 1300	259 ± 27	582 ± 56
	$Z+$jets	$19\,000 \pm 1400$	383 ± 29	955 ± 69
	Top quarks	3280 ± 480	277 ± 28	276 ± 32
	Diboson	720 ± 120	69 ± 12	68 ± 14
	Total	$32\,100 \pm 2000$	988 ± 50	1881 ± 96
Signal	$W(\ell\nu)W(qq')$	56 ± 22	8.0 ± 3.2	5.4 ± 2.2
	$W(\ell\nu)Z(qq)$	12.0 ± 4.7	2.1 ± 0.8	1.6 ± 0.6
	$Z(\nu\nu)W(qq')$	66 ± 25	9.0 ± 3.5	7.4 ± 2.9
	$Z(\nu\nu)Z(qq)$	27 ± 10	5.1 ± 2.0	3.1 ± 1.2
	Total	161 ± 35	24.3 ± 5.2	17.5 ± 3.9
SM		$32\,300 \pm 2000$	1012 ± 50	1898 ± 96
Data		32 299	1002	1935

TABLE VII. Numbers of events observed and predicted for signal and background processes in the 1-lepton channel signal regions, obtained from signal-plus-background fits to the signal and control regions (Sec. X). The signal yields are calculated after the fit with the observed signal strength of 1.05 applied. The uncertainties combine statistical and systematic contributions. The fit constrains the background estimate towards the observed data, which reduces the total background uncertainty by correlating those uncertainties from the individual backgrounds.

Sample		Resolved	Merged HP	Merged LP
Background	$W+$jets	$69\,100 \pm 1900$	1201 ± 65	2828 ± 97
	$Z+$jets	2770 ± 370	39 ± 3	83 ± 6
	Top quarks	7100 ± 1100	394 ± 56	422 ± 63
	Diboson	2660 ± 600	163 ± 35	229 ± 57
	Multijet	$13\,400 \pm 1600$	⋯	⋯
	Total	$95\,100 \pm 2800$	1797 ± 93	3560 ± 130
Signal	$W(\ell\nu)W(qq')$	330 ± 120	45 ± 17	34 ± 13
	$W(\ell\nu)Z(qq)$	78 ± 29	11 ± 4	5 ± 2
	Total	410 ± 130	57 ± 18	39 ± 13
SM		$95\,500 \pm 2800$	1854 ± 95	3600 ± 130
Data		95 366	1864	3571

TABLE VIII. Numbers of events observed and predicted for signal and background processes in the 2-lepton channel signal regions, obtained from signal-plus-background fits to the signal and control regions (Sec. X). The signal yields are calculated after the fit with the observed signal strength of 1.05 applied. The uncertainties combine statistical and systematic contributions. The fit constrains the background estimate towards the observed data, which reduces the total background uncertainty by correlating those uncertainties from the individual backgrounds.

Sample		Resolved	Merged HP	Merged LP
Background	$Z+$jets	$37\,090 \pm 310$	331 ± 14	775 ± 24
	Top quarks	645 ± 99	5.8 ± 0.9	9.9 ± 2.7
	Diboson	830 ± 170	34.6 ± 7.6	36.7 ± 8.2
	Total	$38\,570 \pm 370$	371 ± 16	821 ± 25
Signal	$Z(\ell\ell)W(qq')$	138 ± 53	8.6 ± 3.3	7.0 ± 2.7
	$Z(\ell\ell)Z(qq)$	46 ± 18	4.3 ± 1.7	2.9 ± 1.1
	Total	185 ± 56	12.9 ± 3.7	9.8 ± 2.9
SM		$38\,760 \pm 370$	384 ± 17	831 ± 25
Data		38 734	371	810

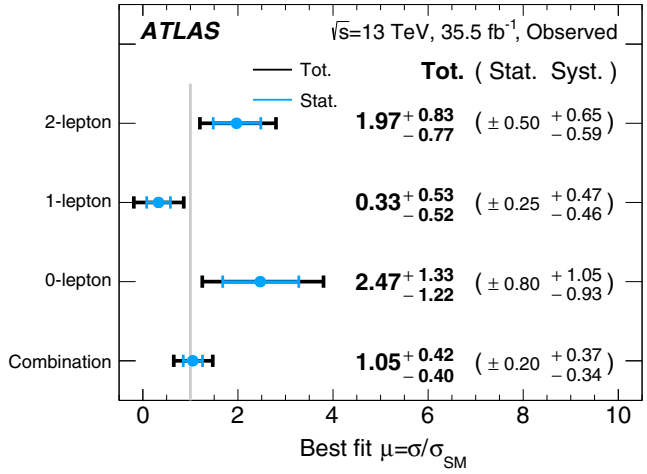

FIG. 7. The fitted values of the signal-strength parameter $\mu^{\text{obs}}_{\text{EW}\,VVjj}$ for the 0-, 1- and 2-lepton channels and their combination. The individual $\mu^{\text{obs}}_{\text{EW}\,VVjj}$ values for the lepton channels are obtained from a simultaneous fit with the signal-strength parameter for each of the lepton channels floating independently. The probability that the signal strengths measured in the three lepton channels are compatible is 36%.

studied using the signal-strength parameter $\mu^{\text{obs}}_{\text{EW}\,VVjj}$. The relative uncertainties in the best-fit $\mu^{\text{obs}}_{\text{EW}\,VVjj}$ value from the leading sources of systematic uncertainty are shown in Table IX. The individual sources of systematic uncertainty

TABLE IX. The symmetrized uncertainty σ_μ from each source in the best-fit signal-strength parameter $\mu^{\text{obs}}_{\text{EW}\,VVjj}$. The floating normalizations include uncertainties of normalization scale factors for $Z+$jets, $W+$jets and top quark contributions.

Uncertainty source	σ_μ
Total uncertainty	0.41
Statistical	0.20
Systematic	0.35
Theoretical and modeling uncertainties	
Floating normalizations	0.09
$Z+$jets	0.13
$W+$jets	0.09
$t\bar{t}$	0.06
Diboson	0.09
Multijet	0.04
Signal	0.07
MC statistics	0.17
Experimental uncertainties	
Large-R jets	0.08
Small-R jets	0.06
Leptons	0.02
$E_{\text{T}}^{\text{miss}}$	0.04
b-tagging	0.07
Pileup	0.04
Luminosity	0.03

TABLE X. Summary of predicted and measured fiducial cross sections for EW $VVjj$ production. The three lepton channels are combined. For the measured fiducial cross sections in the merged and resolved categories, two signal-strength parameters are used in the combined fit, one for the merged category and the other one for the resolved category; while for the measured fiducial cross section in the inclusive fiducial phase space, a single signal-strength parameter is used. For the SM predicted cross section, the error is the theoretical uncertainty (theo.). For the measured cross section, the first error is the statistical uncertainty (stat.), and the second error is the systematic uncertainty (syst.).

Fiducial phase space	Predicted $\sigma^{\text{fid,SM}}_{\text{EW}\,VVjj}$ [fb]	Measured $\sigma^{\text{fid,obs}}_{\text{EW}\,VVjj}$ [fb]
Merged	11.4 ± 0.7 (theo.)	$12.7 \pm 3.8(\text{stat.})^{+4.8}_{-4.2}(\text{syst.})$
Resolved	31.6 ± 1.8 (theo.)	$26.5 \pm 8.2(\text{stat.})^{+17.4}_{-17.1}(\text{syst.})$
Inclusive	43.0 ± 2.4 (theo.)	$45.1 \pm 8.6(\text{stat.})^{+15.9}_{-14.6}(\text{syst.})$

detailed in Sec. VIII are combined into categories. Apart from the statistics of the data, the uncertainties with the largest impact on the sensitivity of EW $VVjj$ production are from the modeling of background ($Z+$jets, $W+$jets and QCD-induced diboson processes), the modeling of the signal, b-tagging, and reconstruction of small-R and large-R jets.

B. Cross-section measurements

The determination of the fiducial cross section is performed by scaling the measured signal strengths with the corresponding SM predicted fiducial cross sections, $\sigma^{\text{fid,obs}}_{\text{EW}\,VVjj} = \mu^{\text{obs}}_{\text{EW}\,VVjj} \cdot \sigma^{\text{fid,SM}}_{\text{EW}\,VVjj}$. It is assumed that there is no new physics that could cause sizable kinematic modifications of the background and signal. Therefore, the only new physics signals that can be detected in an unbiased way are those leading to an enhanced EW $VVjj$ signal strength in the search region of this analysis. The fiducial cross sections for EW $VVjj$ are measured in the merged and resolved fiducial phase-space regions described in Sec. VII and inclusively. The merged HP SR and LP SR are combined to form one single merged fiducial phase-space region. The systematic uncertainties of the measured fiducial cross sections include contributions from experimental systematic uncertainties, theory modeling uncertainties in the backgrounds, theory modeling uncertainties in the shapes of signal kinematic distributions, and luminosity uncertainties. The measured and SM predicted fiducial cross sections for EW $VVjj$ processes are summarized in Table X, where the measured values are obtained from two different simultaneous fits. In the first fit, two signal-strength parameters are used, one for the merged category (both HP and LP), and the other one for the resolved category; while in the second fit, a single signal-strength parameter is used. The measured and SM predicted fiducial cross sections in each lepton channel are

TABLE XI. Summary of predicted and measured fiducial cross sections for EW $VVjj$ production in the three lepton channels. The measured values are obtained from a simultaneous fit where each lepton channel has its own signal-strength parameter, and in each lepton channel the same signal-strength parameter is applied to both the merged and resolved categories. For the SM predicted cross section, the error is the theoretical uncertainty (theo.). For the measured cross section, the first error is the statistical uncertainty (stat.), and the second error is the systematic uncertainty (syst.).

Fiducial phase space		Predicted $\sigma^{\mathrm{fid,SM}}_{\mathrm{EW}\,VVjj}$ [fb]	Measured $\sigma^{\mathrm{fid,obs}}_{\mathrm{EW}\,VVjj}$ [fb]
Merged	0-lepton	4.1 ± 0.3 (theo.)	$10.1 \pm 3.3(\mathrm{stat.})^{+4.2}_{-3.8}(\mathrm{syst.})$
	1-lepton	6.1 ± 0.5 (theo.)	$2.0 \pm 1.5(\mathrm{stat.})^{+2.9}_{-2.8}(\mathrm{syst.})$
	2-lepton	1.2 ± 0.1 (theo.)	$2.4 \pm 0.6(\mathrm{stat.})^{+0.8}_{-0.7}(\mathrm{syst.})$
Resolved	0-lepton	9.2 ± 0.6 (theo.)	$22.8 \pm 7.4(\mathrm{stat.})^{+9.4}_{-8.5}(\mathrm{syst.})$
	1-lepton	16.4 ± 1.0 (theo.)	$5.5 \pm 4.1(\mathrm{stat.})^{+7.7}_{-7.5}(\mathrm{syst.})$
	2-lepton	6.0 ± 0.4 (theo.)	$11.8 \pm 3.0(\mathrm{stat.})^{+3.8}_{-3.5}(\mathrm{syst.})$
Inclusive	0-lepton	13.3 ± 0.8 (theo.)	$32.9 \pm 10.7(\mathrm{stat.})^{+13.5}_{-12.3}(\mathrm{syst.})$
	1-lepton	22.5 ± 1.5 (theo.)	$7.5 \pm 5.6(\mathrm{stat.})^{+10.5}_{-10.2}(\mathrm{syst.})$
	2-lepton	7.2 ± 0.4 (theo.)	$14.2 \pm 3.6(\mathrm{stat.})^{+4.6}_{-4.2}(\mathrm{syst.})$

also reported in Table XI. The measured values are obtained from a simultaneous fit where each lepton channel has its own signal-strength parameter, and in each lepton channel the same signal-strength parameter is applied to both the merged and resolved categories. The predictions are from MadGraph5_aMC@NLO 2.4.3 at LO only, and no higher order corrections are included; the theoretical uncertainties due to the PDF, missing higher-order corrections, and parton-shower modeling are estimated as described in Sec. VIII. The measured fiducial cross sections are generally consistent with the SM predictions.

XI. CONCLUSION

A measurement of $VVjj$ ($V = W,\ Z$) electroweak production using $\sqrt{s} = 13$ TeV pp collisions at the LHC is presented. The data were collected with the ATLAS detector in 2015 and 2016 and correspond to a total integrated luminosity of 35.5 fb^{-1}. The study explores the final states with one boson decaying leptonically, and the other boson decaying into a pair of quarks, identified either as two separate jets or as one large-radius jet.

The $VVjj$ electroweak production cross section is measured with a significance of 2.7 standard deviations over the background-only hypothesis. The expected significance is 2.5 standard deviations. The measured signal strength relative to the leading-order SM prediction is $\mu^{\mathrm{obs}}_{\mathrm{EW}\,VVjj} = 1.05 \pm 0.20(\mathrm{stat.})^{+0.37}_{-0.34}(\mathrm{syst.})$. The fiducial cross section of $VVjj$ electroweak production is measured to be $\sigma^{\mathrm{fid,obs}}_{\mathrm{EW}\,VVjj} = 45.1 \pm 8.6(\mathrm{stat.})^{+15.9}_{-14.6}(\mathrm{syst.})$ fb.

ACKNOWLEDGMENTS

We thank CERN for the very successful operation of the LHC, as well as the support staff from our institutions without whom ATLAS could not be operated efficiently. We acknowledge the support of ANPCyT, Argentina; Yerevan Physics Institute (YerPhI), Armenia; ARC, Australia; BMWFW and FWF, Austria; Azerbaijan National Academy of Sciences (ANAS), Azerbaijan; State Science and Technology Committee (SSTC), Belarus; CNPq and FAPESP, Brazil; NSERC, NRC and CFI, Canada; CERN; CONICYT, Chile; CAS, MOST and NSFC, China; COLCIENCIAS, Colombia; MSMT CR, MPO CR and Committee for Collaboration of the Czech Republic with CERN (VSC CR), Czech Republic; DNRF and Danish Natural Science Research Council (DNSRC), Denmark; IN2P3-CNRS, CEA-DRF/IRFU, France; Shota Rustaveli National Science Foundation of Georgia (SRNSFG), Georgia; BMBF, HGF, and MPG, Germany; GSRT, Greece; RGC, Hong Kong SAR, China; ISF and Benoziyo Center, Israel; INFN, Italy; MEXT and JSPS, Japan; CNRST, Morocco; NWO, Netherlands; Research Council of Norway (RCN), Norway; MNiSW and NCN, Poland; FCT, Portugal; Ministry of National Education, Institute of Atomic Physics (MNE/IFA), Romania; Ministry of Education and Science of the Russian Federation (MES) of Russia and National Research Centre Kurchatov Institute, Russian Federation; JINR; Ministry of Education, Science and Technological Development (MESTD), Serbia; Ministry of Education, Science, Research and Sport (MSSR), Slovakia; ARRS and MIZŠ, Slovenia; DST/NRF, South Africa; MINECO, Spain; Swedish Research Council (SRC) and Wallenberg Foundation, Sweden; Secretariat for Education and Research (SERI), SNSF and Cantons of Bern and Geneva, Switzerland; MOST, Taiwan; TAEK, Turkey; STFC, United Kingdom; DOE and NSF, United States of America. In addition, individual groups and members have received support from BCKDF,

CANARIE, CRC and Compute Canada, Canada; COST, ERC, ERDF, Horizon 2020, and Marie Skłodowska-Curie Actions, European Union; Investissements d' Avenir Labex and Idex, ANR, France; DFG and AvH Foundation, Germany; Herakleitos, Thales and Aristeia programmes co-financed by EU-ESF and the Greek NSRF, Greece; BSF-NSF and GIF, Israel; CERCA Programme Generalitat de Catalunya, Spain; The Royal Society and Leverhulme Trust, United Kingdom. The crucial computing support from all WLCG partners is acknowledged gratefully, in particular from CERN, the ATLAS Tier-1 facilities at TRIUMF (Canada), NDGF (Denmark, Norway, Sweden), CC-IN2P3 (France), KIT/GridKA (Germany), INFN-CNAF (Italy), NL-T1 (Netherlands), PIC (Spain), ASGC (Taiwan), RAL (UK) and BNL (USA), the Tier-2 facilities worldwide and large non-WLCG resource providers. Major contributors of computing resources are listed in Ref. [102].

[1] B. W. Lee, C. Quigg, and H. B. Thacker, Strength of Weak Interactions at Very High Energies and the Higgs Boson Mass, Phys. Rev. Lett. **38**, 883 (1977).
[2] B. W. Lee, C. Quigg, and H. B. Thacker, Weak interactions at very high energies: The role of the Higgs-boson mass, Phys. Rev. D **16**, 1519 (1977).
[3] ATLAS Collaboration, Observation of a new particle in the search for the standard model Higgs boson with the ATLAS detector at the LHC, Phys. Lett. B **716**, 1 (2012).
[4] CMS Collaboration, Observation of a new boson at a mass of 125 GeV with the CMS experiment at the LHC, Phys. Lett. B **716**, 30 (2012).
[5] ATLAS Collaboration, Measurements of the Higgs boson production and decay rates and coupling strengths using pp collision data at $\sqrt{s} = 7$ and 8 TeV in the ATLAS experiment, Eur. Phys. J. C **76**, 6 (2016).
[6] ATLAS Collaboration, Study of the spin and parity of the Higgs boson in diboson decays with the ATLAS detector, Eur. Phys. J. C **75**, 476 (2015); Erratum **76**, 152 (2016).
[7] CMS Collaboration, Precise determination of the mass of the Higgs boson and tests of compatibility of its couplings with the standard model predictions using proton collisions at 7 and 8 TeV, Eur. Phys. J. C **75**, 212 (2015).
[8] CMS Collaboration, Constraints on the spin-parity and anomalous HVV couplings of the Higgs boson in proton collisions at 7 and 8 TeV, Phys. Rev. D **92**, 012004 (2015).
[9] O. J. P. Eboli, M. C. Gonzalez-Garcia, and S. M. Lietti, Bosonic quartic couplings at CERN LHC, Phys. Rev. D **69**, 095005 (2004).
[10] O. J. P. Eboli, M. C. Gonzalez-Garcia, and J. K. Mizukoshi, $pp \to jje^{\pm}\mu^{\pm}\nu\nu$ and $jje^{\pm}\mu^{\mp}\nu\nu$ at $\mathcal{O}(\alpha_{\rm em}^6)$ and $\mathcal{O}(\alpha_{\rm em}^4\alpha_s^2)$ for the study of the quartic electroweak gauge boson vertex at CERN LHC, Phys. Rev. D **74**, 073005 (2006).
[11] J. Chang, K. Cheung, C.-T. Lu, and T.-C. Yuan, WW scattering in the era of post-Higgs-boson discovery, Phys. Rev. D **87**, 093005 (2013).
[12] D. Espriu and B. Yencho, Longitudinal WW scattering in light of the Higgs boson discovery, Phys. Rev. D **87**, 055017 (2013).
[13] V. D. Barger, K. Cheung, T. Han, and R. J. N. Phillips, Strong W^+W^+ scattering signals at pp supercolliders, Phys. Rev. D **42**, 3052 (1990).
[14] CMS Collaboration, Observation of Electroweak Production of Same-Sign W Boson Pairs in the Two Jet and Two Same-Sign Lepton Final State in Proton-Proton Collisions at 13 TeV, Phys. Rev. Lett. **120**, 081801 (2018).
[15] ATLAS Collaboration, Observation of electroweak $W^{\pm}Z$ boson pair production in association with two jets in pp collisions at $\sqrt{s} = 13$ TeV with the ATLAS detector, Phys. Lett. B **793**, 469 (2019).
[16] ATLAS Collaboration, Evidence for Electroweak Production of $W^{\pm}W^{\pm}jj$ in pp Collisions at $\sqrt{s} = 8$ TeV with the ATLAS Detector, Phys. Rev. Lett. **113**, 141803 (2014).
[17] ATLAS Collaboration, Measurements of electroweak Wjj production and constraints on anomalous gauge couplings with the ATLAS detector, Eur. Phys. J. C **77**, 474 (2017).
[18] CMS Collaboration, Study of Vector Boson Scattering and Search for New Physics in Events with Two Same-Sign Leptons and Two Jets, Phys. Rev. Lett. **114**, 051801 (2015).
[19] CMS Collaboration, Measurement of the cross section for electroweak production of $Z\gamma$ in association with two jets and constraints on anomalous quartic gauge couplings in proton-proton collisions at $\sqrt{s} = 8$ TeV, Phys. Lett. B **770**, 380 (2017).
[20] CMS Collaboration, Measurement of electroweak WZ boson production and search for new physics in $WZ+$ two jets events in pp collisions at $\sqrt{s} = 13$ TeV, Phys. Lett. B **795**, 281 (2019).
[21] ATLAS Collaboration, Measurements of $W^{\pm}Z$ production cross sections in pp collisions at $\sqrt{s} = 8$ TeV with the ATLAS detector and limits on anomalous gauge boson self-couplings, Phys. Rev. D **93**, 092004 (2016).
[22] CMS Collaboration, Measurement of vector boson scattering and constraints on anomalous quartic couplings from events with four leptons and two jets in proton-proton collisions at $\sqrt{s} = 13$ TeV, Phys. Lett. B **774**, 682 (2017).
[23] ATLAS Collaboration, Studies of $Z\gamma$ production in association with a high-mass dijet system in pp collisions at $\sqrt{s} = 8$ TeV with the ATLAS detector, J. High Energy Phys. 07 (2017) 107.
[24] CMS Collaboration, Measurement of electroweak-induced production of $W\gamma$ with two jets in pp collisions at $\sqrt{s} =$ 8 TeV and constraints on anomalous quartic gauge couplings, J. High Energy Phys. 06 (2017) 106.

[25] CMS Collaboration, Evidence for exclusive $\gamma\gamma \to W^+W^-$ production and constraints on anomalous quartic gauge couplings in pp collisions at $\sqrt{s} = 7$ and 8 TeV, J. High Energy Phys. 08 (2016) 119.
[26] ATLAS Collaboration, Search for anomalous electroweak production of WW/WZ in association with a high-mass dijet system in pp collisions at $\sqrt{s} = 8$ TeV with the ATLAS detector, Phys. Rev. D **95**, 032001 (2017).
[27] CMS Collaboration, Search for anomalous electroweak production of vector boson pairs in association with two jets in proton-proton collisions at 13 TeV, arXiv:1905.07445.
[28] ATLAS Collaboration, The ATLAS experiment at the CERN large hadron collider, J. Instrum. **3**, S08003 (2008).
[29] ATLAS Collaboration, Performance of the ATLAS trigger system in 2015, Eur. Phys. J. C **77**, 317 (2017).
[30] J. Alwall, R. Frederix, S. Frixione, V. Hirschi, F. Maltoni, O. Mattelaer, H.-S. Shao, T. Stelzer, P. Torrielli, and M. Zaro, The automated computation of tree-level and next-to-leading order differential cross sections, and their matching to parton shower simulations, J. High Energy Phys. 07 (2014) 079.
[31] R. D. Ball *et al.*, Parton distributions with LHC data, Nucl. Phys. **B867**, 244 (2013).
[32] T. Sjöstrand, S. Mrenna, and P. Z. Skands, A brief introduction to PYTHIA 8.1, Comput. Phys. Commun. **178**, 852 (2008).
[33] ATLAS Collaboration, ATLAS Pythia 8 tunes to 7 TeV data, Report No. ATL-PHYS-PUB-2014-021, 2014, https://cds.cern.ch/record/1966419.
[34] T. Gleisberg, S. Höche, F. Krauss, M. Schönherr, S. Schumann, F. Siegert, and J. Winter, , Event generation with SHERPA 1.1, J. High Energy Phys. 02 (2009) 007.
[35] T. Gleisberg and S. Höche, Comix, a new matrix element generator, J. High Energy Phys. 12 (2008) 039.
[36] F. Cascioli, P. Maierhofer, and S. Pozzorini, Scattering Amplitudes with Open Loops, Phys. Rev. Lett. **108**, 111601 (2012).
[37] S. Höche, F. Krauss, M. Schönherr, and F. Siegert, QCD matrix elements + parton showers: The NLO case, J. High Energy Phys. 04 (2013) 027.
[38] R. D. Ball *et al.* (NNPDF Collaboration), Parton distributions for the LHC Run II, J. High Energy Phys. 04 (2015) 040.
[39] P. Nason, A new method for combining NLO QCD with shower Monte Carlo algorithms, J. High Energy Phys. 11 (2004) 040.
[40] S. Frixione, P. Nason, and G. Ridolfi, A positive-weight next-to-leading-order Monte Carlo for heavy flavour hadroproduction, J. High Energy Phys. 09 (2007) 126.
[41] S. Alioli, P. Nason, C. Oleari, and E. Re, A general framework for implementing NLO calculations in shower Monte Carlo programs: The POWHEG BOX, J. High Energy Phys. 06 (2010) 043.
[42] H.-L. Lai, M. Guzzi, J. Huston, Z. Li, P. M. Nadolsky, J. Pumplin, and C.-P. Yuan, New parton distributions for collider physics, Phys. Rev. D **82**, 074024 (2010).
[43] S. Alioli, P. Nason, C. Oleari, and E. Re, NLO single-top production matched with shower in POWHEG: s- and t-channel contributions, J. High Energy Phys. 09 (2009) 111; Erratum, J. High Energy Phys. 02 (2010) 11.
[44] R. Frederix, E. Re, and P. Torrielli, Single-top t-channel hadroproduction in the four-flavour scheme with POWHEG and aMC@NLO, J. High Energy Phys. 09 (2012) 130.
[45] E. Re, Single-top Wt-channel production matched with parton showers using the POWHEG method, Eur. Phys. J. C **71**, 1547 (2011).
[46] P. Artoisenet, R. Frederix, O. Mattelaer, and R. Rietkerk, Automatic spin-entangled decays of heavy resonances in Monte Carlo simulations, J. High Energy Phys. 03 (2013) 015.
[47] T. Sjöstrand, S. Mrenna, and P. Z. Skands, PYTHIA 6.4 physics and manual, J. High Energy Phys. 05 (2006) 026.
[48] J. Pumplin, D. R. Stump, J. Huston, H.-L. Lai, P. Nadolsky, and W.-K. Tung, New generation of parton distributions with uncertainties from global QCD analysis, J. High Energy Phys. 07 (2002) 012.
[49] P. Z. Skands, Tuning Monte Carlo generators: The Perugia tunes, Phys. Rev. D **82**, 074018 (2010).
[50] D. J. Lange, The EvtGen particle decay simulation package, Nucl. Instrum. Methods Phys. Res., Sect. A **462**, 152 (2001).
[51] C. Anastasiou, L. J. Dixon, K. Melnikov, and F. Petriello, High-precision QCD at hadron colliders: Electroweak gauge boson rapidity distributions at next-to-next-to leading order, Phys. Rev. D **69**, 094008 (2004).
[52] S. Höche, F. Krauss, M. Schonherr, and F. Siegert, NLO matrix elements and truncated showers, J. High Energy Phys. 08 (2011) 123.
[53] M. Czakon, P. Fiedler, and A. Mitov, Total Top-Quark Pair-Production Cross Section at Hadron Colliders through $O(\alpha_s^4)$, Phys. Rev. Lett. **110**, 252004 (2013).
[54] M. Czakon and A. Mitov, Top++: A program for the calculation of the top-pair cross-section at hadron colliders, Comput. Phys. Commun. **185**, 2930 (2014).
[55] N. Kidonakis, Next-to-next-to-leading logarithm resummation for s-channel single top quark production, Phys. Rev. D **81**, 054028 (2010).
[56] N. Kidonakis, Two-loop soft anomalous dimensions for single top quark associated production with a W^- or H^-, Phys. Rev. D **82**, 054018 (2010).
[57] ATLAS Collaboration, The ATLAS Simulation Infrastructure, Eur. Phys. J. C **70**, 823 (2010).
[58] S. Agostinelli *et al.*, GEANT4: A simulation toolkit, Nucl. Instrum. Methods Phys. Res., Sect. A **506**, 250 (2003).
[59] ATLAS Collaboration, Summary of ATLAS Pythia 8 tunes, Report No. ATL-PHYS-PUB-2012-003, 2012, https://cds.cern.ch/record/1474107.
[60] A. D. Martin, W. J. Stirling, R. S. Thorne, and G. Watt, Parton distributions for the LHC, Eur. Phys. J. C **63**, 189 (2009).
[61] ATLAS Collaboration, Electron reconstruction and identification in the ATLAS experiment using the 2015 and 2016 LHC proton-proton collision data at $\sqrt{s} = 13$ TeV, arXiv:1902.04655.
[62] ATLAS Collaboration, Muon reconstruction performance of the ATLAS detector in proton-proton collision data at $\sqrt{s} = 13$ TeV, Eur. Phys. J. C **76**, 292 (2016).
[63] ATLAS Collaboration, Topological cell clustering in the ATLAS calorimeters and its performance in LHC Run 1, Eur. Phys. J. C **77**, 490 (2017).

[64] M. Cacciari, G. P. Salam, and G. Soyez, The anti-k_t jet clustering algorithm, J. High Energy Phys. 04 (2008) 063.

[65] M. Cacciari, G. P. Salam, and G. Soyez, FastJet user manual, Eur. Phys. J. C **72**, 1896 (2012).

[66] ATLAS Collaboration, Jet energy scale measurements and their systematic uncertainties in proton-proton collisions at $\sqrt{s} = 13$ TeV with the ATLAS detector, Phys. Rev. D **96**, 072002 (2017).

[67] ATLAS Collaboration, Performance of pile-up mitigation techniques for jets in pp collisions at $\sqrt{s} = 8$ TeV using the ATLAS detector, Eur. Phys. J. C **76**, 581 (2016).

[68] M. Cacciari and G. P. Salam, Pileup subtraction using jet areas, Phys. Lett. B **659**, 119 (2008).

[69] ATLAS Collaboration, Performance of b-jet identification in the ATLAS experiment, J. Instrum. **11**, P04008 (2016).

[70] ATLAS Collaboration, Optimisation of the ATLAS b-tagging performance for the 2016 LHC run, Report No. ATL-PHYS-PUB-2016-012, 2016, https://cds.cern.ch/record/2160731.

[71] D. Krohn, J. Thaler, and L.-T. Wang, Jet trimming, J. High Energy Phys. 02 (2010) 084.

[72] S. D. Ellis and D. E. Soper, Successive combination jet algorithm for hadron collisions, Phys. Rev. D **48**, 3160 (1993).

[73] ATLAS Collaboration, Performance of jet substructure techniques for large-R jets in proton-proton collisions at $\sqrt{s} = 7$ TeV using the ATLAS detector, J. High Energy Phys. 09 (2013) 076.

[74] ATLAS Collaboration, Jet mass reconstruction with the ATLAS Detector in early Run 2 data, Report No. ATLAS-CONF-2016-035, 2016, https://cds.cern.ch/record/2200211.

[75] ATLAS Collaboration, Flavor tagging with track-jets in boosted topologies with the ATLAS detector, Report No. ATL-PHYS-PUB-2014-013, 2014, https://cds.cern.ch/record/1750681.

[76] A. J. Larkoski, I. Moult, and D. Neill, Power counting to better jet observables, J. High Energy Phys. 12 (2014) 009.

[77] A. J. Larkoski, I. Moult, and D. Neill, Analytic boosted boson discrimination, J. High Energy Phys. 05 (2016) 117.

[78] ATLAS Collaboration, Performance of top-quark and W-boson tagging with ATLAS in Run 2 of the LHC, Eur. Phys. J. C **79**, 375 (2019).

[79] ATLAS Collaboration, Performance of missing transverse momentum reconstruction with the ATLAS detector using proton-proton collisions at $\sqrt{s} = 13$ TeV, Eur. Phys. J. C **78**, 903 (2018).

[80] ATLAS Collaboration, Searches for heavy ZZ and ZW resonances in the $\ell\ell qq$ and $\nu\nu qq$ final states in pp collisions at $\sqrt{s} = 13$ TeV with the ATLAS detector, J. High Energy Phys. 03 (2018) 009.

[81] ATLAS Collaboration, Search for WW/WZ resonance production in $\ell\nu qq$ final states in pp collisions at $\sqrt{s} =$ 13 TeV with the ATLAS detector, J. High Energy Phys. 03 (2018) 042.

[82] A. Hoecker *et al.*, TMVA: Toolkit for multivariate data analysis, arXiv:physics/0703039.

[83] ATLAS Collaboration, Evidence for the $H \to b\bar{b}$ decay with the ATLAS detector, J. High Energy Phys. 12 (2017) 024.

[84] ATLAS Collaboration, Discrimination between light quark and gluon jets in pp collisions at $\sqrt{s} = 8$ TeV with the ATLAS Detector, Report No. ATLAS-CONF-2016-034, 2016, https://cds.cern.ch/record/2200202.

[85] ATLAS Collaboration, Proposal for particle-level object and observable definitions for use in physics measurements at the LHC, Report No. ATL-PHYS-PUB-2015-013, 2015, https://cds.cern.ch/record/2022743.

[86] ATLAS Collaboration, Luminosity determination in pp collisions at $\sqrt{s} = 8$ TeV using the ATLAS detector at the LHC, Eur. Phys. J. C **76**, 653 (2016).

[87] G. Avoni *et al.*, The new LUCID-2 detector for luminosity measurement and monitoring in ATLAS, J. Instrum. **13**, P07017 (2018).

[88] ATLAS Collaboration, Measurement of the Inelastic Proton-Proton Cross Section at $\sqrt{s} = 13$ TeV with the ATLAS Detector at the LHC, Phys. Rev. Lett. **117**, 182002 (2016).

[89] ATLAS Collaboration, Electron and photon energy calibration with the ATLAS detector using 2015–2016 LHC proton-proton collision data, J. Instrum. **14**, P03017 (2019).

[90] ATLAS Collaboration, Commissioning of the ATLAS b-tagging algorithms using $t\bar{t}$ events in early Run 2 data, Report No. ATL-PHYS-PUB-2015-039, 2015, https://cds.cern.ch/record/2047871.

[91] ATLAS Collaboration, Expected performance of the ATLAS b-tagging algorithms in Run-2, Report No. ATL-PHYS-PUB-2015-022, 2015, https://cds.cern.ch/record/2037697.

[92] J. Gao, M. Guzzi, J. Huston, H.-L. Lai, Z. Li, P. Nadolsky, J. Pumplin, D. Stump, and C.-P. Yuan, CT10 next-to-next-to-leading order global analysis of QCD, Phys. Rev. D **89**, 033009 (2014).

[93] L. A. Harland-Lang, A. D. Martin, P. Motylinski, and R. S. Thorne, Parton distributions in the LHC era: MMHT 2014 PDFs, Eur. Phys. J. C **75**, 204 (2015).

[94] ATLAS Collaboration, Measurement of the cross-section for producing a W boson in association with a single top quark in pp collisions at $\sqrt{s} = 13$ TeV with ATLAS, J. High Energy Phys. 01 (2018) 063.

[95] G. Corcella, I. G. Knowles, G. Marchesini, S. Moretti, K. Odagiri, P. Richardson, M. H. Seymour, and B. R. Webber, HERWIG 6: An event generator for hadron emission reactions with interfering gluons (including supersymmetric processes), J. High Energy Phys. 01 (2001) 010.

[96] S. Gieseke, C. Rohr, and A. Siodmok, Colour reconnections in Herwig++, Eur. Phys. J. C **72**, 2225 (2012).

[97] ATLAS Collaboration, Combined search for the Standard Model Higgs boson in pp collisions at $\sqrt{s} = 7$ TeV with the ATLAS detector, Phys. Rev. D **86**, 032003 (2012).

[98] W. Verkerke and D. P. Kirkby, The RooFit toolkit for data modeling, arXiv:physics/0306116.

[99] L. Moneta, K. Belasco, K. Cranmer, S. Kreiss, A. Lazzaro, D. Piparo, G. Schott, W. Verkerke, M. Wolf, The RooStats Project, Proc. Sci., ACAT2010 (**2010**) 057 [arXiv:1009.1003].

[100] ATLAS Collaboration, Procedure for the LHC Higgs boson search combination in summer 2011, Report No. ATL-PHYS-PUB-2011-011, 2011, https://cds.cern.ch/record/1375842.

[101] N. D. Gagunashvili, Comparison of weighted and unweighted histograms, Proc. Sci., ACAT2007 (**2007**) 054 [arXiv:physics/0605123].

[102] ATLAS Collaboration, ATLAS computing acknowledgements, Report No. ATL-GEN-PUB-2016-002, https://cds.cern.ch/record/2202407.

G. Aad,[101] B. Abbott,[128] D. C. Abbott,[102] O. Abdinov,[13,a] A. Abed Abud,[70a,70b] K. Abeling,[53] D. K. Abhayasinghe,[93] S. H. Abidi,[167] O. S. AbouZeid,[40] N. L. Abraham,[156] H. Abramowicz,[161] H. Abreu,[160] Y. Abulaiti,[6] B. S. Acharya,[66a,66b,b] B. Achkar,[53] S. Adachi,[163] L. Adam,[99] C. Adam Bourdarios,[132] L. Adamczyk,[83a] L. Adamek,[167] J. Adelman,[121] M. Adersberger,[114] A. Adiguzel,[12c,c] S. Adorni,[54] T. Adye,[144] A. A. Affolder,[146] Y. Afik,[160] C. Agapopoulou,[132] M. N. Agaras,[38] A. Aggarwal,[119] C. Agheorghiesei,[27c] J. A. Aguilar-Saavedra,[140f,140a,d] F. Ahmadov,[79] X. Ai,[15a] G. Aielli,[73a,73b] S. Akatsuka,[85] T. P. A. Åkesson,[96] E. Akilli,[54] A. V. Akimov,[110] K. Al Khoury,[132] G. L. Alberghi,[23b,23a] J. Albert,[176] M. J. Alconada Verzini,[88] S. Alderweireldt,[119] M. Aleksa,[36] I. N. Aleksandrov,[79] C. Alexa,[27b] D. Alexandre,[19] T. Alexopoulos,[10] A. Alfonsi,[120] M. Alhroob,[128] B. Ali,[142] G. Alimonti,[68a] J. Alison,[37] S. P. Alkire,[148] C. Allaire,[132] B. M. M. Allbrooke,[156] B. W. Allen,[131] P. P. Allport,[21] A. Aloisio,[69a,69b] A. Alonso,[40] F. Alonso,[88] C. Alpigiani,[148] A. A. Alshehri,[57] M. Alvarez Estevez,[98] B. Alvarez Gonzalez,[36] D. Álvarez Piqueras,[174] M. G. Alviggi,[69a,69b] Y. Amaral Coutinho,[80b] A. Ambler,[103] L. Ambroz,[135] C. Amelung,[26] D. Amidei,[105] S. P. Amor Dos Santos,[140a] S. Amoroso,[46] C. S. Amrouche,[54] F. An,[78] C. Anastopoulos,[149] N. Andari,[145] T. Andeen,[11] C. F. Anders,[61b] J. K. Anders,[20] A. Andreazza,[68a,68b] V. Andrei,[61a] C. R. Anelli,[176] S. Angelidakis,[38] A. Angerami,[39] A. V. Anisenkov,[122b,122a] A. Annovi,[71a] C. Antel,[61a] M. T. Anthony,[149] M. Antonelli,[51] D. J. A. Antrim,[171] F. Anulli,[72a] M. Aoki,[81] J. A. Aparisi Pozo,[174] L. Aperio Bella,[36] G. Arabidze,[106] J. P. Araque,[140a] V. Araujo Ferraz,[80b] R. Araujo Pereira,[80b] C. Arcangeletti,[51] A. T. H. Arce,[49] F. A. Arduh,[88] J-F. Arguin,[109] S. Argyropoulos,[77] J.-H. Arling,[46] A. J. Armbruster,[36] L. J. Armitage,[92] A. Armstrong,[171] O. Arnaez,[167] H. Arnold,[120] A. Artamonov,[111,a] G. Artoni,[135] S. Artz,[99] S. Asai,[163] N. Asbah,[59] E. M. Asimakopoulou,[172] L. Asquith,[156] K. Assamagan,[29] R. Astalos,[28a] R. J. Atkin,[33a] M. Atkinson,[173] N. B. Atlay,[151] H. Atmani,[132] K. Augsten,[142] G. Avolio,[36] R. Avramidou,[60a] M. K. Ayoub,[15a] A. M. Azoulay,[168b] G. Azuelos,[109,e] M. J. Baca,[21] H. Bachacou,[145] K. Bachas,[67a,67b] M. Backes,[135] F. Backman,[45a,45b] P. Bagnaia,[72a,72b] M. Bahmani,[84] H. Bahrasemani,[152] A. J. Bailey,[174] V. R. Bailey,[173] J. T. Baines,[144] M. Bajic,[40] C. Bakalis,[10] O. K. Baker,[183] P. J. Bakker,[120] D. Bakshi Gupta,[8] S. Balaji,[157] E. M. Baldin,[122b,122a] P. Balek,[180] F. Balli,[145] W. K. Balunas,[135] J. Balz,[99] E. Banas,[84] A. Bandyopadhyay,[24] Sw. Banerjee,[181,f] A. A. E. Bannoura,[182] L. Barak,[161] W. M. Barbe,[38] E. L. Barberio,[104] D. Barberis,[55b,55a] M. Barbero,[101] T. Barillari,[115] M-S. Barisits,[36] J. Barkeloo,[131] T. Barklow,[153] R. Barnea,[160] S. L. Barnes,[60c] B. M. Barnett,[144] R. M. Barnett,[18] Z. Barnovska-Blenessy,[60a] A. Baroncelli,[60a] G. Barone,[29] A. J. Barr,[135] L. Barranco Navarro,[174] F. Barreiro,[98] J. Barreiro Guimarães da Costa,[15a] S. Barsov,[138] R. Bartoldus,[153] G. Bartolini,[101] A. E. Barton,[89] P. Bartos,[28a] A. Basalaev,[46] A. Bassalat,[132,g] R. L. Bates,[57] S. J. Batista,[167] S. Batlamous,[35e] J. R. Batley,[32] B. Batool,[151] M. Battaglia,[146] M. Bauce,[72a,72b] F. Bauer,[145] K. T. Bauer,[171] H. S. Bawa,[31,h] J. B. Beacham,[49] T. Beau,[136] P. H. Beauchemin,[170] F. Becherer,[52] P. Bechtle,[24] H. C. Beck,[53] H. P. Beck,[20,i] K. Becker,[52] M. Becker,[99] C. Becot,[46] A. Beddall,[12d] A. J. Beddall,[12a] V. A. Bednyakov,[79] M. Bedognetti,[120] C. P. Bee,[155] T. A. Beermann,[76] M. Begalli,[80b] M. Begel,[29] A. Behera,[155] J. K. Behr,[46] F. Beisiegel,[24] A. S. Bell,[94] G. Bella,[161] L. Bellagamba,[23b] A. Bellerive,[34] P. Bellos,[9] K. Beloborodov,[122b,122a] K. Belotskiy,[112] N. L. Belyaev,[112] D. Benchekroun,[35a] N. Benekos,[10] Y. Benhammou,[161] D. P. Benjamin,[6] M. Benoit,[54] J. R. Bensinger,[26] S. Bentvelsen,[120] L. Beresford,[135] M. Beretta,[51] D. Berge,[46] E. Bergeaas Kuutmann,[172] N. Berger,[5] B. Bergmann,[142] L. J. Bergsten,[26] J. Beringer,[18] S. Berlendis,[7] N. R. Bernard,[102] G. Bernardi,[136] C. Bernius,[153] F. U. Bernlochner,[24] T. Berry,[93] P. Berta,[99] C. Bertella,[15a] I. A. Bertram,[89] G. J. Besjes,[40] O. Bessidskaia Bylund,[182] N. Besson,[145] A. Bethani,[100] S. Bethke,[115] A. Betti,[24] A. J. Bevan,[92] J. Beyer,[115] R. Bi,[139] R. M. Bianchi,[139] O. Biebel,[114] D. Biedermann,[19] R. Bielski,[36] K. Bierwagen,[99] N. V. Biesuz,[71a,71b] M. Biglietti,[74a] T. R. V. Billoud,[109] M. Bindi,[53] A. Bingul,[12d] C. Bini,[72a,72b] S. Biondi,[23b,23a] M. Birman,[180] T. Bisanz,[53] J. P. Biswal,[161] A. Bitadze,[100] C. Bittrich,[48] K. Bjørke,[134] K. M. Black,[25] T. Blazek,[28a] I. Bloch,[46] C. Blocker,[26] A. Blue,[57] U. Blumenschein,[92] G. J. Bobbink,[120] V. S. Bobrovnikov,[122b,122a] S. S. Bocchetta,[96] A. Bocci,[49] D. Boerner,[46] D. Bogavac,[14] A. G. Bogdanchikov,[122b,122a] C. Bohm,[45a] V. Boisvert,[93] P. Bokan,[53,172] T. Bold,[83a] A. S. Boldyrev,[113] A. E. Bolz,[61b] M. Bomben,[136] M. Bona,[92] J. S. Bonilla,[131] M. Boonekamp,[145] H. M. Borecka-Bielska,[90] A. Borisov,[123] G. Borissov,[89] J. Bortfeldt,[36] D. Bortoletto,[135] V. Bortolotto,[73a,73b] D. Boscherini,[23b] M. Bosman,[14] J. D. Bossio Sola,[103] K. Bouaouda,[35a]

J. Boudreau,[139] E. V. Bouhova-Thacker,[89] D. Boumediene,[38] S. K. Boutle,[57] A. Boveia,[126] J. Boyd,[36] D. Boye,[33b,j] I. R. Boyko,[79] A. J. Bozson,[93] J. Bracinik,[21] N. Brahimi,[101] G. Brandt,[182] O. Brandt,[61a] F. Braren,[46] B. Brau,[102] J. E. Brau,[131] W. D. Breaden Madden,[57] K. Brendlinger,[46] L. Brenner,[46] R. Brenner,[172] S. Bressler,[180] B. Brickwedde,[99] D. L. Briglin,[21] D. Britton,[57] D. Britzger,[115] I. Brock,[24] R. Brock,[106] G. Brooijmans,[39] W. K. Brooks,[147b] E. Brost,[121] J. H Broughton,[21] P. A. Bruckman de Renstrom,[84] D. Bruncko,[28b] A. Bruni,[23b] G. Bruni,[23b] L. S. Bruni,[120] S. Bruno,[73a,73b] B. H. Brunt,[32] M. Bruschi,[23b] N. Bruscino,[139] P. Bryant,[37] L. Bryngemark,[96] T. Buanes,[17] Q. Buat,[36] P. Buchholz,[151] A. G. Buckley,[57] I. A. Budagov,[79] M. K. Bugge,[134] F. Bührer,[52] O. Bulekov,[112] T. J. Burch,[121] S. Burdin,[90] C. D. Burgard,[120] A. M. Burger,[129] B. Burghgrave,[8] K. Burka,[84] J. T. P. Burr,[46] V. Büscher,[99] E. Buschmann,[53] P. J. Bussey,[57] J. M. Butler,[25] C. M. Buttar,[57] J. M. Butterworth,[94] P. Butti,[36] W. Buttinger,[36] A. Buzatu,[158] A. R. Buzykaev,[122b,122a] G. Cabras,[23b,23a] S. Cabrera Urbán,[174] D. Caforio,[56] H. Cai,[173] V. M. M. Cairo,[153] O. Cakir,[4a] N. Calace,[36] P. Calafiura,[18] A. Calandri,[101] G. Calderini,[136] P. Calfayan,[65] G. Callea,[57] L. P. Caloba,[80b] S. Calvente Lopez,[98] D. Calvet,[38] S. Calvet,[38] T. P. Calvet,[155] M. Calvetti,[71a,71b] R. Camacho Toro,[136] S. Camarda,[36] D. Camarero Munoz,[98] P. Camarri,[73a,73b] D. Cameron,[134] R. Caminal Armadans,[102] C. Camincher,[36] S. Campana,[36] M. Campanelli,[94] A. Camplani,[40] A. Campoverde,[151] V. Canale,[69a,69b] A. Canesse,[103] M. Cano Bret,[60c] J. Cantero,[129] T. Cao,[161] Y. Cao,[173] M. D. M. Capeans Garrido,[36] M. Capua,[41b,41a] R. Cardarelli,[73a] F. C. Cardillo,[149] I. Carli,[143] T. Carli,[36] G. Carlino,[69a] B. T. Carlson,[139] L. Carminati,[68a,68b] R. M. D. Carney,[45a,45b] S. Caron,[119] E. Carquin,[147b] S. Carrá,[68a,68b] J. W. S. Carter,[167] M. P. Casado,[14,k] A. F. Casha,[167] D. W. Casper,[171] R. Castelijn,[120] F. L. Castillo,[174] V. Castillo Gimenez,[174] N. F. Castro,[140a,140e] A. Catinaccio,[36] J. R. Catmore,[134] A. Cattai,[36] J. Caudron,[24] V. Cavaliere,[29] E. Cavallaro,[14] D. Cavalli,[68a] M. Cavalli-Sforza,[14] V. Cavasinni,[71a,71b] E. Celebi,[12b] F. Ceradini,[74a,74b] L. Cerda Alberich,[174] A. S. Cerqueira,[80a] A. Cerri,[156] L. Cerrito,[73a,73b] F. Cerutti,[18] A. Cervelli,[23b,23a] S. A. Cetin,[12b] D. Chakraborty,[121] S. K. Chan,[59] W. S. Chan,[120] W. Y. Chan,[90] J. D. Chapman,[32] B. Chargeishvili,[159b] D. G. Charlton,[21] T. P. Charman,[92] C. C. Chau,[34] S. Che,[126] A. Chegwidden,[106] S. Chekanov,[6] S. V. Chekulaev,[168a] G. A. Chelkov,[79,l] M. A. Chelstowska,[36] B. Chen,[78] C. Chen,[60a] C. H. Chen,[78] H. Chen,[29] J. Chen,[60a] J. Chen,[39] S. Chen,[137] S. J. Chen,[15c] X. Chen,[15b,m] Y. Chen,[82] Y-H. Chen,[46] H. C. Cheng,[63a] H. J. Cheng,[15a,15d] A. Cheplakov,[79] E. Cheremushkina,[123] R. Cherkaoui El Moursli,[35e] E. Cheu,[7] K. Cheung,[64] T. J. A. Chevalérias,[145] L. Chevalier,[145] V. Chiarella,[51] G. Chiarelli,[71a] G. Chiodini,[67a] A. S. Chisholm,[36,21] A. Chitan,[27b] I. Chiu,[163] Y. H. Chiu,[176] M. V. Chizhov,[79] K. Choi,[65] A. R. Chomont,[72a,72b] S. Chouridou,[162] Y. S. Chow,[120] M. C. Chu,[63a] J. Chudoba,[141] A. J. Chuinard,[103] J. J. Chwastowski,[84] L. Chytka,[130] K. M. Ciesla,[84] D. Cinca,[47] V. Cindro,[91] I. A. Cioară,[27b] A. Ciocio,[18] F. Cirotto,[69a,69b] Z. H. Citron,[180] M. Citterio,[68a] D. A. Ciubotaru,[27b] B. M. Ciungu,[167] A. Clark,[54] M. R. Clark,[39] P. J. Clark,[50] C. Clement,[45a,45b] Y. Coadou,[101] M. Cobal,[66a,66c] A. Coccaro,[55b] J. Cochran,[78] H. Cohen,[161] A. E. C. Coimbra,[36] L. Colasurdo,[119] B. Cole,[39] A. P. Colijn,[120] J. Collot,[58] P. Conde Muiño,[140a,n] E. Coniavitis,[52] S. H. Connell,[33b] I. A. Connelly,[57] S. Constantinescu,[27b] F. Conventi,[69a,o] A. M. Cooper-Sarkar,[135] F. Cormier,[175] K. J. R. Cormier,[167] L. D. Corpe,[94] M. Corradi,[72a,72b] E. E. Corrigan,[96] F. Corriveau,[103,p] A. Cortes-Gonzalez,[36] M. J. Costa,[174] F. Costanza,[5] D. Costanzo,[149] G. Cowan,[93] J. W. Cowley,[32] J. Crane,[100] K. Cranmer,[124] S. J. Crawley,[57] R. A. Creager,[137] S. Crépé-Renaudin,[58] F. Crescioli,[136] M. Cristinziani,[24] V. Croft,[120] G. Crosetti,[41b,41a] A. Cueto,[5] T. Cuhadar Donszelmann,[149] A. R. Cukierman,[153] S. Czekierda,[84] P. Czodrowski,[36] M. J. Da Cunha Sargedas De Sousa,[60b] J. V. Da Fonseca Pinto,[80b] C. Da Via,[100] W. Dabrowski,[83a] T. Dado,[28a] S. Dahbi,[35e] T. Dai,[105] C. Dallapiccola,[102] M. Dam,[40] G. D'amen,[23b,23a] V. D'Amico,[74a,74b] J. Damp,[99] J. R. Dandoy,[137] M. F. Daneri,[30] N. P. Dang,[181,f] N. D Dann,[100] M. Danninger,[175] V. Dao,[36] G. Darbo,[55b] O. Dartsi,[5] A. Dattagupta,[131] T. Daubney,[46] S. D'Auria,[68a,68b] W. Davey,[24] C. David,[46] T. Davidek,[143] D. R. Davis,[49] E. Dawe,[104] I. Dawson,[149] K. De,[8] R. De Asmundis,[69a] M. De Beurs,[120] S. De Castro,[23b,23a] S. De Cecco,[72a,72b] N. De Groot,[119] P. de Jong,[120] H. De la Torre,[106] A. De Maria,[15c] D. De Pedis,[72a] A. De Salvo,[72a] U. De Sanctis,[73a,73b] M. De Santis,[73a,73b] A. De Santo,[156] K. De Vasconcelos Corga,[101] J. B. De Vivie De Regie,[132] C. Debenedetti,[146] D. V. Dedovich,[79] A. M. Deiana,[42] M. Del Gaudio,[41b,41a] J. Del Peso,[98] Y. Delabat Diaz,[46] D. Delgove,[132] F. Deliot,[145] C. M. Delitzsch,[7] M. Della Pietra,[69a,69b] D. Della Volpe,[54] A. Dell'Acqua,[36] L. Dell'Asta,[73a,73b] M. Delmastro,[5] C. Delporte,[132] P. A. Delsart,[58] D. A. DeMarco,[167] S. Demers,[183] M. Demichev,[79] G. Demontigny,[109] S. P. Denisov,[123] D. Denysiuk,[120] L. D'Eramo,[136] D. Derendarz,[84] J. E. Derkaoui,[35d] F. Derue,[136] P. Dervan,[90] K. Desch,[24] C. Deterre,[46] K. Dette,[167] C. Deutsch,[24] M. R. Devesa,[30] P. O. Deviveiros,[36] A. Dewhurst,[144] S. Dhaliwal,[26] F. A. Di Bello,[54] A. Di Ciaccio,[73a,73b] L. Di Ciaccio,[5] W. K. Di Clemente,[137] C. Di Donato,[69a,69b] A. Di Girolamo,[36] G. Di Gregorio,[71a,71b] B. Di Micco,[74a,74b] R. Di Nardo,[102] K. F. Di Petrillo,[59] R. Di Sipio,[167] D. Di Valentino,[34] C. Diaconu,[101] F. A. Dias,[40] T. Dias Do Vale,[140a] M. A. Diaz,[147a] J. Dickinson,[18] E. B. Diehl,[105]

J. Dietrich,[19] S. Díez Cornell,[46] A. Dimitrievska,[18] W. Ding,[15b] J. Dingfelder,[24] F. Dittus,[36] F. Djama,[101] T. Djobava,[159b] J. I. Djuvsland,[17] M. A. B. Do Vale,[80c] M. Dobre,[27b] D. Dodsworth,[26] C. Doglioni,[96] J. Dolejsi,[143] Z. Dolezal,[143] M. Donadelli,[80d] J. Donini,[38] A. D'onofrio,[92] M. D'Onofrio,[90] J. Dopke,[144] A. Doria,[69a] M. T. Dova,[88] A. T. Doyle,[57] E. Drechsler,[152] E. Dreyer,[152] T. Dreyer,[53] A. S. Drobac,[170] Y. Duan,[60b] F. Dubinin,[110] M. Dubovsky,[28a] A. Dubreuil,[54] E. Duchovni,[180] G. Duckeck,[114] A. Ducourthial,[136] O. A. Ducu,[109] D. Duda,[115] A. Dudarev,[36] A. C. Dudder,[99] E. M. Duffield,[18] L. Duflot,[132] M. Dührssen,[36] C. Dülsen,[182] M. Dumancic,[180] A. E. Dumitriu,[27b] A. K. Duncan,[57] M. Dunford,[61a] A. Duperrin,[101] H. Duran Yildiz,[4a] M. Düren,[56] A. Durglishvili,[159b] D. Duschinger,[48] B. Dutta,[46] D. Duvnjak,[1] G. I. Dyckes,[137] M. Dyndal,[36] S. Dysch,[100] B. S. Dziedzic,[84] K. M. Ecker,[115] R. C. Edgar,[105] T. Eifert,[36] G. Eigen,[17] K. Einsweiler,[18] T. Ekelof,[172] M. El Kacimi,[35c] R. El Kosseifi,[101] V. Ellajosyula,[172] M. Ellert,[172] F. Ellinghaus,[182] A. A. Elliot,[92] N. Ellis,[36] J. Elmsheuser,[29] M. Elsing,[36] D. Emeliyanov,[144] A. Emerman,[39] Y. Enari,[163] J. S. Ennis,[178] M. B. Epland,[49] J. Erdmann,[47] A. Ereditato,[20] M. Errenst,[36] M. Escalier,[132] C. Escobar,[174] O. Estrada Pastor,[174] E. Etzion,[161] H. Evans,[65] A. Ezhilov,[138] F. Fabbri,[57] L. Fabbri,[23b,23a] V. Fabiani,[119] G. Facini,[94] R. M. Faisca Rodrigues Pereira,[140a] R. M. Fakhrutdinov,[123] S. Falciano,[72a] P. J. Falke,[5] S. Falke,[5] J. Faltova,[143] Y. Fang,[15a] Y. Fang,[15a] G. Fanourakis,[44] M. Fanti,[68a,68b] A. Farbin,[8] A. Farilla,[74a] E. M. Farina,[70a,70b] T. Farooque,[106] S. Farrell,[18] S. M. Farrington,[178] P. Farthouat,[36] F. Fassi,[35e] P. Fassnacht,[36] D. Fassouliotis,[9] M. Faucci Giannelli,[50] W. J. Fawcett,[32] L. Fayard,[132] O. L. Fedin,[138,q] W. Fedorko,[175] M. Feickert,[42] S. Feigl,[134] L. Feligioni,[101] A. Fell,[149] C. Feng,[60b] E. J. Feng,[36] M. Feng,[49] M. J. Fenton,[57] A. B. Fenyuk,[123] J. Ferrando,[46] A. Ferrante,[173] A. Ferrari,[172] P. Ferrari,[120] R. Ferrari,[70a] D. E. Ferreira de Lima,[61b] A. Ferrer,[174] D. Ferrere,[54] C. Ferretti,[105] F. Fiedler,[99] A. Filipčič,[91] F. Filthaut,[119] K. D. Finelli,[25] M. C. N. Fiolhais,[140a] L. Fiorini,[174] F. Fischer,[114] W. C. Fisher,[106] I. Fleck,[151] P. Fleischmann,[105] R. R. M. Fletcher,[137] T. Flick,[182] B. M. Flierl,[114] L. F. Flores,[137] L. R. Flores Castillo,[63a] F. M. Follega,[75a,75b] N. Fomin,[17] G. T. Forcolin,[75a,75b] A. Formica,[145] F. A. Förster,[14] A. C. Forti,[100] A. G. Foster,[21] M. G. Foti,[135] D. Fournier,[132] H. Fox,[89] P. Francavilla,[71a,71b] S. Francescato,[72a,72b] M. Franchini,[23b,23a] S. Franchino,[61a] D. Francis,[36] L. Franconi,[20] M. Franklin,[59] A. N. Fray,[92] B. Freund,[109] W. S. Freund,[80b] E. M. Freundlich,[47] D. C. Frizzell,[128] D. Froidevaux,[36] J. A. Frost,[135] C. Fukunaga,[164] E. Fullana Torregrosa,[174] E. Fumagalli,[55b,55a] T. Fusayasu,[116] J. Fuster,[174] A. Gabrielli,[23b,23a] A. Gabrielli,[18] G. P. Gach,[83a] S. Gadatsch,[54] P. Gadow,[115] G. Gagliardi,[55b,55a] L. G. Gagnon,[109] C. Galea,[27b] B. Galhardo,[140a] G. E. Gallardo,[135] E. J. Gallas,[135] B. J. Gallop,[144] P. Gallus,[142] G. Galster,[40] R. Gamboa Goni,[92] K. K. Gan,[126] S. Ganguly,[180] J. Gao,[60a] Y. Gao,[90] Y. S. Gao,[31,h] C. García,[174] J. E. García Navarro,[174] J. A. García Pascual,[15a] C. Garcia-Argos,[52] M. Garcia-Sciveres,[18] R. W. Gardner,[37] N. Garelli,[153] S. Gargiulo,[52] V. Garonne,[134] A. Gaudiello,[55b,55a] G. Gaudio,[70a] I. L. Gavrilenko,[110] A. Gavrilyuk,[111] C. Gay,[175] G. Gaycken,[24] E. N. Gazis,[10] A. A. Geanta,[27b] C. N. P. Gee,[144] J. Geisen,[53] M. Geisen,[99] M. P. Geisler,[61a] C. Gemme,[55b] M. H. Genest,[58] C. Geng,[105] S. Gentile,[72a,72b] S. George,[93] T. Geralis,[44] D. Gerbaudo,[14] L. O. Gerlach,[53] P. Gessinger-Befurt,[99] G. Gessner,[47] S. Ghasemi,[151] M. Ghasemi Bostanabad,[176] M. Ghneimat,[24] A. Ghosh,[77] B. Giacobbe,[23b] S. Giagu,[72a,72b] N. Giangiacomi,[23b,23a] P. Giannetti,[71a] A. Giannini,[69a,69b] S. M. Gibson,[93] M. Gignac,[146] D. Gillberg,[34] G. Gilles,[182] D. M. Gingrich,[3,e] M. P. Giordani,[66a,66c] F. M. Giorgi,[23b] P. F. Giraud,[145] G. Giugliarelli,[66a,66c] D. Giugni,[68a] F. Giuli,[73a,73b] S. Gkaitatzis,[162] I. Gkialas,[9,r] E. L. Gkougkousis,[14] P. Gkountoumis,[10] L. K. Gladilin,[113] C. Glasman,[98] J. Glatzer,[14] P. C. F. Glaysher,[46] A. Glazov,[46] M. Goblirsch-Kolb,[26] S. Goldfarb,[104] T. Golling,[54] D. Golubkov,[123] A. Gomes,[140a,140b] R. Goncalves Gama,[53] R. Gonçalo,[140a,140b] G. Gonella,[52] L. Gonella,[21] A. Gongadze,[79] F. Gonnella,[21] J. L. Gonski,[59] S. González de la Hoz,[174] S. Gonzalez-Sevilla,[54] G. R. Gonzalvo Rodriguez,[174] L. Goossens,[36] P. A. Gorbounov,[111] H. A. Gordon,[29] B. Gorini,[36] E. Gorini,[67a,67b] A. Gorišek,[91] A. T. Goshaw,[49] M. I. Gostkin,[79] C. A. Gottardo,[24] M. Gouighri,[35b] D. Goujdami,[35c] A. G. Goussiou,[148] N. Govender,[33b,s] C. Goy,[5] E. Gozani,[160] I. Grabowska-Bold,[83a] E. C. Graham,[90] J. Gramling,[171] E. Gramstad,[134] S. Grancagnolo,[19] M. Grandi,[156] V. Gratchev,[138] P. M. Gravila,[27f] F. G. Gravili,[67a,67b] C. Gray,[57] H. M. Gray,[18] C. Grefe,[24] K. Gregersen,[96] I. M. Gregor,[46] P. Grenier,[153] K. Grevtsov,[46] N. A. Grieser,[128] J. Griffiths,[8] A. A. Grillo,[146] K. Grimm,[31,t] S. Grinstein,[14,u] J.-F. Grivaz,[132] S. Groh,[99] E. Gross,[180] J. Grosse-Knetter,[53] Z. J. Grout,[94] C. Grud,[105] A. Grummer,[118] L. Guan,[105] W. Guan,[181] J. Guenther,[36] A. Guerguichon,[132] F. Guescini,[168a] D. Guest,[171] R. Gugel,[52] B. Gui,[126] T. Guillemin,[5] S. Guindon,[36] U. Gul,[57] J. Guo,[60c] W. Guo,[105] Y. Guo,[60a,v] Z. Guo,[101] R. Gupta,[46] S. Gurbuz,[12c] G. Gustavino,[128] P. Gutierrez,[128] C. Gutschow,[94] C. Guyot,[145] M. P. Guzik,[83a] C. Gwenlan,[135] C. B. Gwilliam,[90] A. Haas,[124] C. Haber,[18] H. K. Hadavand,[8] N. Haddad,[35e] A. Hadef,[60a] S. Hageböck,[36] M. Hagihara,[169] M. Haleem,[177] J. Haley,[129] G. Halladjian,[106] G. D. Hallewell,[101] K. Hamacher,[182] P. Hamal,[130] K. Hamano,[176] H. Hamdaoui,[35e] G. N. Hamity,[149] K. Han,[60a,w] L. Han,[60a] S. Han,[15a,15d] K. Hanagaki,[81,x] M. Hance,[146] D. M. Handl,[114] B. Haney,[137] R. Hankache,[136] E. Hansen,[96] J. B. Hansen,[40] J. D. Hansen,[40] M. C. Hansen,[24]

P. H. Hansen,[40] E. C. Hanson,[100] K. Hara,[169] A. S. Hard,[181] T. Harenberg,[182] S. Harkusha,[107] P. F. Harrison,[178] N. M. Hartmann,[114] Y. Hasegawa,[150] A. Hasib,[50] S. Hassani,[145] S. Haug,[20] R. Hauser,[106] L. B. Havener,[39] M. Havranek,[142] C. M. Hawkes,[21] R. J. Hawkings,[36] D. Hayden,[106] C. Hayes,[155] R. L. Hayes,[175] C. P. Hays,[135] J. M. Hays,[92] H. S. Hayward,[90] S. J. Haywood,[144] F. He,[60a] M. P. Heath,[50] V. Hedberg,[96] L. Heelan,[8] S. Heer,[24] K. K. Heidegger,[52] J. Heilman,[34] S. Heim,[46] T. Heim,[18] B. Heinemann,[46,y] J. J. Heinrich,[131] L. Heinrich,[36] C. Heinz,[56] J. Hejbal,[141] L. Helary,[61b] A. Held,[175] S. Hellesund,[134] C. M. Helling,[146] S. Hellman,[45a,45b] C. Helsens,[36] R. C. W. Henderson,[89] Y. Heng,[181] S. Henkelmann,[175] A. M. Henriques Correia,[36] G. H. Herbert,[19] H. Herde,[26] V. Herget,[177] Y. Hernández Jiménez,[33c] H. Herr,[99] M. G. Herrmann,[114] T. Herrmann,[48] G. Herten,[52] R. Hertenberger,[114] L. Hervas,[36] T. C. Herwig,[137] G. G. Hesketh,[94] N. P. Hessey,[168a] A. Higashida,[163] S. Higashino,[81] E. Higón-Rodriguez,[174] K. Hildebrand,[37] E. Hill,[176] J. C. Hill,[32] K. K. Hill,[29] K. H. Hiller,[46] S. J. Hillier,[21] M. Hils,[48] I. Hinchliffe,[18] F. Hinterkeuser,[24] M. Hirose,[133] S. Hirose,[52] D. Hirschbuehl,[182] B. Hiti,[91] O. Hladik,[141] D. R. Hlaluku,[33c] X. Hoad,[50] J. Hobbs,[155] N. Hod,[180] M. C. Hodgkinson,[149] A. Hoecker,[36] F. Hoenig,[114] D. Hohn,[52] D. Hohov,[132] T. R. Holmes,[37] M. Holzbock,[114] L. B. A. H Hommels,[32] S. Honda,[169] T. Honda,[81] T. M. Hong,[139] A. Hönle,[115] B. H. Hooberman,[173] W. H. Hopkins,[6] Y. Horii,[117] P. Horn,[48] A. J. Horton,[152] L. A. Horyn,[37] J-Y. Hostachy,[58] A. Hostiuc,[148] S. Hou,[158] A. Hoummada,[35a] J. Howarth,[100] J. Hoya,[88] M. Hrabovsky,[130] J. Hrdinka,[76] I. Hristova,[19] J. Hrivnac,[132] A. Hrynevich,[108] T. Hryn'ova,[5] P. J. Hsu,[64] S.-C. Hsu,[148] Q. Hu,[29] S. Hu,[60c] Y. Huang,[15a] Z. Hubacek,[142] F. Hubaut,[101] M. Huebner,[24] F. Huegging,[24] T. B. Huffman,[135] M. Huhtinen,[36] R. F. H. Hunter,[34] P. Huo,[155] A. M. Hupe,[34] N. Huseynov,[79,z] J. Huston,[106] J. Huth,[59] R. Hyneman,[105] S. Hyrych,[28a] G. Iacobucci,[54] G. Iakovidis,[29] I. Ibragimov,[151] L. Iconomidou-Fayard,[132] Z. Idrissi,[35e] P. I. Iengo,[36] R. Ignazzi,[40] O. Igonkina,[120,a,aa] R. Iguchi,[163] T. Iizawa,[54] Y. Ikegami,[81] M. Ikeno,[81] D. Iliadis,[162] N. Ilic,[119] F. Iltzsche,[48] G. Introzzi,[70a,70b] M. Iodice,[74a] K. Iordanidou,[39] V. Ippolito,[72a,72b] M. F. Isacson,[172] N. Ishijima,[133] M. Ishino,[163] M. Ishitsuka,[165] W. Islam,[129] C. Issever,[135] S. Istin,[160] F. Ito,[169] J. M. Iturbe Ponce,[63a] R. Iuppa,[75a,75b] A. Ivina,[180] H. Iwasaki,[81] J. M. Izen,[43] V. Izzo,[69a] P. Jacka,[141] P. Jackson,[1] R. M. Jacobs,[24] V. Jain,[2] G. Jäkel,[182] K. B. Jakobi,[99] K. Jakobs,[52] S. Jakobsen,[76] T. Jakoubek,[141] J. Jamieson,[57] K. W. Janas,[83a] R. Jansky,[54] J. Janssen,[24] M. Janus,[53] P. A. Janus,[83a] G. Jarlskog,[96] N. Javadov,[79,z] T. Javůrek,[36] M. Javurkova,[52] F. Jeanneau,[145] L. Jeanty,[131] J. Jejelava,[159a,bb] A. Jelinskas,[178] P. Jenni,[52,cc] J. Jeong,[46] N. Jeong,[46] S. Jézéquel,[5] H. Ji,[181] J. Jia,[155] H. Jiang,[78] Y. Jiang,[60a] Z. Jiang,[153,dd] S. Jiggins,[52] F. A. Jimenez Morales,[38] J. Jimenez Pena,[174] S. Jin,[15c] A. Jinaru,[27b] O. Jinnouchi,[165] H. Jivan,[33c] P. Johansson,[149] K. A. Johns,[7] C. A. Johnson,[65] K. Jon-And,[45a,45b] R. W. L. Jones,[89] S. D. Jones,[156] S. Jones,[7] T. J. Jones,[90] J. Jongmanns,[61a] P. M. Jorge,[140a] J. Jovicevic,[36] X. Ju,[18] J. J. Junggeburth,[115] A. Juste Rozas,[14,u] A. Kaczmarska,[84] M. Kado,[72a,72b] H. Kagan,[126] M. Kagan,[153] C. Kahra,[99] T. Kaji,[179] E. Kajomovitz,[160] C. W. Kalderon,[96] A. Kaluza,[99] A. Kamenshchikov,[123] L. Kanjir,[91] Y. Kano,[163] V. A. Kantserov,[112] J. Kanzaki,[81] L. S. Kaplan,[181] D. Kar,[33c] M. J. Kareem,[168b] E. Karentzos,[10] S. N. Karpov,[79] Z. M. Karpova,[79] V. Kartvelishvili,[89] A. N. Karyukhin,[123] L. Kashif,[181] R. D. Kass,[126] A. Kastanas,[45a,45b] Y. Kataoka,[163] C. Kato,[60d,60c] J. Katzy,[46] K. Kawade,[82] K. Kawagoe,[87] T. Kawaguchi,[117] T. Kawamoto,[163] G. Kawamura,[53] E. F. Kay,[176] V. F. Kazanin,[122b,122a] R. Keeler,[176] R. Kehoe,[42] J. S. Keller,[34] E. Kellermann,[96] D. Kelsey,[156] J. J. Kempster,[21] J. Kendrick,[21] O. Kepka,[141] S. Kersten,[182] B. P. Kerševan,[91] S. Ketabchi Haghighat,[167] M. Khader,[173] F. Khalil-Zada,[13] M. Khandoga,[145] A. Khanov,[129] A. G. Kharlamov,[122b,122a] T. Kharlamova,[122b,122a] E. E. Khoda,[175] A. Khodinov,[166] T. J. Khoo,[54] E. Khramov,[79] J. Khubua,[159b] S. Kido,[82] M. Kiehn,[54] C. R. Kilby,[93] Y. K. Kim,[37] N. Kimura,[66a,66c] O. M. Kind,[19] B. T. King,[90,a] D. Kirchmeier,[48] J. Kirk,[144] A. E. Kiryunin,[115] T. Kishimoto,[163] D. P. Kisliuk,[167] V. Kitali,[46] O. Kivernyk,[5] E. Kladiva,[28b,a] T. Klapdor-Kleingrothaus,[52] M. H. Klein,[105] M. Klein,[90] U. Klein,[90] K. Kleinknecht,[99] P. Klimek,[121] A. Klimentov,[29] T. Klingl,[24] T. Klioutchnikova,[36] F. F. Klitzner,[114] P. Kluit,[120] S. Kluth,[115] E. Kneringer,[76] E. B. F. G. Knoops,[101] A. Knue,[52] D. Kobayashi,[87] T. Kobayashi,[163] M. Kobel,[48] M. Kocian,[153] P. Kodys,[143] P. T. Koenig,[24] T. Koffas,[34] N. M. Köhler,[115] T. Koi,[153] M. Kolb,[61b] I. Koletsou,[5] T. Komarek,[130] T. Kondo,[81] N. Kondrashova,[60c] K. Köneke,[52] A. C. König,[119] T. Kono,[125] R. Konoplich,[124,ee] V. Konstantinides,[94] N. Konstantinidis,[94] B. Konya,[96] R. Kopeliansky,[65] S. Koperny,[83a] K. Korcyl,[84] K. Kordas,[162] G. Koren,[161] A. Korn,[94] I. Korolkov,[14] E. V. Korolkova,[149] N. Korotkova,[113] O. Kortner,[115] S. Kortner,[115] T. Kosek,[143] V. V. Kostyukhin,[24] A. Kotwal,[49] A. Koulouris,[10] A. Kourkoumeli-Charalampidi,[70a,70b] C. Kourkoumelis,[9] E. Kourlitis,[149] V. Kouskoura,[29] A. B. Kowalewska,[84] R. Kowalewski,[176] C. Kozakai,[163] W. Kozanecki,[145] A. S. Kozhin,[123] V. A. Kramarenko,[113] G. Kramberger,[91] D. Krasnopevtsev,[60a] M. W. Krasny,[136] A. Krasznahorkay,[36] D. Krauss,[115] J. A. Kremer,[83a] J. Kretzschmar,[90] P. Krieger,[167] F. Krieter,[114] A. Krishnan,[61b] K. Krizka,[18] K. Kroeninger,[47] H. Kroha,[115] J. Kroll,[141] J. Kroll,[137] J. Krstic,[16] U. Kruchonak,[79] H. Krüger,[24] N. Krumnack,[78] M. C. Kruse,[49] T. Kubota,[104] S. Kuday,[4b] J. T. Kuechler,[46] S. Kuehn,[36] A. Kugel,[61a] T. Kuhl,[46] V. Kukhtin,[79] R. Kukla,[101]

Y. Kulchitsky,[107,ff] S. Kuleshov,[147b] Y. P. Kulinich,[173] M. Kuna,[58] T. Kunigo,[85] A. Kupco,[141] T. Kupfer,[47] O. Kuprash,[52] H. Kurashige,[82] L. L. Kurchaninov,[168a] Y. A. Kurochkin,[107] A. Kurova,[112] M. G. Kurth,[15a,15d] E. S. Kuwertz,[36] M. Kuze,[165] A. K. Kvam,[148] J. Kvita,[130] T. Kwan,[103] A. La Rosa,[115] L. La Rotonda,[41b,41a] F. La Ruffa,[41b,41a] C. Lacasta,[174] F. Lacava,[72a,72b] D. P. J. Lack,[100] H. Lacker,[19] D. Lacour,[136] E. Ladygin,[79] R. Lafaye,[5] B. Laforge,[136] T. Lagouri,[33c] S. Lai,[53] S. Lammers,[65] W. Lampl,[7] C. Lampoudis,[162] E. Lançon,[29] U. Landgraf,[52] M. P. J. Landon,[92] M. C. Lanfermann,[54] V. S. Lang,[46] J. C. Lange,[53] R. J. Langenberg,[36] A. J. Lankford,[171] F. Lanni,[29] K. Lantzsch,[24] A. Lanza,[70a] A. Lapertosa,[55b,55a] S. Laplace,[136] J. F. Laporte,[145] T. Lari,[68a] F. Lasagni Manghi,[23b,23a] M. Lassnig,[36] T. S. Lau,[63a] A. Laudrain,[132] A. Laurier,[34] M. Lavorgna,[69a,69b] M. Lazzaroni,[68a,68b] B. Le,[104] E. Le Guirriec,[101] M. LeBlanc,[7] T. LeCompte,[6] F. Ledroit-Guillon,[58] C. A. Lee,[29] G. R. Lee,[17] L. Lee,[59] S. C. Lee,[158] S. J. Lee,[34] B. Lefebvre,[168a] M. Lefebvre,[176] F. Legger,[114] C. Leggett,[18] K. Lehmann,[152] N. Lehmann,[182] G. Lehmann Miotto,[36] W. A. Leight,[46] A. Leisos,[162,gg] M. A. L. Leite,[80d] R. Leitner,[143] D. Lellouch,[180,a] K. J. C. Leney,[42] T. Lenz,[24] B. Lenzi,[36] R. Leone,[7] S. Leone,[71a] C. Leonidopoulos,[50] A. Leopold,[136] G. Lerner,[156] C. Leroy,[109] R. Les,[167] C. G. Lester,[32] M. Levchenko,[138] J. Levêque,[5] D. Levin,[105] L. J. Levinson,[180] D. J. Lewis,[21] B. Li,[15b] B. Li,[105] C-Q. Li,[60a] F. Li,[60c] H. Li,[60a] H. Li,[60b] J. Li,[60c] K. Li,[153] L. Li,[60c] M. Li,[15a] Q. Li,[15a,15d] Q. Y. Li,[60a] S. Li,[60d,60c] X. Li,[46] Y. Li,[46] Z. Li,[60b] Z. Liang,[15a] B. Liberti,[73a] A. Liblong,[167] K. Lie,[63c] S. Liem,[120] C. Y. Lin,[32] K. Lin,[106] T. H. Lin,[99] R. A. Linck,[65] J. H. Lindon,[21] A. L. Lionti,[54] E. Lipeles,[137] A. Lipniacka,[17] M. Lisovyi,[61b] T. M. Liss,[173,hh] A. Lister,[175] A. M. Litke,[146] J. D. Little,[8] B. Liu,[78,ii] B. L Liu,[6] H. B. Liu,[29] H. Liu,[105] J. B. Liu,[60a] J. K. K. Liu,[135] K. Liu,[136] M. Liu,[60a] P. Liu,[18] Y. Liu,[15a,15d] Y. L. Liu,[105] Y. W. Liu,[60a] M. Livan,[70a,70b] A. Lleres,[58] J. Llorente Merino,[15a] S. L. Lloyd,[92] C. Y. Lo,[63b] F. Lo Sterzo,[42] E. M. Lobodzinska,[46] P. Loch,[7] S. Loffredo,[73a,73b] T. Lohse,[19] K. Lohwasser,[149] M. Lokajicek,[141] J. D. Long,[173] R. E. Long,[89] L. Longo,[36] K. A. Looper,[126] J. A. Lopez,[147b] I. Lopez Paz,[100] A. Lopez Solis,[149] J. Lorenz,[114] N. Lorenzo Martinez,[5] M. Losada,[22] P. J. Lösel,[114] A. Lösle,[52] X. Lou,[46] X. Lou,[15a] A. Lounis,[132] J. Love,[6] P. A. Love,[89] J. J. Lozano Bahilo,[174] M. Lu,[60a] Y. J. Lu,[64] H. J. Lubatti,[148] C. Luci,[72a,72b] A. Lucotte,[58] C. Luedtke,[52] F. Luehring,[65] I. Luise,[136] L. Luminari,[72a] B. Lund-Jensen,[154] M. S. Lutz,[102] D. Lynn,[29] R. Lysak,[141] E. Lytken,[96] F. Lyu,[15a] V. Lyubushkin,[79] T. Lyubushkina,[79] H. Ma,[29] L. L. Ma,[60b] Y. Ma,[60b] G. Maccarrone,[51] A. Macchiolo,[115] C. M. Macdonald,[149] J. Machado Miguens,[137] D. Madaffari,[174] R. Madar,[38] W. F. Mader,[48] N. Madysa,[48] J. Maeda,[82] K. Maekawa,[163] S. Maeland,[17] T. Maeno,[29] M. Maerker,[48] A. S. Maevskiy,[113] V. Magerl,[52] N. Magini,[78] D. J. Mahon,[39] C. Maidantchik,[80b] T. Maier,[114] A. Maio,[140a,140b,140d] O. Majersky,[28a] S. Majewski,[131] Y. Makida,[81] N. Makovec,[132] B. Malaescu,[136] Pa. Malecki,[84] V. P. Maleev,[138] F. Malek,[58] U. Mallik,[77] D. Malon,[6] C. Malone,[32] S. Maltezos,[10] S. Malyukov,[36] J. Mamuzic,[174] G. Mancini,[51] I. Mandić,[91] L. Manhaes de Andrade Filho,[80a] I. M. Maniatis,[162] J. Manjarres Ramos,[48] K. H. Mankinen,[96] A. Mann,[114] A. Manousos,[76] B. Mansoulie,[145] I. Manthos,[162] S. Manzoni,[120] A. Marantis,[162] G. Marceca,[30] L. Marchese,[135] G. Marchiori,[136] M. Marcisovsky,[141] C. Marcon,[96] C. A. Marin Tobon,[36] M. Marjanovic,[38] Z. Marshall,[18] M. U. F Martensson,[172] S. Marti-Garcia,[174] C. B. Martin,[126] T. A. Martin,[178] V. J. Martin,[50] B. Martin dit Latour,[17] L. Martinelli,[74a,74b] M. Martinez,[14,u] V. I. Martinez Outschoorn,[102] S. Martin-Haugh,[144] V. S. Martoiu,[27b] A. C. Martyniuk,[94] A. Marzin,[36] S. R. Maschek,[115] L. Masetti,[99] T. Mashimo,[163] R. Mashinistov,[110] J. Masik,[100] A. L. Maslennikov,[122b,122a] L. H. Mason,[104] L. Massa,[73a,73b] P. Massarotti,[69a,69b] P. Mastrandrea,[71a,71b] A. Mastroberardino,[41b,41a] T. Masubuchi,[163] A. Matic,[114] P. Mättig,[24] J. Maurer,[27b] B. Maček,[91] D. A. Maximov,[122b,122a] R. Mazini,[158] I. Maznas,[162] S. M. Mazza,[146] S. P. Mc Kee,[105] T. G. McCarthy,[115] L. I. McClymont,[94] W. P. McCormack,[18] E. F. McDonald,[104] J. A. Mcfayden,[36] M. A. McKay,[42] K. D. McLean,[176] S. J. McMahon,[144] P. C. McNamara,[104] C. J. McNicol,[178] R. A. McPherson,[176,p] J. E. Mdhluli,[33c] Z. A. Meadows,[102] S. Meehan,[148] T. Megy,[52] S. Mehlhase,[114] A. Mehta,[90] T. Meideck,[58] B. Meirose,[43] D. Melini,[174] B. R. Mellado Garcia,[33c] J. D. Mellenthin,[53] M. Melo,[28a] F. Meloni,[46] A. Melzer,[24] S. B. Menary,[100] E. D. Mendes Gouveia,[140a,140e] L. Meng,[36] X. T. Meng,[105] S. Menke,[115] E. Meoni,[41b,41a] S. Mergelmeyer,[19] S. A. M. Merkt,[139] C. Merlassino,[20] P. Mermod,[54] L. Merola,[69a,69b] C. Meroni,[68a] O. Meshkov,[113,110] J. K. R. Meshreki,[151] A. Messina,[72a,72b] J. Metcalfe,[6] A. S. Mete,[171] C. Meyer,[65] J. Meyer,[160] J-P. Meyer,[145] H. Meyer Zu Theenhausen,[61a] F. Miano,[156] R. P. Middleton,[144] L. Mijović,[50] G. Mikenberg,[180] M. Mikestikova,[141] M. Mikuž,[91] H. Mildner,[149] M. Milesi,[104] A. Milic,[167] D. A. Millar,[92] D. W. Miller,[37] A. Milov,[180] D. A. Milstead,[45a,45b] R. A. Mina,[153,dd] A. A. Minaenko,[123] M. Miñano Moya,[174] I. A. Minashvili,[159b] A. I. Mincer,[124] B. Mindur,[83a] M. Mineev,[79] Y. Minegishi,[163] Y. Ming,[181] L. M. Mir,[14] A. Mirto,[67a,67b] K. P. Mistry,[137] T. Mitani,[179] J. Mitrevski,[114] V. A. Mitsou,[174] M. Mittal,[60c] A. Miucci,[20] P. S. Miyagawa,[149] A. Mizukami,[81] J. U. Mjörnmark,[96] T. Mkrtchyan,[184] M. Mlynarikova,[143] T. Moa,[45a,45b] K. Mochizuki,[109] P. Mogg,[52] S. Mohapatra,[39] R. Moles-Valls,[24] M. C. Mondragon,[106] K. Mönig,[46] J. Monk,[40] E. Monnier,[101] A. Montalbano,[152] J. Montejo Berlingen,[36] M. Montella,[94] F. Monticelli,[88] S. Monzani,[68a] N. Morange,[132]

D. Moreno,[22] M. Moreno Llácer,[36] C. Moreno Martinez,[14] P. Morettini,[55b] M. Morgenstern,[120] S. Morgenstern,[48] D. Mori,[152] M. Morii,[59] M. Morinaga,[179] V. Morisbak,[134] A. K. Morley,[36] G. Mornacchi,[36] A. P. Morris,[94] L. Morvaj,[155] P. Moschovakos,[36] B. Moser,[120] M. Mosidze,[159b] T. Moskalets,[145] H. J. Moss,[149] J. Moss,[31,jj] K. Motohashi,[165] E. Mountricha,[36] E. J. W. Moyse,[102] S. Muanza,[101] J. Mueller,[139] R. S. P. Mueller,[114] D. Muenstermann,[89] G. A. Mullier,[96] J. L. Munoz Martinez,[14] F. J. Munoz Sanchez,[100] P. Murin,[28b] W. J. Murray,[178,144] A. Murrone,[68a,68b] M. Muškinja,[18] C. Mwewa,[33a] A. G. Myagkov,[123,kk] J. Myers,[131] M. Myska,[142] B. P. Nachman,[18] O. Nackenhorst,[47] A. Nag Nag,[48] K. Nagai,[135] K. Nagano,[81] Y. Nagasaka,[62] M. Nagel,[52] E. Nagy,[101] A. M. Nairz,[36] Y. Nakahama,[117] K. Nakamura,[81] T. Nakamura,[163] I. Nakano,[127] H. Nanjo,[133] F. Napolitano,[61a] R. F. Naranjo Garcia,[46] R. Narayan,[11] D. I. Narrias Villar,[61a] I. Naryshkin,[138] T. Naumann,[46] G. Navarro,[22] H. A. Neal,[105,a] P. Y. Nechaeva,[110] F. Nechansky,[46] T. J. Neep,[21] A. Negri,[70a,70b] M. Negrini,[23b] C. Nellist,[53] M. E. Nelson,[135] S. Nemecek,[141] P. Nemethy,[124] M. Nessi,[36,ll] M. S. Neubauer,[173] M. Neumann,[182] P. R. Newman,[21] T. Y. Ng,[63c] Y. S. Ng,[19] Y. W. Y. Ng,[171] H. D. N. Nguyen,[101] T. Nguyen Manh,[109] E. Nibigira,[38] R. B. Nickerson,[135] R. Nicolaidou,[145] D. S. Nielsen,[40] J. Nielsen,[146] N. Nikiforou,[11] V. Nikolaenko,[123,kk] I. Nikolic-Audit,[136] K. Nikolopoulos,[21] P. Nilsson,[29] H. R. Nindhito,[54] Y. Ninomiya,[81] A. Nisati,[72a] N. Nishu,[60c] R. Nisius,[115] I. Nitsche,[47] T. Nitta,[179] T. Nobe,[163] Y. Noguchi,[85] M. Nomachi,[133] I. Nomidis,[136] M. A. Nomura,[29] M. Nordberg,[36] N. Norjoharuddeen,[135] T. Novak,[91] O. Novgorodova,[48] R. Novotny,[142] L. Nozka,[130] K. Ntekas,[171] E. Nurse,[94] F. G. Oakham,[34,e] H. Oberlack,[115] J. Ocariz,[136] A. Ochi,[82] I. Ochoa,[39] J. P. Ochoa-Ricoux,[147a] K. O'Connor,[26] S. Oda,[87] S. Odaka,[81] S. Oerdek,[53] A. Ogrodnik,[83a] A. Oh,[100] S. H. Oh,[49] C. C. Ohm,[154] H. Oide,[55b,55a] M. L. Ojeda,[167] H. Okawa,[169] Y. Okazaki,[85] Y. Okumura,[163] T. Okuyama,[81] A. Olariu,[27b] L. F. Oleiro Seabra,[140a] S. A. Olivares Pino,[147a] D. Oliveira Damazio,[29] J. L. Oliver,[1] M. J. R. Olsson,[171] A. Olszewski,[84] J. Olszowska,[84] D. C. O'Neil,[152] A. Onofre,[140a,140e] K. Onogi,[117] P. U. E. Onyisi,[11] H. Oppen,[134] M. J. Oreglia,[37] G. E. Orellana,[88] D. Orestano,[74a,74b] N. Orlando,[14] R. S. Orr,[167] V. O'Shea,[57] R. Ospanov,[60a] G. Otero y Garzon,[30] H. Otono,[87] M. Ouchrif,[35d] F. Ould-Saada,[134] A. Ouraou,[145] Q. Ouyang,[15a] M. Owen,[57] R. E. Owen,[21] V. E. Ozcan,[12c] N. Ozturk,[8] J. Pacalt,[130] H. A. Pacey,[32] K. Pachal,[49] A. Pacheco Pages,[14] C. Padilla Aranda,[14] S. Pagan Griso,[18] M. Paganini,[183] G. Palacino,[65] S. Palazzo,[50] S. Palestini,[36] M. Palka,[83b] D. Pallin,[38] I. Panagoulias,[10] C. E. Pandini,[36] J. G. Panduro Vazquez,[93] P. Pani,[46] G. Panizzo,[66a,66c] L. Paolozzi,[54] C. Papadatos,[109] K. Papageorgiou,[9,r] A. Paramonov,[6] D. Paredes Hernandez,[63b] S. R. Paredes Saenz,[135] B. Parida,[166] T. H. Park,[167] A. J. Parker,[89] M. A. Parker,[32] F. Parodi,[55b,55a] E. W. P. Parrish,[121] J. A. Parsons,[39] U. Parzefall,[52] L. Pascual Dominguez,[136] V. R. Pascuzzi,[167] J. M. P. Pasner,[146] E. Pasqualucci,[72a] S. Passaggio,[55b] F. Pastore,[93] P. Pasuwan,[45a,45b] S. Pataraia,[99] J. R. Pater,[100] A. Pathak,[181] T. Pauly,[36] B. Pearson,[115] M. Pedersen,[134] L. Pedraza Diaz,[119] R. Pedro,[140a] T. Peiffer,[53] S. V. Peleganchuk,[122b,122a] O. Penc,[141] H. Peng,[60a] B. S. Peralva,[80a] M. M. Perego,[132] A. P. Pereira Peixoto,[140a] D. V. Perepelitsa,[29] F. Peri,[19] L. Perini,[68a,68b] H. Pernegger,[36] S. Perrella,[69a,69b] K. Peters,[46] R. F. Y. Peters,[100] B. A. Petersen,[36] T. C. Petersen,[40] E. Petit,[101] A. Petridis,[1] C. Petridou,[162] P. Petroff,[132] M. Petrov,[135] F. Petrucci,[74a,74b] M. Pettee,[183] N. E. Pettersson,[102] K. Petukhova,[143] A. Peyaud,[145] R. Pezoa,[147b] L. Pezzotti,[70a,70b] T. Pham,[104] F. H. Phillips,[106] P. W. Phillips,[144] M. W. Phipps,[173] G. Piacquadio,[155] E. Pianori,[18] A. Picazio,[102] R. H. Pickles,[100] R. Piegaia,[30] D. Pietreanu,[27b] J. E. Pilcher,[37] A. D. Pilkington,[100] M. Pinamonti,[73a,73b] J. L. Pinfold,[3] M. Pitt,[180] L. Pizzimento,[73a,73b] M.-A. Pleier,[29] V. Pleskot,[143] E. Plotnikova,[79] D. Pluth,[78] P. Podberezko,[122b,122a] R. Poettgen,[96] R. Poggi,[54] L. Poggioli,[132] I. Pogrebnyak,[106] D. Pohl,[24] I. Pokharel,[53] G. Polesello,[70a] A. Poley,[18] A. Policicchio,[72a,72b] R. Polifka,[143] A. Polini,[23b] C. S. Pollard,[46] V. Polychronakos,[29] D. Ponomarenko,[112] L. Pontecorvo,[36] S. Popa,[27a] G. A. Popeneciu,[27d] D. M. Portillo Quintero,[58] S. Pospisil,[142] K. Potamianos,[46] I. N. Potrap,[79] C. J. Potter,[32] H. Potti,[11] T. Poulsen,[96] J. Poveda,[36] T. D. Powell,[149] G. Pownall,[46] M. E. Pozo Astigarraga,[36] P. Pralavorio,[101] S. Prell,[78] D. Price,[100] M. Primavera,[67a] S. Prince,[103] M. L. Proffitt,[148] N. Proklova,[112] K. Prokofiev,[63c] F. Prokoshin,[147b] S. Protopopescu,[29] J. Proudfoot,[6] M. Przybycien,[83a] D. Pudzha,[138] A. Puri,[173] P. Puzo,[132] J. Qian,[105] Y. Qin,[100] A. Quadt,[53] M. Queitsch-Maitland,[46] A. Qureshi,[1] P. Rados,[104] F. Ragusa,[68a,68b] G. Rahal,[97] J. A. Raine,[54] S. Rajagopalan,[29] A. Ramirez Morales,[92] K. Ran,[15a,15d] T. Rashid,[132] S. Raspopov,[5] M. G. Ratti,[68a,68b] D. M. Rauch,[46] F. Rauscher,[114] S. Rave,[99] B. Ravina,[149] I. Ravinovich,[180] J. H. Rawling,[100] M. Raymond,[36] A. L. Read,[134] N. P. Readioff,[58] M. Reale,[67a,67b] D. M. Rebuzzi,[70a,70b] A. Redelbach,[177] G. Redlinger,[29] K. Reeves,[43] L. Rehnisch,[19] J. Reichert,[137] D. Reikher,[161] A. Reiss,[99] A. Rej,[151] C. Rembser,[36] M. Renda,[27b] M. Rescigno,[72a] S. Resconi,[68a] E. D. Resseguie,[137] S. Rettie,[175] E. Reynolds,[21] O. L. Rezanova,[122b,122a] P. Reznicek,[143] E. Ricci,[75a,75b] R. Richter,[115] S. Richter,[46] E. Richter-Was,[83b] O. Ricken,[24] M. Ridel,[136] P. Rieck,[115] C. J. Riegel,[182] O. Rifki,[46] M. Rijssenbeek,[155] A. Rimoldi,[70a,70b] M. Rimoldi,[20] L. Rinaldi,[23b] G. Ripellino,[154] B. Ristić,[89] E. Ritsch,[36] I. Riu,[14] J. C. Rivera Vergara,[147a] F. Rizatdinova,[129] E. Rizvi,[92] C. Rizzi,[36] R. T. Roberts,[100] S. H. Robertson,[103,p] M. Robin,[46]

D. Robinson,[32] J. E. M. Robinson,[46] A. Robson,[57] E. Rocco,[99] C. Roda,[71a,71b] S. Rodriguez Bosca,[174] A. Rodriguez Perez,[14] D. Rodriguez Rodriguez,[174] A. M. Rodríguez Vera,[168b] S. Roe,[36] O. Røhne,[134] R. Röhrig,[115] C. P. A. Roland,[65] J. Roloff,[59] A. Romaniouk,[112] M. Romano,[23b,23a] N. Rompotis,[90] M. Ronzani,[124] L. Roos,[136] S. Rosati,[72a] K. Rosbach,[52] N-A. Rosien,[53] G. Rosin,[102] B. J. Rosser,[137] E. Rossi,[46] E. Rossi,[74a,74b] E. Rossi,[69a,69b] L. P. Rossi,[55b] L. Rossini,[68a,68b] R. Rosten,[14] M. Rotaru,[27b] J. Rothberg,[148] D. Rousseau,[132] G. Rovelli,[70a,70b] D. Roy,[33c] A. Rozanov,[101] Y. Rozen,[160] X. Ruan,[33c] F. Rubbo,[153] F. Rühr,[52] A. Ruiz-Martinez,[174] A. Rummler,[36] Z. Rurikova,[52] N. A. Rusakovich,[79] H. L. Russell,[103] L. Rustige,[38,47] J. P. Rutherfoord,[7] E. M. Rüttinger,[46,mm] Y. F. Ryabov,[138] M. Rybar,[39] G. Rybkin,[132] A. Ryzhov,[123] G. F. Rzehorz,[53] P. Sabatini,[53] G. Sabato,[120] S. Sacerdoti,[132] H. F-W. Sadrozinski,[146] R. Sadykov,[79] F. Safai Tehrani,[72a] B. Safarzadeh Samani,[156] P. Saha,[121] S. Saha,[103] M. Sahinsoy,[61a] A. Sahu,[182] M. Saimpert,[46] M. Saito,[163] T. Saito,[163] H. Sakamoto,[163] A. Sakharov,[124,ee] D. Salamani,[54] G. Salamanna,[74a,74b] J. E. Salazar Loyola,[147b] P. H. Sales De Bruin,[172] D. Salihagic,[115,a] A. Salnikov,[153] J. Salt,[174] D. Salvatore,[41b,41a] F. Salvatore,[156] A. Salvucci,[63a,63b,63c] A. Salzburger,[36] J. Samarati,[36] D. Sammel,[52] D. Sampsonidis,[162] D. Sampsonidou,[162] J. Sánchez,[174] A. Sanchez Pineda,[66a,66c] H. Sandaker,[134] C. O. Sander,[46] I. G. Sanderswood,[89] M. Sandhoff,[182] C. Sandoval,[22] D. P. C. Sankey,[144] M. Sannino,[55b,55a] Y. Sano,[117] A. Sansoni,[51] C. Santoni,[38] H. Santos,[140a,140b] S. N. Santpur,[18] A. Santra,[174] A. Sapronov,[79] J. G. Saraiva,[140a,140d] O. Sasaki,[81] K. Sato,[169] E. Sauvan,[5] P. Savard,[167,e] N. Savic,[115] R. Sawada,[163] C. Sawyer,[144] L. Sawyer,[95,nn] C. Sbarra,[23b] A. Sbrizzi,[23a] T. Scanlon,[94] J. Schaarschmidt,[148] P. Schacht,[115] B. M. Schachtner,[114] D. Schaefer,[37] L. Schaefer,[137] J. Schaeffer,[99] S. Schaepe,[36] U. Schäfer,[99] A. C. Schaffer,[132] D. Schaile,[114] R. D. Schamberger,[155] N. Scharmberg,[100] V. A. Schegelsky,[138] D. Scheirich,[143] F. Schenck,[19] M. Schernau,[171] C. Schiavi,[55b,55a] S. Schier,[146] L. K. Schildgen,[24] Z. M. Schillaci,[26] E. J. Schioppa,[36] M. Schioppa,[41b,41a] K. E. Schleicher,[52] S. Schlenker,[36] K. R. Schmidt-Sommerfeld,[115] K. Schmieden,[36] C. Schmitt,[99] S. Schmitt,[46] S. Schmitz,[99] J. C. Schmoeckel,[46] U. Schnoor,[52] L. Schoeffel,[145] A. Schoening,[61b] E. Schopf,[135] M. Schott,[99] J. F. P. Schouwenberg,[119] J. Schovancova,[36] S. Schramm,[54] F. Schroeder,[182] A. Schulte,[99] H-C. Schultz-Coulon,[61a] M. Schumacher,[52] B. A. Schumm,[146] Ph. Schune,[145] A. Schwartzman,[153] T. A. Schwarz,[105] Ph. Schwemling,[145] R. Schwienhorst,[106] A. Sciandra,[146] G. Sciolla,[26] M. Scodeggio,[46] M. Scornajenghi,[41b,41a] F. Scuri,[71a] F. Scutti,[104] L. M. Scyboz,[115] C. D. Sebastiani,[72a,72b] P. Seema,[19] S. C. Seidel,[118] A. Seiden,[146] T. Seiss,[37] J. M. Seixas,[80b] G. Sekhniaidze,[69a] K. Sekhon,[105] S. J. Sekula,[42] N. Semprini-Cesari,[23b,23a] S. Sen,[49] S. Senkin,[38] C. Serfon,[76] L. Serin,[132] L. Serkin,[66a,66b] M. Sessa,[60a] H. Severini,[128] F. Sforza,[170] A. Sfyrla,[54] E. Shabalina,[53] J. D. Shahinian,[146] N. W. Shaikh,[45a,45b] D. Shaked Renous,[180] L. Y. Shan,[15a] R. Shang,[173] J. T. Shank,[25] M. Shapiro,[18] A. Sharma,[135] A. S. Sharma,[1] P. B. Shatalov,[111] K. Shaw,[156] S. M. Shaw,[100] A. Shcherbakova,[138] Y. Shen,[128] N. Sherafati,[34] A. D. Sherman,[25] P. Sherwood,[94] L. Shi,[158,oo] S. Shimizu,[81] C. O. Shimmin,[183] Y. Shimogama,[179] M. Shimojima,[116] I. P. J. Shipsey,[135] S. Shirabe,[87] M. Shiyakova,[79,pp] J. Shlomi,[180] A. Shmeleva,[110] M. J. Shochet,[37] J. Shojaii,[104] D. R. Shope,[128] S. Shrestha,[126] E. Shulga,[180] P. Sicho,[141] A. M. Sickles,[173] P. E. Sidebo,[154] E. Sideras Haddad,[33c] O. Sidiropoulou,[36] A. Sidoti,[23b,23a] F. Siegert,[48] Dj. Sijacki,[16] M. Silva Jr.,[181] M. V. Silva Oliveira,[80a] S. B. Silverstein,[45a] S. Simion,[132] E. Simioni,[99] R. Simoniello,[99] P. Sinervo,[167] N. B. Sinev,[131] M. Sioli,[23b,23a] I. Siral,[105] S. Yu. Sivoklokov,[113] J. Sjölin,[45a,45b] E. Skorda,[96] P. Skubic,[128] M. Slawinska,[84] K. Sliwa,[170] R. Slovak,[143] V. Smakhtin,[180] B. H. Smart,[144] J. Smiesko,[28a] N. Smirnov,[112] S. Yu. Smirnov,[112] Y. Smirnov,[112] L. N. Smirnova,[113,qq] O. Smirnova,[96] J. W. Smith,[53] M. Smizanska,[89] K. Smolek,[142] A. Smykiewicz,[84] A. A. Snesarev,[110] H. L. Snoek,[120] I. M. Snyder,[131] S. Snyder,[29] R. Sobie,[176,p] A. M. Soffa,[171] A. Soffer,[161] A. Søgaard,[50] F. Sohns,[53] C. A. Solans Sanchez,[36] E. Yu. Soldatov,[112] U. Soldevila,[174] A. A. Solodkov,[123] A. Soloshenko,[79] O. V. Solovyanov,[123] V. Solovyev,[138] P. Sommer,[149] H. Son,[170] W. Song,[144] W. Y. Song,[168b] A. Sopczak,[142] F. Sopkova,[28b] C. L. Sotiropoulou,[71a,71b] S. Sottocornola,[70a,70b] R. Soualah,[66a,66c,rr] A. M. Soukharev,[122b,122a] D. South,[46] S. Spagnolo,[67a,67b] M. Spalla,[115] M. Spangenberg,[178] F. Spanò,[93] D. Sperlich,[52] T. M. Spieker,[61a] R. Spighi,[23b] G. Spigo,[36] M. Spina,[156] D. P. Spiteri,[57] M. Spousta,[143] A. Stabile,[68a,68b] B. L. Stamas,[121] R. Stamen,[61a] M. Stamenkovic,[120] E. Stanecka,[84] R. W. Stanek,[6] B. Stanislaus,[135] M. M. Stanitzki,[46] M. Stankaityte,[135] B. Stapf,[120] E. A. Starchenko,[123] G. H. Stark,[146] J. Stark,[58] S. H Stark,[40] P. Staroba,[141] P. Starovoitov,[61a] S. Stärz,[103] R. Staszewski,[84] G. Stavropoulos,[44] M. Stegler,[46] P. Steinberg,[29] A. L. Steinhebel,[131] B. Stelzer,[152] H. J. Stelzer,[139] O. Stelzer-Chilton,[168a] H. Stenzel,[56] T. J. Stevenson,[156] G. A. Stewart,[36] M. C. Stockton,[36] G. Stoicea,[27b] M. Stolarski,[140a] P. Stolte,[53] S. Stonjek,[115] A. Straessner,[48] J. Strandberg,[154] S. Strandberg,[45a,45b] M. Strauss,[128] P. Strizenec,[28b] R. Ströhmer,[177] D. M. Strom,[131] R. Stroynowski,[42] A. Strubig,[50] S. A. Stucci,[29] B. Stugu,[17] J. Stupak,[128] N. A. Styles,[46] D. Su,[153] S. Suchek,[61a] Y. Sugaya,[133] V. V. Sulin,[110] M. J. Sullivan,[90] D. M. S. Sultan,[54] S. Sultansoy,[4c] T. Sumida,[85] S. Sun,[105] X. Sun,[3] K. Suruliz,[156] C. J. E. Suster,[157] M. R. Sutton,[156] S. Suzuki,[81] M. Svatos,[141] M. Swiatlowski,[37] S. P. Swift,[2] T. Swirski,[177] A. Sydorenko,[99] I. Sykora,[28a] M. Sykora,[143]

T. Sykora,[143] D. Ta,[99] K. Tackmann,[46,ss] J. Taenzer,[161] A. Taffard,[171] R. Tafirout,[168a] E. Tahirovic,[92] H. Takai,[29] R. Takashima,[86] K. Takeda,[82] T. Takeshita,[150] E. P. Takeva,[50] Y. Takubo,[81] M. Talby,[101] A. A. Talyshev,[122b,122a] N. M. Tamir,[161] J. Tanaka,[163] M. Tanaka,[165] R. Tanaka,[132] B. B. Tannenwald,[126] S. Tapia Araya,[173] S. Tapprogge,[99] A. Tarek Abouelfadl Mohamed,[136] S. Tarem,[160] G. Tarna,[27b,tt] G. F. Tartarelli,[68a] P. Tas,[143] M. Tasevsky,[141] T. Tashiro,[85] E. Tassi,[41b,41a] A. Tavares Delgado,[140a,140b] Y. Tayalati,[35e] A. J. Taylor,[50] G. N. Taylor,[104] W. Taylor,[168b] A. S. Tee,[89] R. Teixeira De Lima,[153] P. Teixeira-Dias,[93] H. Ten Kate,[36] J. J. Teoh,[120] S. Terada,[81] K. Terashi,[163] J. Terron,[98] S. Terzo,[14] M. Testa,[51] R. J. Teuscher,[167,p] S. J. Thais,[183] T. Theveneaux-Pelzer,[46] F. Thiele,[40] D. W. Thomas,[93] J. O. Thomas,[42] J. P. Thomas,[21] A. S. Thompson,[57] P. D. Thompson,[21] L. A. Thomsen,[183] E. Thomson,[137] Y. Tian,[39] R. E. Ticse Torres,[53] V. O. Tikhomirov,[110,uu] Yu. A. Tikhonov,[122b,122a] S. Timoshenko,[112] P. Tipton,[183] S. Tisserant,[101] K. Todome,[23b,23a] S. Todorova-Nova,[5] S. Todt,[48] J. Tojo,[87] S. Tokár,[28a] K. Tokushuku,[81] E. Tolley,[126] K. G. Tomiwa,[33c] M. Tomoto,[117] L. Tompkins,[153,dd] K. Toms,[118] B. Tong,[59] P. Tornambe,[102] E. Torrence,[131] H. Torres,[48] E. Torró Pastor,[148] C. Tosciri,[135] J. Toth,[101,vv] D. R. Tovey,[149] C. J. Treado,[124] T. Trefzger,[177] F. Tresoldi,[156] A. Tricoli,[29] I. M. Trigger,[168a] S. Trincaz-Duvoid,[136] W. Trischuk,[167] B. Trocmé,[58] A. Trofymov,[132] C. Troncon,[68a] M. Trovatelli,[176] F. Trovato,[156] L. Truong,[33b] M. Trzebinski,[84] A. Trzupek,[84] F. Tsai,[46] J. C-L. Tseng,[135] P. V. Tsiareshka,[107,ff] A. Tsirigotis,[162] N. Tsirintanis,[9] V. Tsiskaridze,[155] E. G. Tskhadadze,[159a] M. Tsopoulou,[162] I. I. Tsukerman,[111] V. Tsulaia,[18] S. Tsuno,[81] D. Tsybychev,[155] Y. Tu,[63b] A. Tudorache,[27b] V. Tudorache,[27b] T. T. Tulbure,[27a] A. N. Tuna,[59] S. Turchikhin,[79] D. Turgeman,[180] I. Turk Cakir,[4b,ww] R. J. Turner,[21] R. T. Turra,[68a] P. M. Tuts,[39] S. Tzamarias,[162] E. Tzovara,[99] G. Ucchielli,[47] K. Uchida,[163] I. Ueda,[81] M. Ughetto,[45a,45b] F. Ukegawa,[169] G. Unal,[36] A. Undrus,[29] G. Unel,[171] F. C. Ungaro,[104] Y. Unno,[81] K. Uno,[163] J. Urban,[28b] P. Urquijo,[104] G. Usai,[8] J. Usui,[81] L. Vacavant,[101] V. Vacek,[142] B. Vachon,[103] K. O. H. Vadla,[134] A. Vaidya,[94] C. Valderanis,[114] E. Valdes Santurio,[45a,45b] M. Valente,[54] S. Valentinetti,[23b,23a] A. Valero,[174] L. Valéry,[46] R. A. Vallance,[21] A. Vallier,[36] J. A. Valls Ferrer,[174] T. R. Van Daalen,[14] P. Van Gemmeren,[6] I. Van Vulpen,[120] M. Vanadia,[73a,73b] W. Vandelli,[36] A. Vaniachine,[166] D. Vannicola,[72a,72b] R. Vari,[72a] E. W. Varnes,[7] C. Varni,[55b,55a] T. Varol,[42] D. Varouchas,[132] K. E. Varvell,[157] M. E. Vasile,[27b] G. A. Vasquez,[176] J. G. Vasquez,[183] F. Vazeille,[38] D. Vazquez Furelos,[14] T. Vazquez Schroeder,[36] J. Veatch,[53] V. Vecchio,[74a,74b] M. J. Veen,[120] L. M. Veloce,[167] F. Veloso,[140a,140c] S. Veneziano,[72a] A. Ventura,[67a,67b] N. Venturi,[36] A. Verbytskyi,[115] V. Vercesi,[70a] M. Verducci,[74a,74b] C. M. Vergel Infante,[78] C. Vergis,[24] W. Verkerke,[120] A. T. Vermeulen,[120] J. C. Vermeulen,[120] M. C. Vetterli,[152,e] N. Viaux Maira,[147b] M. Vicente Barreto Pinto,[54] T. Vickey,[149] O. E. Vickey Boeriu,[149] G. H. A. Viehhauser,[135] L. Vigani,[135] M. Villa,[23b,23a] M. Villaplana Perez,[68a,68b] E. Vilucchi,[51] M. G. Vincter,[34] V. B. Vinogradov,[79] A. Vishwakarma,[46] C. Vittori,[23b,23a] I. Vivarelli,[156] M. Vogel,[182] P. Vokac,[142] S. E. von Buddenbrock,[33c] E. Von Toerne,[24] V. Vorobel,[143] K. Vorobev,[112] M. Vos,[174] J. H. Vossebeld,[90] N. Vranjes,[16] M. Vranjes Milosavljevic,[16] V. Vrba,[142] M. Vreeswijk,[120] T. Šfiligoj,[91] R. Vuillermet,[36] I. Vukotic,[37] T. Ženiš,[28a] L. Živković,[16] P. Wagner,[24] W. Wagner,[182] J. Wagner-Kuhr,[114] H. Wahlberg,[88] K. Wakamiya,[82] V. M. Walbrecht,[115] J. Walder,[89] R. Walker,[114] S. D. Walker,[93] W. Walkowiak,[151] V. Wallangen,[45a,45b] A. M. Wang,[59] C. Wang,[60c] C. Wang,[60b] F. Wang,[181] H. Wang,[18] H. Wang,[3] J. Wang,[157] J. Wang,[61b] P. Wang,[42] Q. Wang,[128] R.-J. Wang,[99] R. Wang,[60a] R. Wang,[6] S. M. Wang,[158] W. T. Wang,[60a] W. Wang,[15c,xx] W. X. Wang,[60a,xx] Y. Wang,[60a,yy] Z. Wang,[60c] C. Wanotayaroj,[46] A. Warburton,[103] C. P. Ward,[32] D. R. Wardrope,[94] N. Warrack,[57] A. Washbrook,[50] A. T. Watson,[21] M. F. Watson,[21] G. Watts,[148] B. M. Waugh,[94] A. F. Webb,[11] S. Webb,[99] C. Weber,[183] M. S. Weber,[20] S. A. Weber,[34] S. M. Weber,[61a] A. R. Weidberg,[135] J. Weingarten,[47] M. Weirich,[99] C. Weiser,[52] P. S. Wells,[36] T. Wenaus,[29] T. Wengler,[36] S. Wenig,[36] N. Wermes,[24] M. D. Werner,[78] P. Werner,[36] M. Wessels,[61a] T. D. Weston,[20] K. Whalen,[131] N. L. Whallon,[148] A. M. Wharton,[89] A. S. White,[105] A. White,[8] M. J. White,[1] D. Whiteson,[171] B. W. Whitmore,[89] F. J. Wickens,[144] W. Wiedenmann,[181] M. Wielers,[144] N. Wieseotte,[99] C. Wiglesworth,[40] L. A. M. Wiik-Fuchs,[52] F. Wilk,[100] H. G. Wilkens,[36] L. J. Wilkins,[93] H. H. Williams,[137] S. Williams,[32] C. Willis,[106] S. Willocq,[102] J. A. Wilson,[21] I. Wingerter-Seez,[5] E. Winkels,[156] F. Winklmeier,[131] O. J. Winston,[156] B. T. Winter,[52] M. Wittgen,[153] M. Wobisch,[95] A. Wolf,[99] T. M. H. Wolf,[120] R. Wolff,[101] R. W. Wölker,[135] J. Wollrath,[52] M. W. Wolter,[84] H. Wolters,[140a,140c] V. W. S. Wong,[175] N. L. Woods,[146] S. D. Worm,[21] B. K. Wosiek,[84] K. W. Woźniak,[84] K. Wraight,[57] S. L. Wu,[181] X. Wu,[54] Y. Wu,[60a] T. R. Wyatt,[100] B. M. Wynne,[50] S. Xella,[40] Z. Xi,[105] L. Xia,[178] D. Xu,[15a] H. Xu,[60a,tt] L. Xu,[29] T. Xu,[145] W. Xu,[105] Z. Xu,[60b] Z. Xu,[153] B. Yabsley,[157] S. Yacoob,[33a] K. Yajima,[133] D. P. Yallup,[94] D. Yamaguchi,[165] Y. Yamaguchi,[165] A. Yamamoto,[81] T. Yamanaka,[163] F. Yamane,[82] M. Yamatani,[163] T. Yamazaki,[163] Y. Yamazaki,[82] Z. Yan,[25] H. J. Yang,[60c,60d] H. T. Yang,[18] S. Yang,[77] X. Yang,[60b,58] Y. Yang,[163] Z. Yang,[17] W-M. Yao,[18] Y. C. Yap,[46] Y. Yasu,[81] E. Yatsenko,[60c,60d] J. Ye,[42] S. Ye,[29] I. Yeletskikh,[79] M. R. Yexley,[89] E. Yigitbasi,[25] E. Yildirim,[99] K. Yorita,[179] K. Yoshihara,[137] C. J. S. Young,[36] C. Young,[153]

J. Yu,[78] R. Yuan,[60b] X. Yue,[61a] S. P. Y. Yuen,[24] B. Zabinski,[84] G. Zacharis,[10] E. Zaffaroni,[54] J. Zahreddine,[136] R. Zaidan,[14] A. M. Zaitsev,[123,kk] T. Zakareishvili,[159b] N. Zakharchuk,[34] S. Zambito,[59] D. Zanzi,[36] D. R. Zaripovas,[57] S. V. Zeißner,[47] C. Zeitnitz,[182] G. Zemaityte,[135] J. C. Zeng,[173] O. Zenin,[123] D. Zerwas,[132] M. Zgubič,[135] D. F. Zhang,[15b] F. Zhang,[181] G. Zhang,[60a] G. Zhang,[15b] H. Zhang,[15c] J. Zhang,[6] L. Zhang,[15c] L. Zhang,[60a] M. Zhang,[173] R. Zhang,[60a] R. Zhang,[24] X. Zhang,[60b] Y. Zhang,[15a,15d] Z. Zhang,[63a] Z. Zhang,[132] P. Zhao,[49] Y. Zhao,[60b] Z. Zhao,[60a] A. Zhemchugov,[79] Z. Zheng,[105] D. Zhong,[173] B. Zhou,[105] C. Zhou,[181] M. S. Zhou,[15a,15d] M. Zhou,[155] N. Zhou,[60c] Y. Zhou,[7] C. G. Zhu,[60b] H. L. Zhu,[60a] H. Zhu,[15a] J. Zhu,[105] Y. Zhu,[60a] X. Zhuang,[15a] K. Zhukov,[110] V. Zhulanov,[122b,122a] D. Zieminska,[65] N. I. Zimine,[79] S. Zimmermann,[52] Z. Zinonos,[115] M. Ziolkowski,[151] G. Zobernig,[181] A. Zoccoli,[23b,23a] K. Zoch,[53] T. G. Zorbas,[149] R. Zou,[37] and L. Zwalinski[36]

(ATLAS Collaboration)

[1]*Department of Physics, University of Adelaide, Adelaide, Australia*
[2]*Physics Department, SUNY Albany, Albany, New York, USA*
[3]*Department of Physics, University of Alberta, Edmonton, Alberta, Canada*
[4a]*Department of Physics, Ankara University, Ankara, Turkey*
[4b]*Istanbul Aydin University, Istanbul, Turkey*
[4c]*Division of Physics, TOBB University of Economics and Technology, Ankara, Turkey*
[5]*LAPP, Université Grenoble Alpes, Université Savoie Mont Blanc, CNRS/IN2P3, Annecy, France*
[6]*High Energy Physics Division, Argonne National Laboratory, Argonne, Illinois, USA*
[7]*Department of Physics, University of Arizona, Tucson, Arizona, USA*
[8]*Department of Physics, University of Texas at Arlington, Arlington, Texas, USA*
[9]*Physics Department, National and Kapodistrian University of Athens, Athens, Greece*
[10]*Physics Department, National Technical University of Athens, Zografou, Greece*
[11]*Department of Physics, University of Texas at Austin, Austin, Texas, USA*
[12a]*Bahcesehir University, Faculty of Engineering and Natural Sciences, Istanbul, Turkey*
[12b]*Istanbul Bilgi University, Faculty of Engineering and Natural Sciences, Istanbul, Turkey*
[12c]*Department of Physics, Bogazici University, Istanbul, Turkey*
[12d]*Department of Physics Engineering, Gaziantep University, Gaziantep, Turkey*
[13]*Institute of Physics, Azerbaijan Academy of Sciences, Baku, Azerbaijan*
[14]*Institut de Física d'Altes Energies (IFAE), Barcelona Institute of Science and Technology, Barcelona, Spain*
[15a]*Institute of High Energy Physics, Chinese Academy of Sciences, Beijing, China*
[15b]*Physics Department, Tsinghua University, Beijing, China*
[15c]*Department of Physics, Nanjing University, Nanjing, China*
[15d]*University of Chinese Academy of Science (UCAS), Beijing, China*
[16]*Institute of Physics, University of Belgrade, Belgrade, Serbia*
[17]*Department for Physics and Technology, University of Bergen, Bergen, Norway*
[18]*Physics Division, Lawrence Berkeley National Laboratory and University of California, Berkeley, California, USA*
[19]*Institut für Physik, Humboldt Universität zu Berlin, Berlin, Germany*
[20]*Albert Einstein Center for Fundamental Physics and Laboratory for High Energy Physics, University of Bern, Bern, Switzerland*
[21]*School of Physics and Astronomy, University of Birmingham, Birmingham, United Kingdom*
[22]*Facultad de Ciencias y Centro de Investigaciónes, Universidad Antonio Nariño, Bogota, Colombia*
[23a]*INFN Bologna and Universita' di Bologna, Dipartimento di Fisica, Italy*
[23b]*INFN Sezione di Bologna, Italy*
[24]*Physikalisches Institut, Universität Bonn, Bonn, Germany*
[25]*Department of Physics, Boston University, Boston, Massachusetts, USA*
[26]*Department of Physics, Brandeis University, Waltham, Massachusetts, USA*
[27a]*Transilvania University of Brasov, Brasov, Romania*
[27b]*Horia Hulubei National Institute of Physics and Nuclear Engineering, Bucharest, Romania*
[27c]*Department of Physics, Alexandru Ioan Cuza University of Iasi, Iasi, Romania*
[27d]*National Institute for Research and Development of Isotopic and Molecular Technologies, Physics Department, Cluj-Napoca, Romania*
[27e]*University Politehnica Bucharest, Bucharest, Romania*
[27f]*West University in Timisoara, Timisoara, Romania*
[28a]*Faculty of Mathematics, Physics and Informatics, Comenius University, Bratislava, Slovak Republic*

[28b]Department of Subnuclear Physics, Institute of Experimental Physics of the Slovak Academy of Sciences, Kosice, Slovak Republic
[29]Physics Department, Brookhaven National Laboratory, Upton, New York, USA
[30]Departamento de Física, Universidad de Buenos Aires, Buenos Aires, Argentina
[31]California State University, California, USA
[32]Cavendish Laboratory, University of Cambridge, Cambridge, United Kingdom
[33a]Department of Physics, University of Cape Town, Cape Town, South Africa
[33b]Department of Mechanical Engineering Science, University of Johannesburg, Johannesburg, South Africa
[33c]School of Physics, University of the Witwatersrand, Johannesburg, South Africa
[34]Department of Physics, Carleton University, Ottawa, Ontario, Canada
[35a]Faculté des Sciences Ain Chock, Réseau Universitaire de Physique des Hautes Energies—Université Hassan II, Casablanca, Morocco
[35b]Faculté des Sciences, Université Ibn-Tofail, Kénitra, Morocco
[35c]Faculté des Sciences Semlalia, Université Cadi Ayyad, LPHEA-Marrakech, Morocco
[35d]Faculté des Sciences, Université Mohamed Premier and LPTPM, Oujda, Morocco
[35e]Faculté des sciences, Université Mohammed V, Rabat, Morocco
[36]CERN, Geneva, Switzerland
[37]Enrico Fermi Institute, University of Chicago, Chicago, Illinois, USA
[38]LPC, Université Clermont Auvergne, CNRS/IN2P3, Clermont-Ferrand, France
[39]Nevis Laboratory, Columbia University, Irvington, New York, USA
[40]Niels Bohr Institute, University of Copenhagen, Copenhagen, Denmark
[41a]Dipartimento di Fisica, Università della Calabria, Rende, Italy
[41b]INFN Gruppo Collegato di Cosenza, Laboratori Nazionali di Frascati, Italy
[42]Physics Department, Southern Methodist University, Dallas, Texas, USA
[43]Physics Department, University of Texas at Dallas, Richardson, Texas, USA
[44]National Centre for Scientific Research "Demokritos", Agia Paraskevi, Greece
[45a]Department of Physics, Stockholm University, Sweden
[45b]Oskar Klein Centre, Stockholm, Sweden
[46]Deutsches Elektronen-Synchrotron DESY, Hamburg and Zeuthen, Germany
[47]Lehrstuhl für Experimentelle Physik IV, Technische Universität Dortmund, Dortmund, Germany
[48]Institut für Kern- und Teilchenphysik, Technische Universität Dresden, Dresden, Germany
[49]Department of Physics, Duke University, Durham, North Carolina, USA
[50]SUPA—School of Physics and Astronomy, University of Edinburgh, Edinburgh, United Kingdom
[51]INFN e Laboratori Nazionali di Frascati, Frascati, Italy
[52]Physikalisches Institut, Albert-Ludwigs-Universität Freiburg, Freiburg, Germany
[53]II. Physikalisches Institut, Georg-August-Universität Göttingen, Göttingen, Germany
[54]Département de Physique Nucléaire et Corpusculaire, Université de Genève, Genève, Switzerland
[55a]Dipartimento di Fisica, Università di Genova, Genova, Italy
[55b]INFN Sezione di Genova, Italy
[56]II. Physikalisches Institut, Justus-Liebig-Universität Giessen, Giessen, Germany
[57]SUPA—School of Physics and Astronomy, University of Glasgow, Glasgow, United Kingdom
[58]LPSC, Université Grenoble Alpes, CNRS/IN2P3, Grenoble INP, Grenoble, France
[59]Laboratory for Particle Physics and Cosmology, Harvard University, Cambridge, Massachusetts, USA
[60a]Department of Modern Physics and State Key Laboratory of Particle Detection and Electronics, University of Science and Technology of China, Hefei, China
[60b]Institute of Frontier and Interdisciplinary Science and Key Laboratory of Particle Physics and Particle Irradiation (MOE), Shandong University, Qingdao, China
[60c]School of Physics and Astronomy, Shanghai Jiao Tong University, KLPPAC-MoE, SKLPPC, Shanghai, China
[60d]Tsung-Dao Lee Institute, Shanghai, China
[61a]Kirchhoff-Institut für Physik, Ruprecht-Karls-Universität Heidelberg, Heidelberg, Germany
[61b]Physikalisches Institut, Ruprecht-Karls-Universität Heidelberg, Heidelberg, Germany
[62]Faculty of Applied Information Science, Hiroshima Institute of Technology, Hiroshima, Japan
[63a]Department of Physics, Chinese University of Hong Kong, Shatin, N.T., Hong Kong, China
[63b]Department of Physics, University of Hong Kong, Hong Kong, China
[63c]Department of Physics and Institute for Advanced Study, Hong Kong University of Science and Technology, Clear Water Bay, Kowloon, Hong Kong, China
[64]Department of Physics, National Tsing Hua University, Hsinchu, Taiwan
[65]Department of Physics, Indiana University, Bloomington, Indiana, USA

[66a]INFN Gruppo Collegato di Udine, Sezione di Trieste, Udine, Italy
[66b]ICTP, Trieste, Italy
[66c]Dipartimento Politecnico di Ingegneria e Architettura, Università di Udine, Udine, Italy
[67a]INFN Sezione di Lecce, Italy
[67b]Dipartimento di Matematica e Fisica, Università del Salento, Lecce, Italy
[68a]INFN Sezione di Milano, Italy
[68b]Dipartimento di Fisica, Università di Milano, Milano, Italy
[69a]INFN Sezione di Napoli, Italy
[69b]Dipartimento di Fisica, Università di Napoli, Napoli, Italy
[70a]INFN Sezione di Pavia, Italy
[70b]Dipartimento di Fisica, Università di Pavia, Pavia, Italy
[71a]INFN Sezione di Pisa, Italy
[71b]Dipartimento di Fisica E. Fermi, Università di Pisa, Pisa, Italy
[72a]INFN Sezione di Roma, Italy
[72b]Dipartimento di Fisica, Sapienza Università di Roma, Roma, Italy
[73a]INFN Sezione di Roma Tor Vergata, Italy
[73b]Dipartimento di Fisica, Università di Roma Tor Vergata, Roma, Italy
[74a]INFN Sezione di Roma Tre, Italy
[74b]Dipartimento di Matematica e Fisica, Università Roma Tre, Roma, Italy
[75a]INFN-TIFPA, Italy
[75b]Università degli Studi di Trento, Trento, Italy
[76]Institut für Astro- und Teilchenphysik, Leopold-Franzens-Universität, Innsbruck, Austria
[77]University of Iowa, Iowa City, Iowa, USA
[78]Department of Physics and Astronomy, Iowa State University, Ames, Iowa, USA
[79]Joint Institute for Nuclear Research, Dubna, Russia
[80a]Departamento de Engenharia Elétrica, Universidade Federal de Juiz de Fora (UFJF), Juiz de Fora, Brazil
[80b]Universidade Federal do Rio De Janeiro COPPE/EE/IF, Rio de Janeiro, Brazil
[80c]Universidade Federal de São João del Rei (UFSJ), São João del Rei, Brazil
[80d]Instituto de Física, Universidade de São Paulo, São Paulo, Brazil
[81]KEK, High Energy Accelerator Research Organization, Tsukuba, Japan
[82]Graduate School of Science, Kobe University, Kobe, Japan
[83a]AGH University of Science and Technology, Faculty of Physics and Applied Computer Science, Krakow, Poland
[83b]Marian Smoluchowski Institute of Physics, Jagiellonian University, Krakow, Poland
[84]Institute of Nuclear Physics Polish Academy of Sciences, Krakow, Poland
[85]Faculty of Science, Kyoto University, Kyoto, Japan
[86]Kyoto University of Education, Kyoto, Japan
[87]Research Center for Advanced Particle Physics and Department of Physics, Kyushu University, Fukuoka, Japan
[88]Instituto de Física La Plata, Universidad Nacional de La Plata and CONICET, La Plata, Argentina
[89]Physics Department, Lancaster University, Lancaster, United Kingdom
[90]Oliver Lodge Laboratory, University of Liverpool, Liverpool, United Kingdom
[91]Department of Experimental Particle Physics, Jožef Stefan Institute and Department of Physics, University of Ljubljana, Ljubljana, Slovenia
[92]School of Physics and Astronomy, Queen Mary University of London, London, United Kingdom
[93]Department of Physics, Royal Holloway University of London, Egham, United Kingdom
[94]Department of Physics and Astronomy, University College London, London, United Kingdom
[95]Louisiana Tech University, Ruston, Louisiana, USA
[96]Fysiska institutionen, Lunds universitet, Lund, Sweden
[97]Centre de Calcul de l'Institut National de Physique Nucléaire et de Physique des Particules (IN2P3), Villeurbanne, France
[98]Departamento de Física Teorica C-15 and CIAFF, Universidad Autónoma de Madrid, Madrid, Spain
[99]Institut für Physik, Universität Mainz, Mainz, Germany
[100]School of Physics and Astronomy, University of Manchester, Manchester, United Kingdom
[101]CPPM, Aix-Marseille Université, CNRS/IN2P3, Marseille, France
[102]Department of Physics, University of Massachusetts, Amherst, Massachusetts, USA
[103]Department of Physics, McGill University, Montreal, Quebec, Canada
[104]School of Physics, University of Melbourne, Victoria, Australia
[105]Department of Physics, University of Michigan, Ann Arbor, Michigan, USA

[106]*Department of Physics and Astronomy, Michigan State University, East Lansing, Michigan, USA*
[107]*B.I. Stepanov Institute of Physics, National Academy of Sciences of Belarus, Minsk, Belarus*
[108]*Research Institute for Nuclear Problems of Byelorussian State University, Minsk, Belarus*
[109]*Group of Particle Physics, University of Montreal, Montreal, Quebec, Canada*
[110]*P.N. Lebedev Physical Institute of the Russian Academy of Sciences, Moscow, Russia*
[111]*Institute for Theoretical and Experimental Physics of the National Research Centre Kurchatov Institute, Moscow, Russia*
[112]*National Research Nuclear University MEPhI, Moscow, Russia*
[113]*D.V. Skobeltsyn Institute of Nuclear Physics, M.V. Lomonosov Moscow State University, Moscow, Russia*
[114]*Fakultät für Physik, Ludwig-Maximilians-Universität München, München, Germany*
[115]*Max-Planck-Institut für Physik (Werner-Heisenberg-Institut), München, Germany*
[116]*Nagasaki Institute of Applied Science, Nagasaki, Japan*
[117]*Graduate School of Science and Kobayashi-Maskawa Institute, Nagoya University, Nagoya, Japan*
[118]*Department of Physics and Astronomy, University of New Mexico, Albuquerque, New Mexico, USA*
[119]*Institute for Mathematics, Astrophysics and Particle Physics, Radboud University Nijmegen/Nikhef, Nijmegen, Netherlands*
[120]*Nikhef National Institute for Subatomic Physics and University of Amsterdam, Amsterdam, Netherlands*
[121]*Department of Physics, Northern Illinois University, DeKalb, Illinois, USA*
[122a]*Budker Institute of Nuclear Physics and NSU, SB RAS, Novosibirsk, Russia*
[122b]*Novosibirsk State University Novosibirsk, Russia*
[123]*Institute for High Energy Physics of the National Research Centre Kurchatov Institute, Protvino, Russia*
[124]*Department of Physics, New York University, New York, New York, USA*
[125]*Ochanomizu University, Otsuka, Bunkyo-ku, Tokyo, Japan*
[126]*The Ohio State University, Columbus, Ohio, USA*
[127]*Faculty of Science, Okayama University, Okayama, Japan*
[128]*Homer L. Dodge Department of Physics and Astronomy, University of Oklahoma, Norman, Oklahoma, USA*
[129]*Department of Physics, Oklahoma State University, Stillwater, Oklahoma, USA*
[130]*Palacký University, RCPTM, Joint Laboratory of Optics, Olomouc, Czech Republic*
[131]*Center for High Energy Physics, University of Oregon, Eugene, Oregon, USA*
[132]*LAL, Université Paris-Sud, CNRS/IN2P3, Université Paris-Saclay, Orsay, France*
[133]*Graduate School of Science, Osaka University, Osaka, Japan*
[134]*Department of Physics, University of Oslo, Oslo, Norway*
[135]*Department of Physics, Oxford University, Oxford, United Kingdom*
[136]*LPNHE, Sorbonne Université, Paris Diderot Sorbonne Paris Cité, CNRS/IN2P3, Paris, France*
[137]*Department of Physics, University of Pennsylvania, Philadelphia, Pennsylvania, USA*
[138]*Konstantinov Nuclear Physics Institute of National Research Centre "Kurchatov Institute", PNPI, St. Petersburg, Russia*
[139]*Department of Physics and Astronomy, University of Pittsburgh, Pittsburgh, Pennsylvania, USA*
[140a]*Laboratório de Instrumentação e Física Experimental de Partículas—LIP, Portugal*
[140b]*Departamento de Física, Faculdade de Ciências, Universidade de Lisboa, Lisboa, Portugal*
[140c]*Departamento de Física, Universidade de Coimbra, Coimbra, Portugal*
[140d]*Centro de Física Nuclear da Universidade de Lisboa, Lisboa, Portugal*
[140e]*Departamento de Física, Universidade do Minho, Braga, Portugal*
[140f]*Universidad de Granada, Granada (Spain), Spain*
[140g]*Dep Física and CEFITEC of Faculdade de Ciências e Tecnologia, Universidade Nova de Lisboa, Caparica, Portugal*
[141]*Institute of Physics of the Czech Academy of Sciences, Prague, Czech Republic*
[142]*Czech Technical University in Prague, Prague, Czech Republic*
[143]*Charles University, Faculty of Mathematics and Physics, Prague, Czech Republic*
[144]*Particle Physics Department, Rutherford Appleton Laboratory, Didcot, United Kingdom*
[145]*IRFU, CEA, Université Paris-Saclay, Gif-sur-Yvette, France*
[146]*Santa Cruz Institute for Particle Physics, University of California Santa Cruz, Santa Cruz, California, USA*
[147a]*Departamento de Física, Pontificia Universidad Católica de Chile, Santiago, Chile*
[147b]*Departamento de Física, Universidad Técnica Federico Santa María, Valparaíso, Chile*
[148]*Department of Physics, University of Washington, Seattle, Washington, USA*
[149]*Department of Physics and Astronomy, University of Sheffield, Sheffield, United Kingdom*
[150]*Department of Physics, Shinshu University, Nagano, Japan*

[151]Department Physik, Universität Siegen, Siegen, Germany
[152]Department of Physics, Simon Fraser University, Burnaby, British Columbia, Canada
[153]SLAC National Accelerator Laboratory, Stanford, California, USA
[154]Physics Department, Royal Institute of Technology, Stockholm, Sweden
[155]Departments of Physics and Astronomy, Stony Brook University, Stony Brook, New York, USA
[156]Department of Physics and Astronomy, University of Sussex, Brighton, United Kingdom
[157]School of Physics, University of Sydney, Sydney, Australia
[158]Institute of Physics, Academia Sinica, Taipei, Taiwan
[159a]E. Andronikashvili Institute of Physics, Iv. Javakhishvili Tbilisi State University, Tbilisi, Georgia
[159b]High Energy Physics Institute, Tbilisi State University, Tbilisi, Georgia
[160]Department of Physics, Technion, Israel Institute of Technology, Haifa, Israel
[161]Raymond and Beverly Sackler School of Physics and Astronomy, Tel Aviv University, Tel Aviv, Israel
[162]Department of Physics, Aristotle University of Thessaloniki, Thessaloniki, Greece
[163]International Center for Elementary Particle Physics and Department of Physics, University of Tokyo, Tokyo, Japan
[164]Graduate School of Science and Technology, Tokyo Metropolitan University, Tokyo, Japan
[165]Department of Physics, Tokyo Institute of Technology, Tokyo, Japan
[166]Tomsk State University, Tomsk, Russia
[167]Department of Physics, University of Toronto, Toronto, Ontario, Canada
[168a]TRIUMF, Vancouver, British Columbia, Canada
[168b]Department of Physics and Astronomy, York University, Toronto, Ontario, Canada
[169]Division of Physics and Tomonaga Center for the History of the Universe, Faculty of Pure and Applied Sciences, University of Tsukuba, Tsukuba, Japan
[170]Department of Physics and Astronomy, Tufts University, Medford, Massachusetts, USA
[171]Department of Physics and Astronomy, University of California Irvine, Irvine, California, USA
[172]Department of Physics and Astronomy, University of Uppsala, Uppsala, Sweden
[173]Department of Physics, University of Illinois, Urbana, Illinois, USA
[174]Instituto de Física Corpuscular (IFIC), Centro Mixto Universidad de Valencia—CSIC, Valencia, Spain
[175]Department of Physics, University of British Columbia, Vancouver, British Columbia, Canada
[176]Department of Physics and Astronomy, University of Victoria, Victoria, British Columbia, Canada
[177]Fakultät für Physik und Astronomie, Julius-Maximilians-Universität Würzburg, Würzburg, Germany
[178]Department of Physics, University of Warwick, Coventry, United Kingdom
[179]Waseda University, Tokyo, Japan
[180]Department of Particle Physics, Weizmann Institute of Science, Rehovot, Israel
[181]Department of Physics, University of Wisconsin, Madison, Wisconsin, USA
[182]Fakultät für Mathematik und Naturwissenschaften, Fachgruppe Physik, Bergische Universität Wuppertal, Wuppertal, Germany
[183]Department of Physics, Yale University, New Haven, Connecticut, USA
[184]Yerevan Physics Institute, Yerevan, Armenia

[a]Deceased.
[b]Also at Department of Physics, King's College London, London, United Kingdom.
[c]Also at Istanbul University, Dept. of Physics, Istanbul, Turkey.
[d]Also at Instituto de Fisica Teorica, IFT-UAM/CSIC, Madrid, Spain.
[e]Also at TRIUMF, Vancouver, British Columbia, Canada.
[f]Also at Department of Physics and Astronomy, University of Louisville, Louisville, Kentucky, USA.
[g]Also at Physics Department, An-Najah National University, Nablus, Palestine.
[h]Also at Department of Physics, California State University, Fresno, California, USA.
[i]Also at Department of Physics, University of Fribourg, Fribourg, Switzerland.
[j]Also at Physics Dept, University of South Africa, Pretoria, South Africa.
[k]Also at Departament de Fisica de la Universitat Autonoma de Barcelona, Barcelona, Spain.
[l]Also at Tomsk State University, Tomsk, and Moscow Institute of Physics and Technology State University, Dolgoprudny, Russia.
[m]Also at The Collaborative Innovation Center of Quantum Matter (CICQM), Beijing, China.
[n]Also at Departamento de Física, Instituto Superior Técnico, Universidade de Lisboa, Lisboa, Portugal.
[o]Also at Universita di Napoli Parthenope, Napoli, Italy.
[p]Also at Institute of Particle Physics (IPP), Canada.
[q]Also at Department of Physics, St. Petersburg State Polytechnical University, St. Petersburg, Russia.
[r]Also at Department of Financial and Management Engineering, University of the Aegean, Chios, Greece.
[s]Also at Centre for High Performance Computing, CSIR Campus, Rosebank, Cape Town, South Africa.
[t]Also at Department of Physics, California State University, East Bay, California, USA.

[u]Also at Institucio Catalana de Recerca i Estudis Avancats, ICREA, Barcelona, Spain.
[v]Also at Department of Physics, University of Michigan, Ann Arbor, Michigan, USA.
[w]Also at LAL, Université Paris-Sud, CNRS/IN2P3, Université Paris-Saclay, Orsay, France.
[x]Also at Graduate School of Science, Osaka University, Osaka, Japan.
[y]Also at Physikalisches Institut, Albert-Ludwigs-Universität Freiburg, Freiburg, Germany.
[z]Also at Institute of Physics, Azerbaijan Academy of Sciences, Baku, Azerbaijan.
[aa]Also at Institute for Mathematics, Astrophysics and Particle Physics, Radboud University Nijmegen/Nikhef, Nijmegen, Netherlands.
[bb]Also at Institute of Theoretical Physics, Ilia State University, Tbilisi, Georgia.
[cc]Also at CERN, Geneva, Switzerland.
[dd]Also at Department of Physics, Stanford University, Stanford, California, USA.
[ee]Also at Manhattan College, New York, New York, USA.
[ff]Also at Joint Institute for Nuclear Research, Dubna, Russia.
[gg]Also at Hellenic Open University, Patras, Greece.
[hh]Also at The City College of New York, New York, New York, USA.
[ii]Also at Institute of High Energy Physics, Chinese Academy of Sciences, Beijing, China.
[jj]Also at Department of Physics, California State University, Sacramento, USA.
[kk]Also at Moscow Institute of Physics and Technology State University, Dolgoprudny, Russia.
[ll]Also at Département de Physique Nucléaire et Corpusculaire, Université de Genève, Genève, Switzerland.
[mm]Also at Department of Physics and Astronomy, University of Sheffield, Sheffield, United Kingdom.
[nn]Also at Louisiana Tech University, Ruston, Louisiana, USA.
[oo]Also at School of Physics, Sun Yat-sen University, Guangzhou, China.
[pp]Also at Institute for Nuclear Research and Nuclear Energy (INRNE) of the Bulgarian Academy of Sciences, Sofia, Bulgaria.
[qq]Also at Faculty of Physics, M.V. Lomonosov Moscow State University, Moscow, Russia.
[rr]Also at Department of Applied Physics and Astronomy, University of Sharjah, Sharjah, United Arab Emirates.
[ss]Also at Institut für Experimentalphysik, Universität Hamburg, Hamburg, Germany.
[tt]Also at CPPM, Aix-Marseille Université, CNRS/IN2P3, Marseille, France.
[uu]Also at National Research Nuclear University MEPhI, Moscow, Russia.
[vv]Also at Institute for Particle and Nuclear Physics, Wigner Research Centre for Physics, Budapest, Hungary.
[ww]Also at Giresun University, Faculty of Engineering, Giresun, Turkey.
[xx]Also at Institute of Physics, Academia Sinica, Taipei, Taiwan.
[yy]Also at LPNHE, Sorbonne Université, Paris Diderot Sorbonne Paris Cité, CNRS/IN2P3, Paris, France.